UNIVERSITÀ DEGLI STUDI DI TRIESTE

UNIVERSITÀ DEGLI STUDI DI TRIESTE

XXXIV CICLO DEL DOTTORATO DI RICERCA IN

BIOMEDICINA MOLECOLARE

THE JANUS FACE OF BILIRUBIN: FROM NEONATAL TOXICITY TO THE POTENTIAL PROTECTION IN NEURODEGENERATIVE DISEASES

Settore scientifico-disciplinare: **BIO/11**

DOTTORANDO / A
SRI JAYANTI

COORDINATORE
PROF. GERMANA MERONI

SUPERVISORE DI TESI
PROF. CLAUDIO TIRIBELLI

CO-SUPERVISORE DI TESI

SILVIA GAZZIN, PHD

ANNO ACCADEMICO 2020/2021

UNIVERSITÀ DEGLI STUDI DI TRIESTE

UNIVERSITÀ DEGLI STUDI DI TRIESTE

XXXIV CICLO DEL DOTTORATO DI RICERCA IN

BIOMEDICINA MOLECOLARE

THE JANUS FACE OF BILIRUBIN: FROM NEONATAL TOXICITY TO THE POTENTIAL PROTECTION IN NEURODEGENERATIVE DISEASES

Settore scientifico-disciplinare: **BIO/11**

DOTTORANDA
SRI JAYANTI

COORDINATORE
PROF. GERMANA MERONI

SUPERVISORE DI TESI
PROF. CLAUDIO TIRIBELLI

CO-SUPERVISORE DI TESI
DOTT.SSA. SILVIA GAZZIN

ANNO ACCADEMICO 2020/2021

TABLE OF CONTENTS

SUMMARY

The Janus face of bilirubin: from neonatal toxicity to the potential protection in neurodegenerative diseases

Sri Jayanti

TASK 1: Bilirubin-induced neonatal neurotoxicity

Unconjugated bilirubin is a metabolite of heme catabolism, and it exhibits Janus face for owning neurotoxicity and neuroprotective effects. It can induce neurotoxicity to neonates (kernicterus) in the course of severe neonatal hyperbilirubinemia and lead to major neurological impairments or even death as consequences. As a complementary – alternative approach to phototherapy or exchange transfusion, the standard treatment for severe neonatal hyperbilirubinemia (not worldwide accessible, particularly in low-income countries), we tested curcumin (Curc). It has been already used in animal models as well as in clinics in other diseases with relevant results. As a model of kernicterus, we used the Gunn rat. We observed the full protection given by Curc from the bilirubin-induced cerebellar hypoplasia (landmark of bilirubin toxicity in the rodent model of kernicterus), the normalization of the cerebellar weight as well as its cellular number and architectural layer. As a final proof of the protective action of curcumin, hyperbilirubinemic rats treated with Curc performed as the normobilirubinemic littermates in the behavioral tests, with a full recovery of the motor-coordination skills. Among the molecular mechanisms

normalized by Curc, we noticed inflammation (including Tnf-α mRNA and protein levels), redox imbalance, and glutamate neurotoxicity. Notably, the ability of Curc to reverse the damage without lowering serum bilirubin levels indicates its direct effect on the damaging mechanisms in the brain. The results suggest the potential of Curc in the clinical scenario, especially in the settings where phototherapy and exchange transfusion are not feasible to perform.

TASK 2: Bilirubin protection in neurodegenerative diseases

TASK2A: Bilirubin reverses the dopaminergic neuron demise in an ex vivo Parkinson's disease (PD) model

The second face of bilirubin studied in our project is its neuroprotective potential. Despite it having long been considered a cytotoxic pigment, last decades UCB has emerged with its plethora of therapeutic potential. Mildly elevated bilirubin level (as in the Gilbert syndrome population), is protective against an array of diseases associated with increased oxidative stress, such as cardiovascular diseases, diabetes, and cancer, as well as in laboratory models of multiple sclerosis and glioma. However, the role of UCB is still not known in Parkinson's disease (PD), the fastest-growing neurological disorder which is still lacking disease-modifying therapy, and where oxidative stress is considered as one of the main causes of dopaminergic neurons (DOPAn) loss. Based on this background, we aimed to assess UCB therapeutic potential in PD.

To the goal, we used the ex vivo PD model previously developed and characterized in the lab (organotypic brain cultures of substantia nigra –

OBCs-SN challenged with low doses of rotenone - Rot). Our slow-progressing PD model not only mimics the stages of the human disease up to the diagnosis phase but also gives access to the pre-clinical – early events triggering DOPAn loss, including oxidative stress, inflammation, and neurotrophic factor alteration. We followed these indicators to evaluate the effect of UCB in this model. The counting of DOPAn, the key parameter to evaluate bilirubin protection, was performed by immunofluorescence. The molecular effects of the pigment were evaluated by RTqPCR, enzymatic tests, and cytokines/neutralizing Ab usage.

We demonstrated that low amounts of UCB are not toxic to DOPAn *per se* and that 0.5μM and 1μM UCB fully protect from the 40% DOPAn loss observed in the PD model. Redox imbalance, despite being observed in the model, looks not to be the key player in the UCB conferred protection. Importantly, we demonstrated that, among the pro-inflammatory markers altered in PD and modulated by UCB, *Tnfα* is the determinant of DOPAn loss and UCB protection.

TASK2B: Nanobubbles as bilirubin carriers in organotypic brain cultures of substantia nigra: an initial screening step of bilirubin-delivery in Parkinson's disease (*The experiments were performed in collaboration with Department of Drug Science and Technology and Department of Neuroscience, University of Torino, Torino, Italy*)

Despite its milestone as a potential single-therapy candidate for PD in our aforementioned experiment, and the possibility to modulate the UCB systemic levels with drugs, the use of UCB as a therapeutic agent suffers

from the challenge of reaching a so-tuned UCB concentration in the subsantia nigra of PD subjects.

The most solid way for reaching our goal is by delivering the specific UCB concentration we need to SN by nano-bubbles (NBs). In collaboration with the University of Turin that priory developed NBs able to carry therapeutic agents, we started screening different formulations of nanobubbles (glycol chitosan [GC]; GC-deferoxamine [GC-DFO], and para-magnetic NBs, GC-DFO-iron [GC-DFO-Fe] and for their safety and efficacy in protecting from DOPAn loss in the model of PD. To the goal, DOPAn immunofluorescence and viability test (MTT, LDH) have been performed.

Combining the vitality tests, GC and GC-DFO are safe to healthy slices (not challenged with Rot) at dilutions higher than 1:192. After loading different formulations of NBs with UCB, the restoration of DOPAn reach up to 80% under GC-UCB and GC-DFO-UCB treatment. Further experiments to optimize the protection of the selected NBs by loading different amounts of UCB and dissecting the molecular mechanisms involved in DOPAn protection are needed.

TASK2C: Curcumin Protection in an *ex vivo* Parkinson's disease (PD) model

Unlikely, the major clinical problem in PD is the late diagnosis, occurring when the 40-50% of DOPAn has been already lost. While the administration of UCB-loaded NBs at diagnosis to stop the progression of DOPAn loss is rational, it will neither revert nor prevent the already occurred damage, as well as a repeated delivery of NBs to the CNS is not a suitable possibility.

Therefore, we took advantage of two important results obtained in this Ph.D. work. The major result of the thesis was demonstrating that TNF-α is the crucial player in DOPAn loss. As we noticed in Task 1 that curcumin (Curc) protects the Gunn rat brain against the toxicity of very high UCB levels also by normalizing TNF-α, and considering that Curc may be considered as a nutraceutical – lifestyle – prophylactic - chronic approach to Parkinson, we have begun to explore its effect in our ex vivo PD model.

Among the range concentrations of Curc tested, 5μM of the spice fully protected from rotenone-induced DOPAn loss, and the protection was lost at higher concentrations. Preliminary data seems to confirm that Curc also acts through *Tnfα* normalization. Future experiments are needed to unravel the mechanism related to TNF-α production and toxicity to DOPAn, as well as curcumin protection.

CHAPTER 1
INTRODUCTION

1.1.Bilirubin and its metabolism

Bilirubin is the yellow pigment of heme catabolism [1]. Daily formed mainly from the degradation of senescent red blood cells in the spleen [2] [3]. As depicted **in Figure 1.1.**, in the spleen, hemoglobin (Heme) derived from the red blood cells, is converted to unconjugated bilirubin (UCB) by the action of heme-oxygenase (HMOX) and biliverdin reductase (BLVR. BV= biliverdin), thus vehicolated to the liver by blood [3]. In the liver, the lipophilic UCB is converted to the hydrophilic conjugated bilirubin (CB, by the uridine-diphospho glucuronosyl transferase**:** UGT1A1), thereafter excreted in the intestine, where it is transformed in the uro- and sterco-bilinogens before excretion[2] [3]. Bilirubin in blood is present as: CB (or direct bilirubin, the minor part), and UCB (or indirect bilirubin), constituting the major fraction in physiological conditions. In turn, blood UCB is present in two forms: bound to albumin (UCB-A, the 99% of circulating UCB in physiological conditions) and the unbound-UCB (the so-called free bilirubin: Bf) [4].

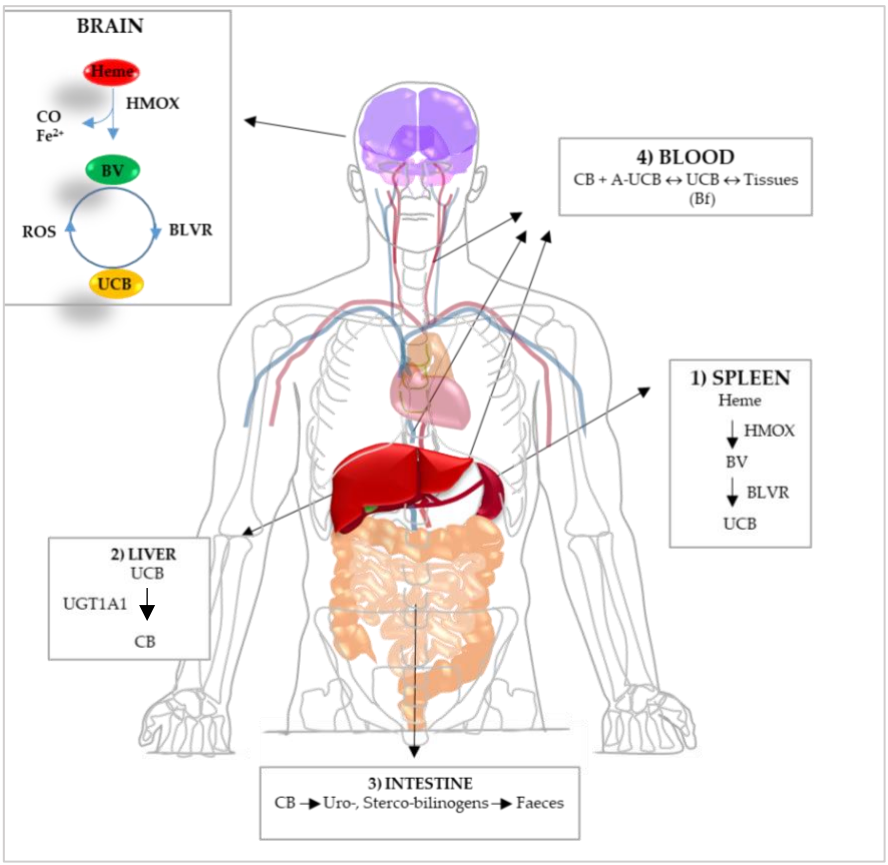

Figure 1.1. Bilirubin Metabolism Sites and [5]

The sum of CB and UCB forms the total serum bilirubin (TSB), routinely quantified in the clinic. Because of the molecular size of the complex, UCB-A is confined to the vascular lumen, while the small-lipophilic Bf easily diffuses across the cellular bilayers entering (in equilibrium with) the tissues [6], [7]. HMOX, BV, BLVR, and UCB (the Yellow Players: YP) are present also in the brain, where they have been hypothesized to act as a potential defensive mechanism toward neurological conditions by reacting on-demand to stressor/pathologic stimuli and producing UCB *in situ* [5], [8].

1.2.Neonatal Hyperbilirubinemia

When blood UCB level exceeds the serum albumin binding capability, the unbound portion of the pigment [free bilirubin (Bf), less than 0.1% in physiological conditions [9], [10] enters the tissues leading to the yellow coloration of the skin, so-called icterus (from the Greek = yellow, or jaundice from the French "jaune" = yellow). Icterus is common in neonates, and mainly due to : (I) the increased red blood cell turnover occurring after birth [11]–[13]; (II) the undeveloped UGT1A1 activity [14]–[16]; and (III) the quite total absence of the intestinal flora in neonates [17]–[19]. At present and in clinical practice, TSB is the value on which the indication of phototherapy (PT) is decided to prevent neurological damage. Nevertheless, due to the large and partly unpredictable variables able to interfere with the bilirubin-albumin binding and altering Bf, the recent advances making easier the quantification of Bf also in the clinic [20] offer the opportunity for a positive impact in the management of the condition.

Neonatal hyperbilirubinemia may present in two distinct: conditions (I) the so-called physiological neonatal hyperbilirubinemia, benign and self-resolving in 1 to 2 weeks [13], [21] not needing medical interventions, and (II) the severe neonatal hyperbilirubinemia, potentially leading to conditions ranging from mild-temporary deficits to permanent neurological alterations, recapped under the definitions of bilirubin induced neurological dysfunction (BIND) and kernicterus spectrum disorder (KSD) or even death [22]–[25].

Frequently considered an event of the past [26], the mortality of neonatal jaundice in the early neonatal period (0–6 days) still accounts for

1,309.3 deaths per 100,000 subjects worldwide [27]. The burden is highest in the low-middle income countries (LMIC), especially in Sub-Saharan Africa and South Asia, where neonatal hyperbilirubinemia is the 7th and 8th leading cause of mortality, respectively. In Western Europe and North America, neonatal hyperbilirubinemia accounts for the 9th and 13th leading cause of mortality, respectively [27].

While the TSB peak plotted as a function of the hours after birth is sufficient to estimate the risk of neurological sequelae in term infants [28], [29], additional factors are required in pre-term babies. In this population, common is the so-called "low bilirubin kernicterus", in which the neurological damage (symptoms and/or neuroimaging findings of brain damage) may be present even with peak TSB under the "safe level" [30]–[33]. Thus, rather than a specific threshold, in pre-term infants a range of TSB levels is more likely to be associated with the onset of neurotoxicity [28]. Both body weight and serum albumin level might be considered additional (possibly personalized) indicators of the developmental maturity of the infant, in addition to the gestational age, all affecting the Bf. In agreement with it, the presence of neurological dysfunctions or even death in extremely low birth weight pre-term infants has been associated with a high level of free/unbound bilirubin [34], suggesting Bf as a more sensitive predictor in respect to TSB [35], [36]. Bf has also been found as a good predictor of auditory dysfunctions in neonates with severe jaundice [37]–[40], as well as for the risk of apnea in pre-term infants [41], [42]. The bilirubin neurotoxicity affecting the auditory system including brainstem auditory nuclei, vestibular nuclei, and the auditory nerve, has been reproduced in the animal model of kernicterus (Gunn rat) [43], [44].

Nevertheless, the interplay between body weight, serum albumin level, Bf and the immaturity of the brain, is one of the reasons for the increased susceptibility to neuronal damage in the pre-term population even at lower bilirubin levels [31], still has to be fully unravelled.

1.2.1. The clinical manifestations

1.2.1.1. Full-term infants

In mature infants, lethargy, hypotonia, and poor sucking are the early non-specific sign of acute bilirubin encephalopathy (ABE), with hypertonia (retrocollis and opisthotonos), fever and high-pitched cry, apnea, and inability to feed representing the signs of advanced stage of ABE [22], [45].

The classical sign of the chronic and permanent clinical sequelae of bilirubin toxicity in the term population includes motor symptoms, hearing loss due to auditory neuropathy spectrum disorder (ANSD) with or without hearing loss, visual impairment (viso-oculomotor, which usually manifests as paralysis of upward gaze, and viso-cortical dysfunction), and dental enamel dysplasia [23], [45], [46]. Those symptoms present a large variability among individuals, recently recapped by the term KSD [22]. In addition, the neurodevelopmental sequelae, later described as spectrum of developmental disorder, have been considered as part of bilirubin-induce neurotoxicity disorders. Bilirubin-induced cognitive delay, developmental delay, specific speech and language disorder, psychological developmental delay, autism spectrum disorder are neurodevelopmental disorders (NDDs) that have been associated with bilirubin neurotoxicity [47]–[50]. However, those results mainly come from observational studies and no

plausible biological mechanisms for this association have been fully established, and the quality of evidence has not been carefully evaluated.

1.2.1.2.Pre-term infants

Pre-term infants less frequently exhibit the conventional bilirubin neurotoxicity signs, likely due to incomplete maturation of neuronal circuit and organization [30], [46], [51]. For this reason, pre-term infants are more at risk of late-diagnosis or even staying undiagnosed, which lead them to suffer from "silent morbidity and mortality" [46], [52]. Meanwhile, the auditory predominant sequelae are more common in pre-term neonates [30], [46], [51]. Pre-term infants with abnormal auditory brain evoke responses (ABR, the common clinical test performed among pre-term infant to evaluate brainstem function related to auditory neural pathway), also present more concurrent apneic events [40], possibly because both these conditions share the same neuronal location targeted by bilirubin. Moreover, increasing are the evidences reporting that hyperbilirubinemia in premature infants is followed by a higher number of apnea events [28], [41], [53].

Concerning the chronic and permanent clinical sequelae of bilirubin toxicity, pre-terms share the same burden as that of the full-term neonates [45], [46]. This may suggest that, under chronic toxic stimuli, inducing the most severe molecular perturbations and cell death [54]–[56], the developmental stage of brain development is irrelevant.

1.2.2. Mechanism of bilirubin induced toxicity

Although the molecular pathogenesis of bilirubin-induced neuronal cell injury is not completely understood, certain recurrent themes resonate in the literature on this topic and include:

1.2.2.1. Cell membrane disruption, mitochondrial damage and oxidative stress

Interaction of UCB with the cells occurs first at the cell membrane in which UCB can rapidly diffuses through membranes [57]. Bilirubin binds avidly to cell membranes, especially myelin-rich membranes, making neurons the principal target of bilirubin toxicity [58]. This process lead to the disruption of neuronal cell membrane structure [59]. These features showed to be associated with oxidative injury to membrane lipids and were not sensed in the more hydrophobic regions. The perturbation in plasma membranes disruption causes oxidative damage and disrupt transport of neurotransmitters[60] as well as on mitochondrial membrane [61]. Mitochondrial damage lead to impaired energy metabolism and apoptosis [60].

Moreover, the role of oxidative stress in bilirubin toxicity was investigated *in vitro* by the observation of an increased level of protein and lipid oxidation and by decreasing the level of antioxidant systems (glutathione)[62]. In different cell lines, bilirubin causes an accumulation of intracellular reactive oxygen species (ROS) that activate the antioxidant cell responses [63], [64]. *In vivo* study in Gunn rats showed high levels of lipid peroxidation by sulfadimethoxine-induced hyperbilirubinemia[65]. However, the inhibition of lipid peroxidation in this model was not able to

confer neuroprotection suggesting that lipid peroxidation is not the primary mechanism in bilirubin induced neuronal damage. This is in agreement with *ex vivo* study demonstrated by Dal ben et *al.* that anti-oxidant alone was not able to protect in bilirubin neurotoxicity indicating that oxidative stress in not a solely mechanism in bilirubin induced neuronal damage [66]. A study in a mice model of hyperbilirubinemia found that bilirubin induces oxidative stress and leads to DNA damage in the cerebellum [67].

Pro-oxidant effects suggested by the impairment of the antioxidant enzyme in brain were observed in a mouse model of Criggler-Najjar syndrome [68]. Pro-oxidant markers consequent to bilirubin exposure were investigated also in newborns and resulted higher in infants with hyperbilirubinemia when compared with normobilirubinemic infants[69]. Another study displayed increase level of malondialdehyde in hyperbilirubinemic infants compared to healthy infants, which significantly decreased after phototherapy [70].

1.2.2.2.Neuroinflammation

Bilirubin neurotoxicity is reported to be enhanced by severe systemic inflammation conditions. (e.g., sepsis, necrotizing enterocolitis, and fetal inflammatory response syndrome) [33]. This enhancing effect may be greater in ongoing maturation cells and preterm neonates [57], [71], [72]. In the experimental setting, chronic bilirubin-induced neuroinflammation (microglial activation) is reported in the Gunn rat and associated with brain development abnormality [46], [73], [74].

Toxic levels of bilirubin trigger an inflammatory response through the release of pro-inflammatory cytokines and the activation of MAPK pathway, triggering the cellular (microglia and astrocyte) release of tumor necrosis factor-α (TNF-α), interleukin (IL)-1b, and IL-6 to produce a proinflammatory milieu leading to cell death [33], [57], [58], [75]–[77]. An *in vivo* study also particularly identified TNFα and NFKβ as key mediators of bilirubin-induced inflammatory response [78]. UCB can cause the reactivity of rat cortical astrocytes and microglia, which in turn exacerbate inflammation [79] and increase BBB permeability by acting on endothelial cells and tight junctions [80]. While the secreted levels of TNF-α are in the same order either in astrocytes or in microglia exposed to UCB, those of IL-1β and IL-6 are increasingly produced by microglia, suggesting that microglia participate in astrocyte reactivity by UCB and corroborating microglia faster response to stimuli [81]. The release of pro-inflammatory cytokines, as well as ROS and NOS, can disrupt nerve terminals activity causing dysfunction and loss of synapses by UCB[82]. Therefore, UCB-induced inflammatory processes have emerged as a critical concept to understand the neurotoxic effects of UCB.

1.2.2.3. Glutamate neurotoxicity

Glutamate is the major excitatory neurotransmitter in the human central nervous system and plays important role in neural development. Bilirubin has been demonstrated to alter the glutamate pathway by excessive stimulation of glutamate release [83]. UCB has shown inhibition of protein kinase C activity in the neuron [84]. This activity is essential to maintain the synaptic transmission between neurons by an influx of Ca^{2+}

through a cation channel in the plasma membrane of the post-synaptic neuron. Membrane depolarization and glutamate binding to N-methyl-D-aspartate (NMDA, class 1) receptors triggered this channel opening. Moreover, UCB exposures to astrocytes decrease the glutamate uptake and prolong the presence of glutamate in the synaptic cleft[85]. This condition overstimulates the NMDA receptor (excitotoxicity), both *in vitro* [84], [86] and *in vivo* (hyperbilirubinemic Gunn rat [87]. Excitotoxicity triggers the excessive influx of Na^+, Ca^{2+}, Cl^- and water and induces neuronal cell swelling that later on will lead to apoptosis and necrosis[88].

1.2.3. Current therapeutical approaches and the caveats

1.2.3.1. Phototherapy

Phototherapy (PT) is the standard treatment for neonatal hyperbilirubinemia to convert bilirubin into water-soluble photoisomers that can be excreted through bile and urine [89]. Effective PT has progressively decreased the need for exchange transfusion (ET) in pre-term infants [90]. Recently, double-PT, which uses two light sources, has been demonstrated more effective for reducing TSB levels compared to single PT among pre-term infants [91].

PT is not a harmless treatment and overtreatment should be avoided. Side effects can include retinal damage, burns, disturbed circadian rhythm, conjunctivitis, rashes, dehydration, hyper- and hypothermia, loose stools, melanotic nevus, bronze baby syndrome, and electrolyte imbalances [92].

A study showed that based on *post hoc* analysis, aggressive PT increased 99% the probability of deaths among extremely low birth weight

(under 750 g) infants [93]. Moreover, moderate bilirubin levels may have clinically important oxidant benefits [94]. A low concentration of bilirubin scavenges reactive oxygen species (ROS), reduces oxidant-induced cellular injury and attenuates oxidant stress. Since the physiologic jaundice recognized as a protective mechanism for the newborn infant against ROS in the first days of life [92], aggressive, prophylactic PT looks to be counterproductive.

In any case, PT has significantly decreased the overall incidence of bilirubin neurotoxicity in most developed countries. Nevertheless, bilirubin neurotoxicity with lifelong neurological sequelae still occurs, and is a major problem in many areas of the world, especially in low- and middle-income countries [95], [96]. The access to health facilities, availability of PT, the possibility to measure TSB at the side of the newborn, and the variation in PT practices (such as the irradiance distances between infants and the light sources) have contributed to the sub-optimal result of this therapeutical approach [95], [97].

1.2.3.2. Exchange Transfusion

Exchange transfusion (ET) ET is the standard therapy for severe hyperbilirubinemia with ABE [98]. ET will be performed if the hyperbilirubinemia exceeds the specific level defined in clinical guidelines and exposes infants tot the risk of bilirubin neurotoxicity [29]. The incidence of severe hyperbilirubinemia adjusted according to the American Academy of Pediatrics thresholds for ET is low, involving ~1.2 per 1,000 live births [99]. The screening of hyperbilirubinemia and its underlying condition [e.g., rhesus and ABO isoimmunization, glucose 6 phosphate deficiency (G6PD)], the treatment of pregnant women who are Rh-negative with Rh-factor therapy, and the increased use of PT, have drastically reduced the number

of ET performed [100]. Nevertheless, premature infants have a tenfold increased risk of eventual bilirubin level meeting or exceeding thresholds for ET compared with term neonates [99].

Furthermore, most studies suggest that sick pre-term infants experience a wide range of complications from ET more frequently than term infants [26], [100]–[102]. In a large cohort study of >1,200 pre-term and term infants who received ET for hyperbilirubinemia, pre-term infants especially those ≤29 weeks of gestational age, have greater odds of death following ET compared to term infants [100].

Moreover, a 30 years prospective study reported that both unaffected hyperbilirubinemia and neurobehavioral affected hyperbilirubinemia subjects were equally received severe hyperbilirubinemia treatments (phototherapy and/or exchange transfusion) are equal in, suggesting that the current treatments are not totally able to prevent the KSD outcome [48].

1.2.3.3. Novel treatment strategies

Despite PT and ET have been widely accepted as standard treatments for severe hyperbilirubinemia to prevent ABE, the limitation of both therapies calls for new neuroprotective treatment.

Minocycline, the anti-inflammatory and antimicrobial drug, has been effectively demonstrated to prevent kernicterus in animal models of hyperbilirubinemia [103]–[105]. However, the use of minocycline in neonates is prevented due to its inevitable side effects including tooth discoloration, increased skin hypersensitivity to light, skin and nail hyperpigmentation, and skin rash [98].

Other drugs under study for treating hyperbilirubinemia is tin-mesoporphyrin (SnMP), the potent competitive inhibitor of heme oxygenase, the key rate-limiting enzyme in the catabolism of heme to bilirubin[1]. Reddy *et al.* have reported a very low birth weight infant with severe hyperbilirubinemia who, while awaiting an ET, underwent a SnMP single-dose treatment. After 10 hours of SnMP administration, TSB was gradually reduced (by 13%) and this eliminated the need for ET. No adverse effects were reported [106]. A clinical trial of SnMP in 213 newborns has shown the early use of a single dose of SnMP decreased the duration of PT, reversed TSB trajectory (mean TSB declined by 18%), and reduced the severity of subsequent hyperbilirubinemia. However, data on long-term risk of BIND still lack in this study [107].

1.3.Bilirubin Potential Protection in Parkinson Disease

Bilirubin, the long-known toxic yellow pigment, has been emerging with its plethora of therapeutic potentials.

The protective role of bilirubin is suggested in Gilbert-syndrome (a condition of mildly elevated bilirubin) subjects toward non-neurological conditions including cardiovascular disease, cancer, and metabolic syndrome [108]. In recent decades, mounting evidence has shown that bilirubin and its enzymatic properties (heme oxygenase and biliverdin reductase, known as yellow players) possess antioxidant, and anti-inflammation, and are even involved in signaling pathways in a wide range of conditions, including neurodegenerative diseases [108]–[110]. However, only a few data are addressing its protective effect in neurodegenerative disease , particularly in PD. In this section, the potential benefical effect of bilirubin in PD will be furtherly explained.

1.3.1. Parkinson's Disease

Found as a rare disorder in 1817 by James Parkinson, nowadays Parkinson's disease (PD) is evolving as the fastest growing neurological disorder and one of the leading causes of disability in the world [111]. Since the improvement of health care is followed by the world's aging population, PD is estimated to be a non-infectious pandemic, with the number of people affected doubling from 6.9 million in 2015 to14.2 million in 2040 [112]. Besides the increase of prevalence, years lived with the disability will be followed by increased different outcomes, including personal, social, and economic burdens that make PD need to be highly concerned [113], [114].

The significant motoric symptoms, tremor, rigidity, and bradykinesia are the consequences of progressive and selective diminished dopaminergic neurons in the substantia nigra pars compacta (SNc) [115], [116]. Moreover, reliable data on the presence of non-motoric symptoms (hyposmia, psychiatric symptoms, rapid eye movement sleep behavior disorder, dementia, pain, fatigue, constipation) have established that PD is not exclusively due to dopaminergic neuron loss but also involves non-dopaminergic neurons [116]. Although the etiology of PD has not been firmly established yet, advanced age, male sex, environmental factors (e.g. toxins and pesticides), and genetic traits have been recognized as relevant risk factors [114], [117], [118]. Multiple mechanisms including mitochondrial dysfunction, oxidative stress, neuroinflammation, and proteostasis disturbances, are increasingly appreciated as key determinants

of dopaminergic neuronal susceptibility in PD and are the feature of both familial and sporadic forms of the disease[119]–[121].

1.3.1.1.Pathogenesis

Although the pathogenesis of PD remains to be fully elucidated, many lines of evidence including postmortem, *in vitro*, and animal model studies unraveled the involved mechanisms of PD (depicted in **Figure 1.2**). These include:

a. Oxidative stress and mitochondrial dysfunction

Due to its high consumption of oxygen, extensive production of reactive oxygen species (ROS), and low level of antioxidant enzymes, the brain is vulnerable to oxidative stress [122], [123]. The involvement of oxidative stress in PD has been explored in post-mortem analysis with the detection of an increased amount of lipid peroxidation markers, carbonyl modification of soluble proteins, and DNA damage [124], [125]. Furthermore, clinical evidence showed the presence of oxidative stress markers in blood and cerebrospinal fluid [126]. In experimental settings, the link between oxidative stress and dopaminergic neuron degeneration has been confirmed. Oxidative stress not only has a direct effect on cellular damages but also influences the activation of signaling pathways leading to cell death [127].

Mitochondrial dysfunction is closely connected to the increased ROS formation in PD. ROS production is physiologic and powers neural activity and maintains cellular homeostasis. However, mitochondrial dysfunction, especially in the electron transfer chain, can lead to excessive

ROS production which is detrimental to cells [123]. On the other hand, ROS also drives further harm to the electron transport chain itself [128]. The deficiency and impairment of mitochondrial complex-I activity, the vital component of the electron transport chain, was found in postmortem studies and dopaminergic cell loss-induced animals by toxin and pesticides [39,40]. The defects of mitochondrial complex-I of the respiratory lead to degeneration of neurons due to lack of ATP production [127].

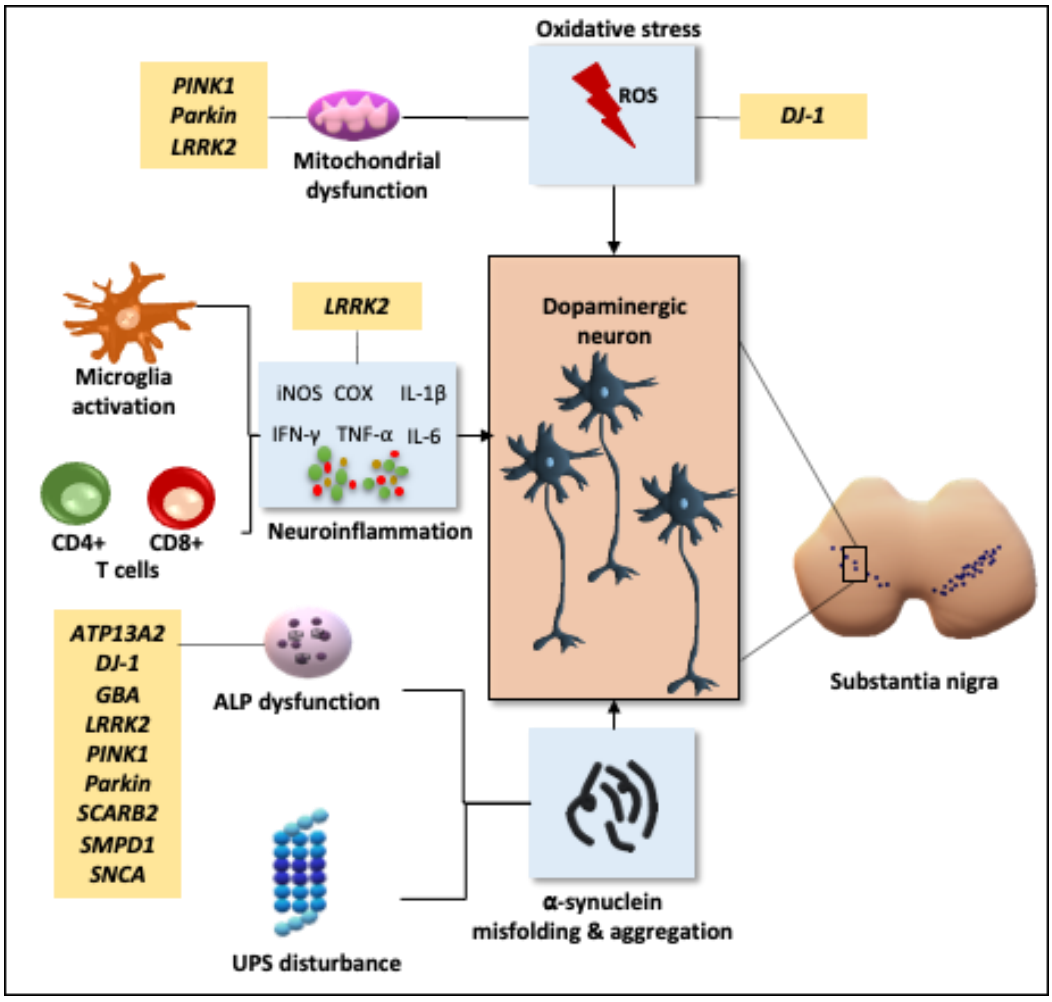

Figure 1.2. The involved mechanism in the pathogenesis of Parkinson's disease. Multiple mechanisms are known to be involved in the pathogenesis of dopaminergic neuron loss including oxidative stress, neuroinflammation, α-synuclein misfolding and aggregation, and genetic influence. Abbreviation: ALP,

autophagy lysosomal pathway; UPS, ubiquitin-proteasome system; iNOS, inducible nitric oxide synthase; COX, cyclooxygenase; TNF-α, tumor necrosis factor-α; IFN-γ, interferon-γ; IL, interleukin -6 and -1β; *DJ1,* Daisuke-Junko-1; *Pink1,* acid protein phosphatase and tensin homolog (PTEN)-induced kinase 1; *ATP13A2,* ATPase type 13A2; *MAPT,* microtubule-associated protein tau; *GBA,* glucocerebrosidase; *SNCA,* α-synuclei, *LRRK2,* Leucine-rich repeat kinase 2; *SMPD1,* acid-sphingomyelinase; *SCARB2,* scavenger receptor class B member 2. [5]

The reasons for dopaminergic neuron SNc vulnerability to mitochondrial dysfunction have been hypothesized to be related to (i) the size and complexity larger than other types of neurons in the brain demands high rates of ATP production to keep resting membrane potential, induce action potential, and allow synaptic transmission, (ii) distinctive physiology of action potential which distinguishes SNc dopaminergic neuron from the majority of neurons in the brain, and (iii) the reliance upon dopamine as a neurotransmitter which is considered as a potentially toxic compound if accumulating into the cytosol [121], [131], [132].

b. Neuroinflammation

Neuroinflammation is one of the main features in PD has been shown in clinical studies as well as experimental settings [133]–[135]. Microglia activation seems to be the primary mediator for the inflammatory process in PD. Microglia have been documented for initiating inflammatory responses in PD [120], [136]. The activation of microglia is due to α-synuclein, as a danger-associated molecular pattern (DAMP), which can directly trigger microglial activation and initiate sterile inflammatory

processes [137], [138]. For instance, in primary cultures, α-synuclein mediates a dose-dependent activation of microglia [139].

α-synuclein is not the only stimulant for microglia activation as multiple agents have been demonstrated to have a microglia activator effect, including debris of degenerating neurons [140]. Additionally, the microglial activation is significantly exacerbated by not only rotenone treatment but also lipopolysaccharides (LPS), indicating multiple mechanisms responsible for microglia activation [141], [142]. Shor-term activation of microglia provides neuroprotection, whereas long-term activation leads to the neurodegeneration process. Noteworthy, activated microglia have been demonstrated as a critical ROS source, further indicating that the inflammation process induces oxidative stress and *vice versa*.

Microglia activation promotes the activity of pro-inflammatory enzymes (such as inducible nitric oxide synthase – NOS and cyclooxygenase – COX) and the release of the pro-inflammatory cytokines, such as C-X-C motif chemokine ligand 12 (CXCL12), tumor necrosis factor-α (TNF-α), interferon-γ (IFN-γ), interleukin (IL)-6 and IL-1β [143]. Moreover, the inflammatory responses of microglia are amplified by astrocytes senescence in the aging brain [144], [145].

Additionally, the involvement of the adaptive immune system has been observed in PD through the presence of CD8+ and CD4+ T cells in the brain in both postmortem human PD specimens and the MPTP mouse model [146]. This conclusion has been supported by Sulzer et al., which found that α -synuclein peptides acted as antigenic epitopes and induced T cell response in PD patients [147]. Finally, a longitudinal study showed that

in PD patients, a more 'pro-inflammatory' components profile (TNF-α, IL1-β, IL-2, and IL-10) in the serum is associated with a faster motor syndrome progression and more cognitive decline [148].

c. Disruption of cellular proteostasis

Protein clearance is an intracellular defense mechanism to ensure protein homeostasis by rapid detection of altered protein and its elimination [149]. Molecular chaperones, the ubiquitin-proteasome system (UPS), and the autophagy-lysosomal pathway (ALP) are the essential pathways that facilitate the clearance of abnormal proteins [150], [151]. UPS selectively shatters short-lived proteins and misfolded or damaged proteins intracellular, whereas ALP degrades the longer-lived proteins, cellular components, and organelle through the lysosomal compartment [152], [153]**.** The proteasome dysfunction exacerbates protein aggregates in PD. Convincing evidence showed that α-synuclein deposition, which later becomes Lewy bodies inclusion in PD subjects, is the consequence of the failure of those degradation pathways [152]. The decrease in UPS activity has been explicitly reported in the substantia nigra of PD brain [154], [155]. It has been demonstrated that the presence of misfolded protein UPS failure in dopaminergic neurons was induced by the expression of mutant α -synuclein [156].

d. Genetic influence

Although the familial forms of PD account for only 5-15% of the cases, these cases have offered essential insights regarding genetic influences in PD pathogenesis [157]. The genetic changes play a role in

molecular pathways, including α-synuclein proteostasis and degradation, mitochondrial function, oxidative stress, and neuroinflammation. Mutation in *DJ1* (Daisuke-Junko-1), *Parkin*, *Pink1* (acid protein phosphatase and tensin homolog (PTEN)-induced kinase 1), and *ATP13A2* (ATPase type 13A2) are responsible for monogenic PD forms and the other genes, including *MAPT* (microtubule-associated protein tau), *GBA* (glucocerebrosidase,), *APOE* (apolipoprotein E), have been associated with an increased risk of developing PD. Meanwhile, *SNCA (*α-Synuclein) and *LRRK2* (Leucine-rich repeat kinase 2) plays a role not only in monogenic form but also as risk factors of PD [158], [159].

The mutation in *SNCA*, the gene encoding for α-synuclein, has been known as the cause of heritable forms of PD by leading to α-synuclein dysfunction and aggregation [160]. Moreover, single nucleotide polymorphism in this gene is associated with the risk for sporadic form [161]. Several genetic mutations related to autophagy lysosomal pathway including *LRRK2, GBA, SMPD1 (*acid-sphingomyelinase), *SNCA, PINK1, Parkin, DJ1, SCARB2 (*scavenger receptor class B member 2) are involved in PD [159]. Some of these genes encode lysosomal enzymes, whereas others correspond to proteins involved in transport to the lysosome, mitophagy, or other autophagic-related functions [162]. Mutations in *PINK1* and *Parkin* involve mitophagy impairment, accelerate the accumulation of defective mitochondria and lead to dopaminergic neuron loss [163]. Mutations in *DJ1*, a gene that encodes a putative antioxidant, are related to enhanced oxidative stress. Recent advances in understanding the genetic influence in PD have uncovered that a gene mutation can be related to multiple molecular pathways. For example, *LRRK2* mutations are not only

associated with autophagy and lysosomal degradation but also neuroinflammation, mitochondrial dysfunction, and neurotransmission [164].

1.3.1.2.Challenges in Management of PD

Despite the numerous efforts directed toward diagnostic modality, the diagnosis of PD still rests on clinical manifestation. Since the prodromal symptoms of PD are non-specific including rapid eye movement, sleep behavior disorder, loss of smell, constipation, urinary dysfunction, orthostatic hypotension, excessive daytime sleepiness, and depression, most PD patients get diagnosed after the cardinal motor symptoms appear. The motor manifestations become apparent after dopaminergic neuron loss in the substantia nigra pars compacta reaches about 40%-50% [165].

The most used therapy is mainly to replace and boost the existing dopamine. Levodopa, the dopamine precursor, is the most frequently used to alleviate motor symptoms. It is usually combined with carbidopa for blocking its metabolism in the periphery and increases its bioavailability in the central nervous system [166]. Levodopa offers significant symptomatic advantages, but its long-term use is followed by motor complications (dyskinesia and motor fluctuation) [167]. Dopamine agonists (pramipexole, ropinirole, and rotigotine), the stimulants for dopamine receptors in the central nervous system, are suitable for the management of mild to moderate PD. However, the side effects such as orthostatic hypotension, hallucinations, confusion, leg edema, and as impulsive disorder have been frequently reported in individuals under dopamine agonist therapy [164], [168]. Catechol-O-methyl transferase inhibitors (entacapone) and

monoamine oxidase aldehyde dehydrogenase B (MAO-B) inhibitors (rasagiline and selegiline) inhibit enzymes involved in the breakdown of levodopa and dopamine [169]. Anticholinergic medications (trihexyphenidyl and benztropine) are not effective in treating bradykinesia but may decrease rigidity, dystonia, and tremor. For the young individual, caution is a must because of the potential of adverse events, particularly relating to cognition [169].

Deep brain stimulation targeting either the subthalamic nucleus or globus pallidus internus has evolved as an important therapy for PD and is usually performed in a relatively early-onset patient [166], [167]. Despite deep brain stimulation being considered as well tolerated, complications due to the surgical techniques such as intracranial hemorrhage, high chance of re-surgery caused by hardware-related complications or infections, and microlesion effects due to electrode penetration (affect cognitive states and psychiatric conditions) are reported [170].

Cell therapy by using pluripotent stem cells, including human embryonic stem cells (hECs) or induced pluripotent stem cells (iPScs), is emerging as a novel experimental approach to tackle this problem. iPScs are preferable over hECS due to similar differentiation potential but fewer ethical concerns [118]. Interestingly, iPScs have been explored as personalized medicine in PD because of its autologous entity (gained from a patient donor), which lowers the chance of graft rejection [169], [171]. However, several issues present in the application of iPScs, including the risk of tumor formation like in hECs implantation and the heterogeneity of iPScs due to the genetic modification, variable transgene expression levels, incomplete reprogramming and reactivation/lack of inactivation of the

transgeness, and. Moreover, PD-patient-derived iPScs may carry mutations and could be susceptible to developing PD-like features [172], [173]. Those issues might be corrected by using genomic editing, particularly CRISPR-Cas9, as performed in iPScs PD model [174].

So far, it is undeniable that all the fore-mentioned pharmacologic and non-pharmacologic approaches can reduce motoric symptoms by targeting the remaining dopaminergic neuron to produce more dopamine, stimulating the dopaminergic receptor, inhibiting the breakdown of dopamine, or replacing dopaminergic neurons. However, none of the intervention strategies mentioned above has a disease-modifying effect of encountering molecular mechanisms involved in PD pathogenesis [116], [165].

1.3.2. Bilirubin as a promising therapy in Parkinson's Disease

Bilirubin is the yellow product of hemoglobin catabolism (**Figure 1.1.**), clinically known as a serum marker of hepatic diseases. Recently, bench-based and epidemiological data point to a health-promoting effect of the pigment toward on chronic diseases[108].

A new interesting perspective in the context of CNS pathologies has also emerged. From clinical studies, low bilirubin level has been associated with multiple neurological conditions including Alzheimer disease, multiple sclerosis, stroke, amyotrophic lateral, and migraine underpinning the beneficial role of bilirubin in CNS [175], [176]. Meanwhile, in context of PD itself, a meta-analysis from eight published clinical studies al showed that the serum bilirubin concentration significantly increased in PD patient

suggesting the involvement of bilirubin in PD pathogenesis and triggering the cause-effect studies via experimental models [177].

Recent data reported the expression and activity of the enzymes involved in UCB production (the yellow players -YPs: HMOX - heme oxygenase 1,2; BV -biliverdin; BLVR - biliverdin reductase A- Figure 2A) in the CNS, making the brain able producing UCB independently from the blood supply. Importantly, the *in situ* UCB production has been shown to increase cellular resistance to damage [3], [108]. Moreover, both HMOX1 and BLVRA, the two key enzymes in UCB production, possess multiple binding sites for transcription factors on the promoter region of the gene, making them promptly inducible by a wide range of stressors stimuli, including those characterizing the neurological conditions [3], [109], [178]–[181]. Finally, each YP may act directly or indirectly (thought signaling pathways) on key biological functions, expanding the potential for protection [182]. These features collectively make the YPs a homeostatic and defensive system that enhances the capability of a neuronal cell to protect itself under a stress condition or even make the CNS independent from the serum UCB level.

Based on epidemiological and experimental data, a minimal increase in the bilirubin level has been suggested to be benefic for both extra-CNS and CNS chronic diseases acting as an anti-oxidant; on immunity and inflammation; on the cell cycle, proliferation, differentiation, migration, and apoptosis; as well as controlling glucose and insulin homeostasis [3], [108], [109], [178]–[181], [183].

1.3.2.1.Potential mechanisms of action

The study of YPs neuroprotection toward PD is at its beginning. Nevertheless, some preliminary interesting information on YPs protective action on the pathological mechanisms of ongoing PD, may be extrapolated from the literature (**Table 1.1**).

a. Antioxidant

Since '80, UCB (or indirect bilirubin in clinical words) is known as the most powerful endogenous antioxidant [6], [184], mostly accounting for the preferential scavenging of lipophilic radicals that can attack lipid membranes [4], [7]. During the ROS/RNS (reactive oxygen / reactive nitrogen species) scavenging activity [185]–[187], UCB is oxidized back to BV, in turn rapidly reconverted to UCB by the BLVRA. As a result, nano-molar concentrations of UCB can neutralize 10,000 times higher levels of cellular ROS [7], [183], without increasing the UCB cellular level to a toxic concentration (Figure 2A). In cell cultures, UCB has been shown to activate the anti-oxidant response genes [101,102]. Moreover, it promotes additional cellular defense against redox stress. Indeed, by reducing ROS, UCB may inhibit the NMDA excitotoxicity, preventing neuronal death [190]. Anti-oxidant defenses (SOD and HMOX1), as well as the protective neuroglobin expression which reduces mitochondrial dysfunction, cytochrome C release, and apoptosis [103,104], and ferritin synthesis (chelating iron) [193], are also induced by intracellular free heme. Besides, BV may scavenge RNS [194], lowering DNA damage [188], [195], and inhibiting lipid peroxidation with an efficacy 2-fold higher than α-tocopherol [196]. As a result, glutamate excitotoxicity [197], inflammation [198], and cell death by

apoptosis [192] are reduced. Despite not studied in the CNS context, BLVRA may also contribute to cellular protection by migrating into the nuclei and acting as a transcription factor on the genes involved in the cellular antioxidant response, immunity, inflammation, autophagy, apoptosis, hypoxia, tumor resistance, etc. [108], [199].

On the other side, the rapid conversion of BV to UCB [200], accumulation of heme and iron (by excessive activation of HMOX1) may lead to brain dysfunctions by including a cell energy failure, increased ROS/RNS production and DNA damage, inhibition of the antioxidant defenses, gliopathy, present in many aging-related neurodegenerative brain disorders, glutamate neurotoxicity, and cell death [61], [67], [109], [195], [201]–[208].

b. Inflammation

Inflammation is the second critical pathological mechanism known to be modified by the YPs. Cytokines production (IL8, TNF-α) is induced by heme, UCB and iron, inducing the neutrophil migration, vascular permeability and edema [203], [204], ER stress[209], activating the microglia [204], and finally reducing the cellular viability [75], [76], [209].

On the other side, BVLRA (acting as a transcription factor), UCB and CO may inhibit the inflammation (TNF-α, Il6, complement, and T-cell response), inhibits NOS, diminish endothelial cell apoptosis, and preventing the alteration of the blood-brain barrier (BBB) [4], [199], [210]–[218].

Table 1.1. Experimental evidences of YPs protective action on the pathological mechanisms of ongoing PD (reviewed in Jayanti *et al*.[5])

Pathological mechanism in PD	**YPs (protective effect)**	**Ref**
REDOX	UCB (↓) Heme (↓) BV (↓)	[6], [184] [7], [183] [210], [219] [193],[194]
Anti-oxidant enzymes	UCB (↑) Heme (↑) BLVRA (↑)	[220], [221] [210], [219] [108], [199]
Carbonylation & lipid-peroxidation	Membrane protection by scavenging lipophilic radicals (↑) BV (↓)	[4], [7], [222] [196]
DNA damage	BV (↓)	[188], [223]
Mitochondrial disfunction	Heme (↓) Heme: cofactor for the mitochondrial electron transport chain (complexes II, III, IV)	[210], [219] [205]
PINK1/DJ1; LRRK2; SNCA; PARK2	No direct experimental data are yet available. Further, devoted studies are needed.	
INFLAMMATION		
Microglia and astrocytes activation	No direct experimental data are yet available. Further, devoted studies are needed.	
α-synuclein		
iNOS & COX	BLVRA, UCB, CO (↓)	[4], [199], [210]–[218]
TNFα	BLVRA, UCB, CO (↓)	[4], [199], [210]–[218]
IL6	BLVRA, UCB, CO (↓)	[4], [199], [210]–[218]
IL1β; IFNγ ; Il2; IL10; CXCLY2	No direct experimental data are yet available. Further, devoted studies are needed.	
CD8+ & CD4+ T cells	BLVRA (↓) BLVRA, UCB, CO (↓)	[108], [199] [4], [199], [210]–[218]

LRRK2; SNCA	No direct experimental data are yet available. Further, devoted studies are needed.	
PROTEIN DEGRADATION		
UPS	No direct experimental data are yet available. Further, devoted studies are needed.	
Autophagy	BLVRA (↓)	[108], [199]
LRKK2; GBA; SMPD1; SNCA; PARK2; PINK1/DJ1; SCARB2	No direct experimental data are yet available. Further, devoted studies are needed.	
GLUTAMATE TOXICITY	UCB (↓) BV (↓)	[190] [197]

UCB: unconjugated bilirubin; Heme: Hemoglobin; BV: biliverdin; BLVRA: biliverdin reductase; PINK7/DJ1: acid protein phosphatase and tensin homolog (PTEN)-induced kinase 1; LRRK2: Leucine-rich repeat kinase 2; SNCA: α-Synuclein; PARK2: Parkinson juvenile disease protein 2; CO: carbon monoxide; HMOX1: heme oxygenase 1; iNOS: inducible nitric oxide synthase; COX: Cyclooxygenase; TNFα: tumor necrosis alpha; IL: interleukin; CXCL12: C-X-C motif chemokine ligand 12; UPS: unfolded protein resonse; GBA: glucocerebrosidase; SMPD1: acid-sphingomyelinase; SCARB2: scavenger receptor class B member 2.

1.3.3. The YPs Modulation in Parkinson Disease (PD)

A two phases HMOX1/UCB modulation, the early induction interpreted as tentative protection toward the ongoing oxidative stress, and the late phase as the failure of the protection is hypothesized. Several pieces of evidence are available.

1) YPs induction in autopsy from PD patients has been described. HMOX1 increased reactivity has been found in the dopaminergic neurons (DOPAn), microglia, and astroglia of the substantia nigra (SN) and in neurons of the neo-cortex presenting Lewy bodies [224]. Since HMOX1 is a redox sensor and an activator of the anti-oxidant response genes, the up-

regulation of HMOX1 in the site of the lesions in PD has been suggested to belong to an early tentative reaction toward the ongoing redox imbalance by the *in situ* production of UCB. 2) In agreement with the protection, in rodent and *in vitro* models, the induction of HMOX1 has been correlated with decreased inflammation and increased DOPAn survival [225], [226] . Interesting for the potential diagnostic applications is the correlation reported between the clinical stage of PD, the serum level of bilirubin (TSB), and HMOX1 induction. 3) Based on the data obtained by Lee [229] and Macias-Garcia [230], a higher TSB (as well as its precursor BV - [231]), is present at the onset of PD, together with an increased presence of UCB degradation products in the urine of PD patients, suggesting the induction of HMOX1 [232]. 4) Notably, patients with higher TSB present less severe symptoms, and needs less L-DOPA administration [233]. And 5) patients receiving L-DOPA, able to improve the symptoms of PD, have a significantly higher TSB *vs.* both drug-naive PD and controls, suggesting that L-DOPA might reduce the redox imbalance, allowing HMOX1 to produce enough bilirubin for alleviating the disease [234]. 6) Supportive are also the recent finding correlating genetic polymorphisms on HMOX genes with PD incidence. Genetic variants on the HMOX1 gene, leading to its decreased transcription and inducibility (thus a reduced UCB/BV production), and HMOX2 (the neuronal constitutive form) have been noticed to be significantly more frequent in subjects with the disease [235]. Specifically for the HMOX1 variants, a correlation with a more early onset of the symptoms has been reported [224]. This data may support the potential protective role of an increased UCB production in the brain. Unlikely the cited paper did not report the TSB level in the PD and control

groups. Based on the described possible role as an early marker of PD, the increase of HMOX1 in saliva has been proposed as an easy-to-do, non-invasive marker of this neurodegenerative condition [236].

On the other side, 7) the up-regulation of HMOX1 has been clinically documented to increase the *in situ* iron deposition, enhance the pro-oxidant milieu, and finally worsening the damage [233], [234], [237]. The data have been supported by experimental models, where the excessive HMOX1 induction, not only will increase the iron deposition in the CNS, but has also been suggested to enhance the oxidation of L-Dopa, an additional highly pro-oxidant molecule [238], [239]. 8) As suggested for Alzheimer's disease, under a condition of extreme redox stress, BLVR might be inactivated, becoming unable to foster the brain with UCB, and finally leading to the failure in protection [240]. 9) In agreement, in the clinical setting, the TSB level in PD patients will decrease with the increase in the severity of the disease. This negative correlation has been interpreted as the failure of the tentative defense with the consumption of UCB [230].

The unraveling of the interplay of YPs with PD progression is currently impossible in the clinical setting due to the late (symptom-based) diagnosis. The confirmation of what was described above, and the dissection of the causative mechanisms from the consequential ones, requires experimental models able to mimic the time course of the disease from the pre-clinical stages, through the stages corresponding to an early diagnosis, to severe disease. Recently, an *ex vivo* model of PD reproducing the whole disease progression in 96 hours has been developed by challenging brain organotypic cultures of substantia nigra with rotenone, a pesticide responsible for PD in'80. This model confirms HMOX1 as one of

the first genes up-regulated in PD (3hours, together with Tnfα and Cox2). The HMOX1 modulation proceed even the DOPAn demise usually detected at the diagnosis in PD patients (-40% vs. controls, 24hours), supporting the potential of the clinical use of HMOX1 as a diagnostic tool [135]. The further use of the model, might allow to demonstrate the effects of an increased UCB in protection against DOPAn loss.

Table 1.2. Evidences of YPs modulation in PD (review in Jayanti *et al*.[5])

YPs	Modulation	Ref
HMOX1	(↑) In DOPAn, microglia, and astroglia of the SN.	[226], [233],
	(↑) In neurons of the neo-cortex with Lewy bodies.	[234], [237]
	(↑) *In vitro* model of PD.	
	Genetic variants of HMOX1 (leading to a reduced transcription and induction of the gene), are more frequent in PD subjects and correlate with an early onset of the disease.	[226] [226], [240] [226]
HMOX2	Genetic variants of the neuronal constitutive HMOX2 (leading to a reduced transcription) are more frequent in PD subjects.	[241]
TSB	(↑) In early clinical stages of PD.	[226], [233]
	(↑) In PD patients with less severe symptoms.	[233]
	(↓) In late/more severe clinical stages of PD.	[226], [242]

HMOX: heme oxygenase; DOPAn: domaninergic neurons; SN: substsntia nigra; PD: Parkinson disease; TSB: total serume bilirubin

1.3.4. Future Prospective: bilirubin as a treatment in PD and its modulatory/delivery system using nanoparticles

From the general knowledge about UCB and the specific information in PD, two point seems clears: a) UCB may protect if given in the non–toxic range, and b) HMOX1 hyperactivation looks inevitable and worsens the ongoing damage. The critical point is how to reach the correct (protective) amount of UCB avoiding the hyperactivation of HMOX1 (**Figure 1.3**).

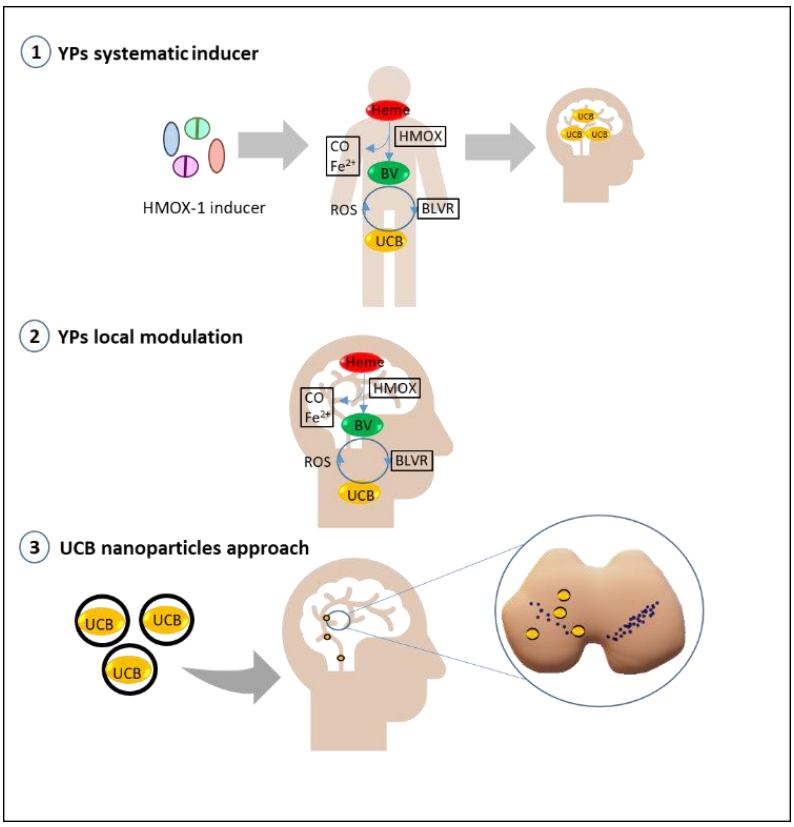

Figure 1.3. Illustration of possible bilirubin modulatory/delivery system in the brain. YPs: Yellow players; HMOX: Heme hoxygenase; BLVR: biliverdin reductase; UCB: unconjugated bilirubin; ROS: reactive oxygen species. [5]

A pharmacological approach targeted in a systemic (whole-body) modulation of the YPs looks the most obvious and is already primarily evaluated in extra-CNS diseases [243]–[245] by inducing HMOX1 and increasing TSB.

A second approach might consist of modulating the YPs directly in the CNS. This approach looks limited beacuse HMOX1 is already induced at the time of the diagnosis. Thus, inducing even more HMOX1 will possibly enhance the side effects and accelerate the disease progression.

A third exciting alternative might be the use of nanoparticles. Nanoparticles designed explicitly for brain delivery (of mRNA, small peptides, chemotherapeutic agents, etc.) are under evaluation and are of routine clinical use as agents in magnetic resonance, magnetic field-directed drug targeting to tumors across the blood-brain interfaces (BBI), and for direct anti-tumor treatment by magnetic hyperthermia [246]–[252]. The potential ways of administration are both invasive (e.g.: intracranial, after the temporary opening of the BBI), marginally invasive (i.p – in animals; i.v.), or non–invasive (nasal route) [247], [249]. Size and charge, selection of the material for the scaffold, engineering of the particles with proteins/antibodies/metals, and/or engineering of the nanoparticles able to use the transporters highly expressed on the BBI and neuronal cell surface, used as Trojan horse [247], [249], [250] are under evaluation. In neurodegenerative diseases (NDs), one of the additional vital points is the need to counteract redox tress, a primary pathological mechanism in NDs [251]. Interestingly, a pro-oxidant milieu may be an advantage, by "opening" the cargo and allowing the release of the principle on the site of the lesion [252].

In the context of PD studies (animal models), nanoparticles delivery of dopamine and levodopa, ropinirole and apomorphine (dopaminergic agonists), and growth factors (NGF, GDNF) have been tested, reporting positive results in term of reaching the target, the release of the content, good efficacy, and tolerance [246]. Hence, the basis for developing UCB-coated nanoparticles possibly loaded with additional therapeutic factors, seems to be a consistent way to explore.

1.4.Curcumin and its therapeutical potential

Curcumin, a low molecular weight, lipophilic, major yellow natural polyphenolic, is extracted from the rhizome of the herb *Curcuma longa*, which belongs to the *Zingiberaceae* family [253]. *Curcuma longa* is a herb that mostly flourishes in tropical as well as in other Indian regions and has multipurpose use as a spice, food preservative, coloring source, and Ayurverdic medicine [254].

Curcumin is categorized as a "generally recognized as safe" (GRAS) compound (EMA and FDA) with no demonstrated side effects even at high dosages[255]. Curcumin has been investigated as an active therapeutic agent for a wide array of diseases including cardiovascular, pulmonary, skin disorders, liver disorders, fatigue, neuropathic pain, bone and muscle loss, and anxiety, due to its well-reported biological activities which include anti-inflammatory, anti-proliferative, anti-angiogenic, pro-apoptotic, anti-oxidant, wound healing, anti-cancer, anti-viral, and anti-diabetic effects [256]–[258].

It was suggested that curcumin alleviates oxidative stress, and inflammation in chronic diseases through the Nrf2-keap1 pathway. Nuclear

factor erythroid-2 related factor 2 (Nrf2) is highly related to oxidative stress in inflammation [259]. Through activation of Nrf2-Keap1 pathway which leads to the increase of antioxidant enzymes, curcumin reduces malondialdehyde (MDA) and ROS levels and promotes cell survival in *in vitro* study [260].

Curcumin has anti-inflammatory properties by inhibiting the pro-inflammatory transcription factor (NF-κB) [261]. It also activates peroxisome proliferator-activated receptor gamma (PPAR-γ), which leads to inhibition of pro-inflammatory cytokine along with expression and release of TNF-α [262]. Curcumin may also be a TNF blocker from *in vitro* and *in vivo* studies by binding to TNF directly [263], [264] . Moreover it also found to suppress IL-1β secretion [265].

1.5.The *ex vivo* model of Parkinson Disease

Lack of representative experimental model is one of the reasons for poor understanding of the early mechanisms of DOPAn demise in PD leading to difficulty in finding effective disease-modifying therapy [266], [267]. The considered ideal criteria of PD model are the measurable DOPAn changes, the appearance of cardinal symptoms, the presence of neuropathology, the type of mutation in the genetic model and the duration of reproducibility of a model to allow rapid and less costly screening of therapeutic agents [267]. So far, not a single type of model, neither toxin-based models nor genetic models, is able to reproduce all these characteristics at once [266], [267] .

Nonetheless, recently, the *ex vivo* PD model using organotypic brain culture of substantia nigra (OBCs-SN) treated with a low dose of rotenone

was able to reproduce the slow progression of DOPAn loss, allowing the time courses mapping of early and late events [135]. Noteworthy, this model gives an important evaluation window at 24 hours post treatment in which also the grade of DOPAn loss in line with clinical human PD (the stage of cardinal PD symptoms are obvious) [135], [262] (**Figure 1.4**).

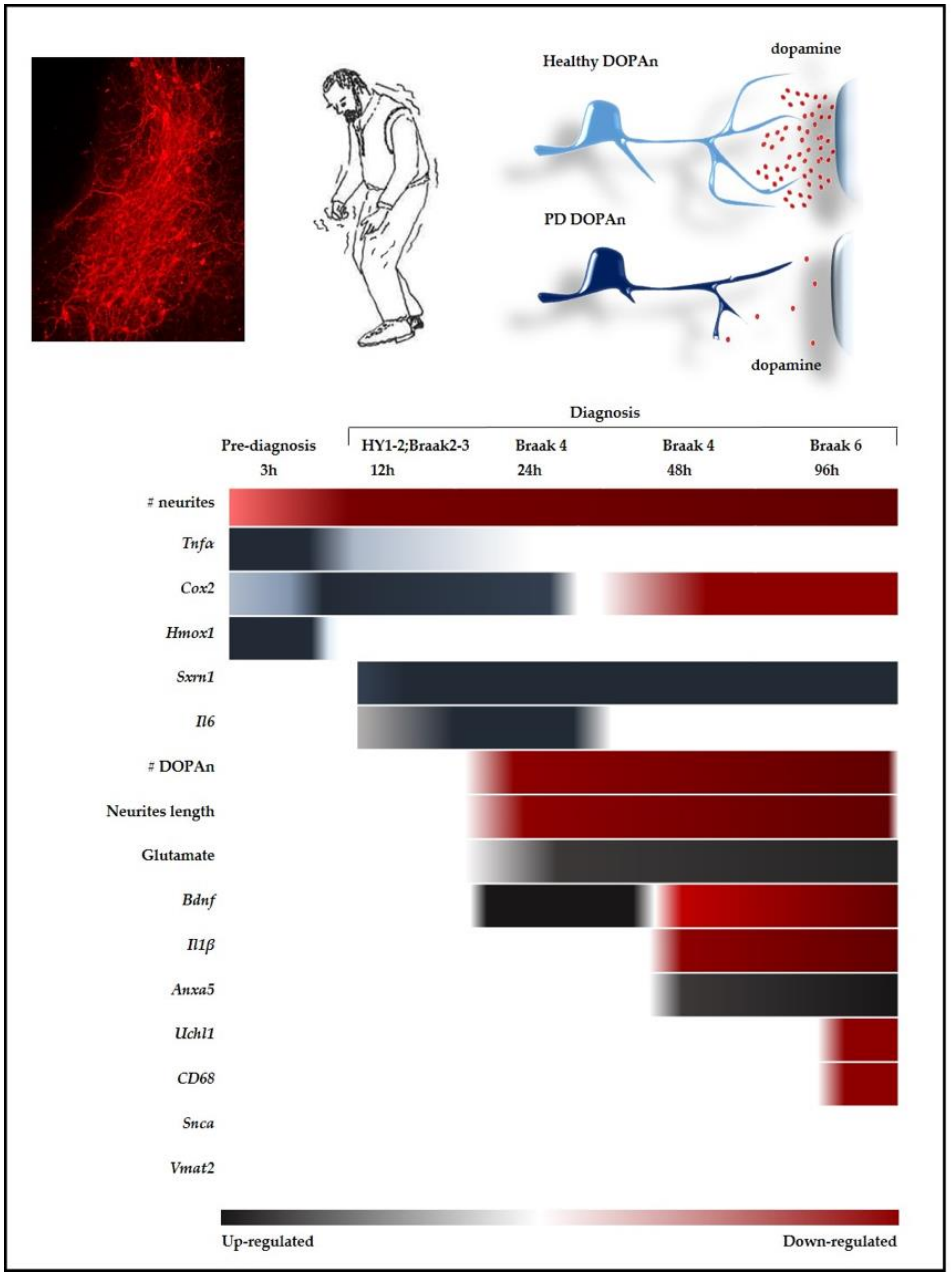

Figure 1.4. Temporal alterations of the markers in *ex vivo* PD model [135].

The OBCs becomes a representative of the physiologically relevant three-dimensional model of the brain that can maintain its architectural and cellular heterogeneity [270]. These benefits bring OBCs as an important bridge between cell lines and *in vivo* models, especially in the evaluation of novel therapy[271]. Moreover, the advantages of the model in reducing not only the number but also the sufferance of animals is an essential ethical concern [272].

CHAPTER 2

AIMS OF STUDY

Bilirubin exhibits a Janus face for owning not only toxicity but also protective effect in neurological conditions. Therefore, we study both effects by dividing the project into two tasks with the following aims of the study.

2.1 TASK 1 – The Effects of Curcumin in Bilirubin-induced Neurotoxicity in Severe Neonatal Hyperbilirubinemia Model

In this work, we aimed to explore the efficacy of curcumin treatment in Gunn rats (a model of severe neonatal hyperbilirubinemia). We assessed histopathological and behavioral changes as parameters of kernicterus spectrum disorder (KSDs) in Gunn rats. To unravel the mechanism of protection, we investigated the effects of curcumin on the main molecular effectors involved in bilirubin brain damage.

2.2 TASK 2 – Bilirubin Neuroprotection in an *ex vivo* Parkinson's disease (PD) model

Concerning the need for disease-modifying therapy in PD, this work was conducted to investigate UCB protective effect in an *ex vivo* PD model [135]. The aim was achieved by performing dopaminergic neuron (DOPAn) count and molecular investigation of early mechanisms triggering the DOPAn loss [135].

Our result show a promising protective effect of UCB in PD. This work continued to explore the feasibility of delivering UCB into the CNS by nanobubbles (NBs). For this purpose, we screened a panel of NBs formulations for their safety. Then the potential protection toward PD of the most suitable candidates was studied in the *ex vivo* PD model.

Finally, to explore a potential prophylactic approach to PD, and by taking advantage of curcumin neuroprotective effect that has been demonstrated in TASK1 [273], we have extended the project to investigate curcumin effect in *ex vivo* model of PD.

CHAPTER 3

MATERIALS AND METHODS

3.1.TASK 1 – The Effects of Curcumin in Bilirubin-induced Neurotoxicity in Severe Neonatal Hyperbilirubinemia Model

3.1.1 Litter Composition and Treatment Scheme

Gunn rats (Hds Blue: Gunn-UDPGTj) were obtained from the SPF animal facility of CBM S.c.a.r.l. (AREA Science Park, Basovizza). Litters were obtained by mating heterozygous normobilirubinemic (Normo) females with heterozygous hyperbilirubinemic (Hyper) males. Animals were housed in a temperature-controlled environment (22 ± 2°C), on a 12h light/dark schedule, and ad-libitum access to food and water. The entire litter composed of both Normo and Hyper pups was used (percentage of Normo/Hyper = 51%/49%, respectively; mean number of pups in each litter: 6.6). Based on our experimental experience demonstrating that the sex is not relevant for the model, both males and females were used (final % of M/F 44%/56%, respectively). Exclusion criteria were litters with less than two Normo, less than two Hyper, or the presence of small, sick animals at the starting of the challenge.

Curcumin (Curc: Curcusoma, 10 mg/Kg, BiosLine, Padova, Italy) treatment (i.p.: intraperitoneal injection) started at P2 (post-natal age in days) when jaundice was visible in Hyper pups and was repeated each day up to P17 (**Figure 3.1**) when the cerebellar hypoplasia in Hyper rats reached the 30% (vs. Normo) [274] and may be used as an immediate indication of the drug efficacy [104].

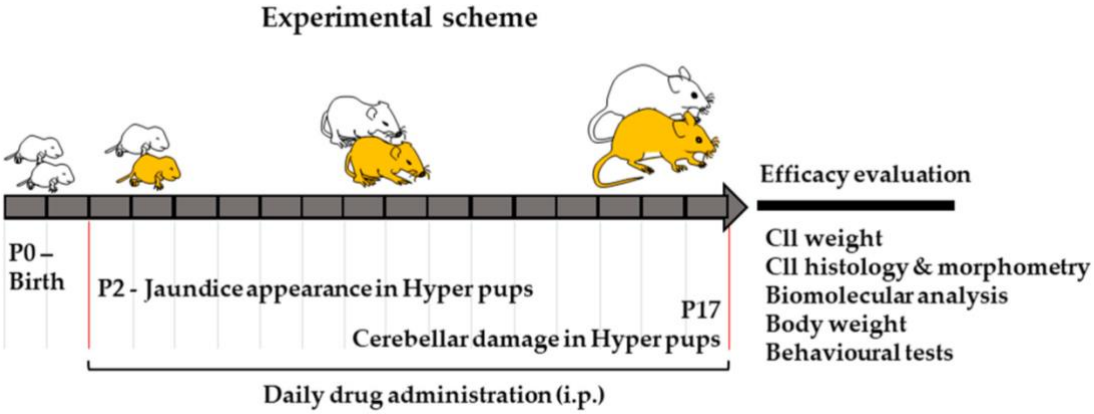

Figure 3.1. Experimental plan and efficacy of curcumin in rescuing cerebellar hypoplasia. (a) Two days after birth (P2: post-natal age in days), the litters composed of both by normobilirubinemic (Normo—white) and hyperbilirubinemic (Hyper—yellow) pups were daily injected intraperitoneally (i.p.) with curcumin (Curc). At P17, the animals were sacrificed, and the cerebellum (Cll) was submitted for different analyses to deeply evaluate the drug efficacy and the mechanisms of action.[273]

Animal distress was monitored daily with an objective distress score table [275]. Bodyweight, as a part of the distress evaluation, was recorded by a bench balance along the treatment (P5, P9, P11, P17; 10 animals in each experimental group were evaluated). Any non-zero observation on any score parameter implied the immediate interruption of the treatment for the affected animal. At the end (P17), animals were sacrificed by decapitation under deep anesthesia (Tiletamina + zolazepam, 35 mg/kg, i.p.), and blood and tissues were collected for analysis as previously described [32,67]. Experiments were performed according to the Italian Law (decree 87-848) and European Community directive (86-606-ECC). The maximal effort was done in respecting the 3R rule. The study was approved by the competent OPBA and by the Italian Ministry (n 1165/2015-PR and n 1024/2020-PR).

3.1.2 Cerebellar weight

To assess the efficacy of the treatment, we considered the reduction of the characteristic cerebellar hypoplasia present in the Gunn rat [104], [276], [277], by recording the cerebellar weight by a precision balance. Data were expressed as mean S.D. and as mg/animal.

3.1.3 Cll histology and morphometry

The architecture of the cerebellum was assessed by hematoxylin-eosin staining, performed in freshly dissected, paraffin-embedded brains, as previously reported [274], [278]. In brief, brains were fixed in neutral buffered formalin and embedded in 4% paraffin. Tissue was sectioned to a thickness of 3–5 m by a microtome (Microm-hm 340e- BioOptica, Milan, Italy), and dried in the oven at 60 C for one hour. Sections were stained with hematoxylin and eosin using an automated Leica ST5020 Multistainer (Leica Microsystem, Milano, Italy). The number of Purkinje cells (PCs) and the thickness of the external granule cell layer (EGL) were evaluated on three different fields, covering almost the whole Cll, by a D-sight plus image digital microscope and scanner (Menarini Diagnostics, Firenze, Italy). Data were expressed as mean S.D., and in fold vs. Normo (reference = 1)

3.1.4 Total serum bilirubin (TSB)

To monitor potential confounding effects of the drug challenge, the total serum bilirubin level was assessed in both Curc-treated pups and control animals. Blood samples were collected during the sacrifice, serum was separated by centrifugation (2000 rpm, 20 min at room temperature)

and the TSB was quantified by the diazo reaction, as previously described [274], [279]. The results were expressed as mean S.D. and in mg/dL.

3.1.5 Behavioural tests

Two tests were selected specifically for assessing the motor and coordination abilities of young rats, the righting reflex, and the negative geotaxis . No training was required, and animals were asked to perform each test only one time a day to avoid fatigue. Since young rats still cannot perfectly keep their body temperature, one animal at a time was separated from the mother, tested, and returned to the mother. Each test does not require more than 2 min in total. The righting reflex was conducted at P9. The pups were gently placed on their back (supine position) on a comfortable surface, and the time required for them to roll on their stomach (prone position), was recorded. The negative geotaxis was performed at P11. The pups were gently placed on an inclined (30°) plane, with the head bottom-oriented. The time required for them to rotate 180° upside-down was recorded. Data were expressed as mean S.D. and in fold vs. Normo (reference = 1).

3.1.6 Real-Time PCR of Selected Markers for Inflammation, Redox Imbalance,and Brain Development

To follow the effect of bilirubin-induced brain damage and Curc protection, we monitored the genes (inflammation and redox state Table 3.1) previously reported [278], and chose because they are known players in bilirubin neurotoxicity (see ref in the Introduction, in addition to [278]). For the Mbp analysis, we compared three different primer pairs (one

designed by us, two from literature). Based on the tests (specificity, efficiency), we used the ones described by Abranches [283]. Total RNA extraction, retrotranscription, and RTqPCR were performed as previously described [274], [278]. In brief, total RNA was extracted using TRI Reagent® RNA Isolation Reagent (Sigma-Aldrich, St. Louis, MO, USA), and the complementary DNA (cDNA) was synthesized with the High Capacity cDNA Reverse Transcription Kit (Applied Biosystems, Monza, Italy), following the manufacturer's instructions. The primers were designed using the Beacon Designer 4.2 software (Premier Biosoft International, Palo Alto, CA, USA) on rat sequences available in GenBank. The reaction was performed in an iQ5 Bio-Rad Thermal cycler (BioRad Laboratories, Hercules, CA, USA), in the SsoAdvanced SYBR green supermix (Bio-Rad Laboratories, Hercules, CA, USA). Amplification of target genes was accomplished using the following protocol: 3 min at 95°C, 40 cycles at 95°C for 20 s, 60°C for 20 s, and 72°C for 30 s. The specificity of the amplification was verified by a melting-curve analysis, and non-specific products of PCR were not found in any case. The relative quantification was made using the iCycleriQ software, version 3.1 (Bio-Rad Laboratories, Hercules, CA, USA) by the DDCt method, taking into account the efficiencies of the individual genes and normalizing the results to the housekeeping genes [284], [285]. Data were expressed as mean ± S.D., and in fold vs. Normo (reference = 1).

Table 3.1. Primers specification[273]

Gene	Accession number	Forward 5′-3′	Reverse 3′-5′
Hprt	NM_012583.2	AGACTGAAGAGCTACT GTAATGAC	GGCTGTACTGCTTGACCA AG
Gapdh	NM_017008.2	CTCTCTGCTCCTCCCTGTT C	CACCGACCTTCACCATCT TG
Hmox1	NM_012580.2	GGTGATGGCCTCCTTGTA	ATAGACTGGGTTCTGCTT GT
Srxn1	NM_001047858.3	AAGGCGGTGACTACTAC T	TTGGCAGGAATGGTCTCT
Tnfα	NM_012675.2	CAACTACGATGCTCAGA AACAC	AGACAGCCTGATCCACTC C
Il1β	NM_031512.2	AACAAGATAGAA G TCAAGA	ATGGTGAAGTCAACTATG
Il6	NM_012589.1	GCCCACCAGGAACGAAA GTC	ATCCTCTGTGAAGTCTCCT CTCC
Cox2	NM_017232.3	CTTTCAATGTGCAAGACC	TACTGTAGGGTTAATGTC ATC
Icam1	NM_012967	ACCTACATACATTCCTAC C	ATGAGACTCCATTGTTGA
Mag	NM_017190	ACCATCCAACCTTCTGTA TC	CTGATTCCGCTCCAAGTG
Mbp	NM_001025291	CACAGAAGAGACCC TCACAGCGACA	TCCATCGGGCGCTTCTTTA GCGG

Hprt: Hypoxanthine-guanine phosphoribosyl-transferase; *Gapdh*: Glyceraldehyde 3-phosphate dehydrogenase; *Hmox1*: Heme oxygenase1; *Srxn1*: Sulfiredoxin 1; *Tnfα*: Tumor necrosis factor alpha; *Il1β*: Interleukin 1 beta; *Il6*: Interleukin 6; *Cox2*: Cyclo-oxygenase 2; *Icam1*: intracellular adhesion molecule 1; *Mag*: myelin-associated glycoprotein; *Mbp*: myelin basic protein.

3.1.7 Glutamate Quantification

The amount of brain glutamate (Glut) was quantified by Glutamate Assay Kit following the producer's instructions (MAK004, Sigma-Aldrich, MO) [278], with some adaptation. Briefly, Cll was mechanically homogenate by a Dounce potter in Glutamate Assay buffer (200 uL each 10 mg tissue), the sample was centrifuged at 13,000 g for 15 min, and the supernatant collected for performing the test. Glutamate content in Hyper

and Curc samples was expressed as fold change compared to Normo, after normalization for the total protein content in each sample, quantified by the Bicinchoninic Acid kit following the supplier's instruction (B9643 and C2284, Sigma-Aldrich, MO). Data were expressed as mean ± S.D., and in fold vs. Normo (reference = 1).

3.1.8 Protein Evaluation of Selected Markers for Inflammation, Redox Imbalance, and Brain Development

Western blot was performed as previously described [274] on 30 μg protein/well for each animal/treatment (except for Hmox1 analysis that required 60 μg protein/well for each animal/treatment). In brief, Cll were mechanically homogenized and the protein concentration was determined by the Bicinchoninic Acid Protein Assay (B-9643 and C2284, Sigma, Missouri, USA). Thus, proteins were separated by 12% SDS-PAGE by electrophoresis in a Hoefer SE 250 System (Amersham BioSciences, UK), transferred onto immune-blot PVDF membranes (0.2 μm; Whatman Schleicher and Schuell, Dassel, Germany) at 100 V for 60 min (Bio-Rad Laboratories, Hercules, CA, USA). Blocking (1.5 h, RT), and incubation with the primary (*Icam1* 2 h RT; *Hmox1* and *Mag* O/N, 4 °C) and secondary antibodies (2 h RT) were performed in 3% defatted milk in 0.2% Tween 20; 20 mM Tris-HCl pH 7.5; 500 mM NaCl. The details of the antibodies used are reported in Table 2. The signal was revealed by chemiluminescence (ECL-Plus Western blotting Detection Reagents, GE-Healthcare Bio-Science, Italy) and visualized on X-ray films (BioMax Light, Kodak Rochester, NY, USA). The results were normalized vs. the actin signal (1h RT), visualized incubating the same membrane. The band intensity was

quantified by the Scion Image software (GE Healthcare Europe GmbH, France) [274].

Table 3.2. Antibodies and ELISA kit specifications [273]

Target	Technique	Ab I Code and Dilution	Ab II Code and dilution
Il1β	ELISA	ER2IL1B (Thermo Scientific, MA, USA)	
Tnfα	ELISA	Ab100785 (Abcam, ProdottiGianni, Milano, Italy)	
Actin	Western blot	A2066 (1:3000) (Sigma-Aldrich, Darmstadt, Germany)	Anti-Rabbit HRP (P0448;1:3000) (Dako, CA, USA)
Hmox1	Western blot	Sc136961 (1:100) (SantaCruz, Aachen, Germany)	Anti-Mouse HRP (P0260;1:3500) (Dako, CA, USA)
Icam1	Western blot	Sc1511 (1:50) (SantaCruz, Aachen, Germany)	Anti-Goat HRP (P0449;1:4000) (Dako, CA, USA)
Mag	Western blot	Sc 166849 (1:1000) (MyBioSource, San Diego,CA, USA)	Anti-Rabbit HRP (1:3000) (Dako, CA, USA)
Mbp	Western blot	MBS175140 (1:100) (MyBioSource, San Diego, CA, USA)	Anti-Rabbit HRP (1:3000) (Dako, CA, USA)

ELISA: enzyme-linked immunosorbent assay. Ab: antibody. Il1β: Interleukin 1 beta; Tnfα: Tumor necrosis factor alpha; Hmox1: Heme oxygenase1; Icam1: intracellular adhesion molecule 1; Mag: myelin-associated glycoprotein, Mbp: myelin basic protein.

Il1β and Tnf*α* level was quantified on tissues homogenates by ELISA kits (see Table 2), following the manufacturer's instructions. The results were normalized for the total protein content in each sample, quantified by the Bicinchoninic Acid Protein Assay (B-9643 and C2284, Sigma, Missouri, USA). Data were expressed as mean ± S.D., and in fold vs. Normo (reference = 1).

3.1.9 Statistical analysis

Data were analyzed with GraphPad Prism version 5.00 for Windows (GraphPad Software, La Jolla, CA, USA). Statistical significance was evaluated the one-way analysis of variance (ANOVA), followed by a

Tukey–Kramer Multiple Comparisons Test when p-value < 0.05. A p-value < 0.05 was considered statistically significant.

3.2.TASK 2 – Bilirubin Neuroprotection in *ex vivo* Parkinson's disease model

3.2.1 General procedures

3.2.1.1. Organotypic brain cultures of substantia nigra (OBCs-SN)

Wistar HanTM Rats, at five (P5) days after birth, were obtained from the animal facility of the University of Trieste, Dept. of Life Sciences, Trieste (AREA Science Park, Basovizza, Italy). Animal experiments were organized according to the Italian Law (decree 87-848) and European Community directive (86-606-ECC). The project has been approved by the local Ethic Committee (Organismo unico Per il Benessere Animale – OPBA, Università degli Studi di Trieste) and by the Italian Ministry (code: 1FF80.N.PZB). Maximal effort to minimize the number of animals used and their sufferance was done (RRR rule). Immediately after sacrifice, brains were removed and maintained in an ice-cold Gey's Balanced Salt Solution plus D-Glucose 10 mg/mL (dissection medium). These experimental conditions were used to prevent damages that could affect neuronal tissue maintained in a non-physiological condition. Mesencephalon was dissected from brains removing both hemispheres and maintained in ice-cold dissection medium until use. A McIIwain tissue chopper (Gomshall Surrey, U.K.) was used to cut coronally 300 μm slices. Healthy slices were selected from the total amount of tissue prepared by the chopper for structural integrity and maintained in ice-cold dissection medium until use. Then, using a razor blade, the dorsal part was discarded and ventral mesencephalon slices were further cut in the midline to obtain two specular slices starting from each one. This allowed us to reduce the dimension of the slice thus improving slice viability. After

cutting into the midline, slices were then transferred to sterile, semi-porous Millicell-CM inserts (PICM03050, Millipore, Darmstadt, Germany), feed by 1 mL of cold medium, and maintained at 37°C, 5% CO2, 95% of humidity in a humidified incubator. Two to six slices were cultured in each filter depending on the aim of the experiment.

3.2.1.2. OBCs-SN medium

For growing an challenging the slices we used the adapted (to free bilirubin - Bf quantification) OBCs-SN medium previoussly identified by Dal Ben et al. [135]. Bf adapted medium was composed of 65% of Basal Medium Eagle (BME) medium, 10% of heat-inactivated Fetal Bovine Serum (FBS), 25% of Hank's Balanced Salt Solution (HBSS), 1% L-Glutamine, 2% Penicillin/Streptomycin, 10 mg/mL D-Glucose. The medium was changed the day after slice preparation and every two days thereafter. Before starting any treatment, slices were maintained in culture 10 for days to allow slices to recover from the stress induced by the slice preparation procedure [135].

3.2.1.3. Chemical and Solutions Used

a. Gey's Balanced Salt Solution + D-Glucose

Calcium Chloride (CaCl2) 0.166 mg/mL, Potassium Chloride (KCl) 0.97 mg/mL, Potassium Phosphate Monobasic (KH2PO4) 0.03 mg/mL, Magnesium Chloride (MgCl2*6H20) 0.21 mg/mL, Magnesium Sulfate (MgSO4-7H2O) 0.07 mg/mL, Sodium Chloride (NaCl) 8.0 mg/mL, Sodium Bicarbonate (NaHCO3) 0.227 mg/mL, Sodium Phosphate Dibasic (Na2HPO4) 0.12 mg/mL, D-Glucose 10 mg/mL.

b. *Hanks' Balanced Salt Solution (HBSS*) (Sigma Aldrich, St. Louis, MO, USA): Calcium Chloride (CaCl2) 0.14 g/L, Potassium Chloride (KCl) 0.40 g/L, Potassium Phosphate Monobasic (KH2PO4) 0.06 g/L, Magnesium Chloride (MgCl2-6H20) 0.10 g/L, Magnesium Sulfate (MgSO4-7H2O) 0.10 g/L, Sodium Chloride (NaCl) 8.00 g/L, Sodium Bicarbonate (NaHCO3) 0.35 g/L, Sodium Phosphate Dibasic (Na2HPO4) 0.048 g/L.

c. Immunofluorescence solution

1. ***Phosphate Buffered-Saline 1x (PBS***), pH=7.4
   Sodium Chloride (NaCl) 8 g/L, Potassium Chloride (KCl) 0.2 g/L, Sodium Phosphate Dibasic (Na2HPO4) 1.44 g/L, Potassium Phosphate Monobasic (KH2PO4) 0.24g/L

2. ***Paraformaldehyde (PFA)*** 4% in PBS (1x, pH=7.4)
   800 mL PBS 1x, 40 g PFA powder; final pH=6.9

3. ***Immunofluorescence Blocking Solution in PBS*** (1x, pH=7.4)
   10% Normal Goat Serum (NGS, Sigma Co., Saint Louis, Missouri, USA) 1% Triton X-100 detergent (Sigma Co., Saint Louis Missouri, USA), 1% Bovine Serum Albumin (BSA, A4503, Sigma Co., Saint Louis, Missouri, USA)

4. ***Immunofluorescence Incubation Solution in PBS*** (1x, pH=7.4)
   1% Normal Goat Serum (NGS, Sigma Co., Saint Louis, Missouri, USA) 1% Triton X-100 detergent (Sigma Co., Saint Louis Missouri,

USA), 1% Bovine Serum Albumin (BSA, A4503, Sigma Co., Saint Louis, Missouri, USA)

3.2.1.4. Immunofluorescence staining and cell counting

Tyrosine hydroxylase immunofluorescence was performed to evaluate morphological and neurobiological changes associated with rotenone, UCB, and additional compounds exposure, as previously described by Dal Ben *et* al. [135]. Slices were fixed in 4% paraformaldehyde (Sigma-Aldrich, St. Louis, MO, USA) for 30 minutes at room temperature and then washed with phosphate-buffered saline (PBS) and glycine 0.1M (Sigma-Aldrich, St. Louis, MO, USA) to remove residues of paraformaldehyde. After washing, slices were pre-incubated for 1 hour in 10% Normal Goat Serum (NGS, Sigma-Aldrich, St. Louis, MO, USA), 1% bovine serum albumin (BSA, Sigma-Aldrich, St. Louis, MO, USA) and 0.1% triton-X100 (Sigma-Aldrich, St. Louis, MO, USA) in PBS (blocking solution). Then, slices were incubated for three days at 4°C with primary polyclonal antibody anti-tyrosine hydroxylase (1:250, AB152, Millipore, Temecula, CA, USA) in an incubation solution containing % NGS, 1% BSA, and 0.1% Triton-X100 for three days at 4 °C.

Slices were then rinsed three times in incubation solution and subsequently incubated with labeled donkey anti-rabbit Alexa Fluor 546 secondary antibody (1:3000, A10040, Life Technologies, Carlsbad, CA, USA) overnight at 4C°. After washing twice with PBS, slices were stained with Hoechst 33258 (1:10,000, Sigma-Aldrich, St. Louis MO, USA), rinsed with Milli-Q water, and mounted with mounting media (Fluorescent Mounting Media, Calbiochem, Germany). Tyrosine hydroxylase-positive (TH+) DOPAn were observed by using fluorescent microscopy Leica

DM2000 (Leica Microsystems Srl, Solms, Germany) and counted under the 20x magnification. Whole slices were counted for each biological condition. The results were expressed as the percentage of TH+ cells in the treated slices relative to the number of cells in the control (100%).

3.2.1.5. RNA extraction and quantification

RNA from both experimental and control groups was extracted using TRI Reagent® RNA Isolation Reagent (T9424, Sigma-Aldrich, St. Louis, MO, USA), following the manufacturer's instructions. This method relies on phase separation by centrifugation of an upper aqueous phase and a lower organic phase. After the addition of 200 μL of purified chloroform (C2432, Sigma-Aldrich, St. Louis, MO, USA) per mL of TRI reagent, vortexing and separation by centrifugation (12,000 rpm for 15 minutes at +4 °C – Microcentrifuge I8 Centrifuge, Beckman Coulter, Brea, California, USA), the RNA separated in the aqueous phase, proteins remain in the organic phase and the DNA in the interface between them. The RNA-containing phase was transferred to a new tube and then 500 μL of isopropyl alcohol (415156, Carlo Erba, Cornaredo, Italy) per mL of TRI reagent was added. Samples were further centrifuged at 10,000 rpm for 10 minutes at +4°C. After removing the supernatant, the resulting RNA pellet was washed with 1 mL of ethanol (02860, Sigma Co., Saint Louis, Missouri; USA) 75 % two times. In the end, ethanol was removed and once the pellet was dried, RNA pellet was dissolved in pure, RNAase-free milliQ water, and stored at -80 °C for further analysis. The concentration and purity of the samples were determined by spectrophotometric (Beckman DU 730, Beckman, Brea, California, USA) validation (Abs

values at 230-260-280 nm). λ 260/ λ 280 ratio allows assessing if the extracted RNA is contaminated with proteins containing aromatic amino acids. λ 260/ λ 230 ratio allows assessing the degree of contamination of the organic ions that bind to the nucleic acid, in particular, thiocyanate and phenolate ions coming from the TRI-zol reagent used in the very first steps of the extraction. Ideally, the proportion between the three Abs values should be Abs230:260:280= 1:2:1 for a pure RNA sample. RNA concentration [μg/μL] was quantified by (using) the formula: [((λ260 x 40 x 100) x (1/1000))]. In particular, 1:100 RNA solution in RNA-ase free pure milliQ water was prepared and read at the spectrophotometer in a 0.1 mL glass cuvette (Beckman DU 730, Beckman, Brea, California, USA).

3.2.1.6. Reverse Transcription PCR

To study gene expression, RNA samples, previously extracted and quantified were reverse transcribed into the corresponding cDNA by the reverse transcription-polymerase chain reaction (RT-PCR). RT-PCR allows generating single-stranded cDNA from total RNA using a reverse transcriptase, which is an RNA-dependent DNA polymerase. Briefly, 1 μg of total RNA of each sample was reverse transcribed using 10μl of RT Master mix from the High Capacity cDNA Reverse Transcription Kit (Applied Biosystems- Life Technologies, Carlsbad, California, USA), in a final volume of 20 μl, according to manufacturer's instructions. Retrotranscription was performed in a Thermal Cycler (T-100 Thermal Cycler, Biorad, Hercules, California, USA) performing the following steps: 10min at 25 °C, 120min at 37 °C, 5min at 85 °C, 4 °C.

a. Real-Time Quantitative PCR (RTqPCR)

The mRNA expression of genes of interest was analyzed by quantitative real-time PCR as previously described [135]. Total RNA was extracted using TRI Reagent® RNA Isolation Reagent (Sigma-Aldrich, St. Louis, MO, USA), following the producer's instructions. The reaction was performed in a final volume of 15 μL in an iQ5 Bio-Rad Thermal cycler (BioRad Laboratories, Hercules, CA, USA). Briefly, 25 ng of cDNA and the corresponding gene-specific sense/antisense primers (250 nM each, except for Cox2 and Il1β, 500 and 750 nM respectively) were diluted in the SSo Advance SYBER green supermix (Bio-Rad Laboratories, Hercules, CA, USA). Amplification protocol consisted of 3 min at 95 °C, 40 cycles at 95 °C for 20 s, 60 °C for 20 s, and 72 °C for 30 s. The specificity of the amplification was verified by a melting-curve analysis, and non-specific products of PCR were not found in any case. The relative quantification was made using the iCycler iQ software, version 3.1 (Bio-Rad Laboratories, Hercules, CA, USA) by the modified ΔΔCt method185, taking into account the efficiencies of the individual genes and normalizing the results to the housekeeping genes, (Glyceraldehyde 3-phosphate dehydrogenase: Gapdh; TATA-binding protein: Tbp) [135]. The quantification of mRNA was expressed relative to the reference sample.

3.2.1.7. Statistical analysis

Data were analyzed with GraphPad Prism version 5.00 for Windows (GraphPad Software, La Jolla, CA, USA). Statistical significance was evaluated the one-way analysis of variance (ANOVA), followed by a Tukey–Kramer Multiple Comparisons Test when p-value < 0.05. A p-value < 0.05 was considered statistically significant. Linear regression was performed using Pearson correlation analysis.

3.2.2 TASK 2A: Bilirubin reverses the dopaminergic neuron demise in an *ex vivo* Parkinson's disease model

3.2.2.1. The treatments

OBCs-SN were challenged with specific compounds immediately after recovery (day 8-10) [135]. All the treatments have been performed for 24h, allowing the reproduction of 40% DOPAn loss in the PD model corresponding to the diagnosis in patients, and a significant modulation of all the early markers of DOPAn loss in the model [135]. The compounds used are

a. Rotenone

   Rotenone (Sigma-Aldrich, St. Louis MO, USA), a pesticide known for inducing PD in human and animal models [286], was dissolved in DMSO and used in a final concentration of 10 nM in the culture medium [135].

b. Unconjugated bilirubin (UCB)

   The specific concentrations of UCB (Sigma-Aldrich, St. Louis, MO, USA), dissolved in DMSO (Sigma-Aldrich, St. Louis, MO, USA), required to reach the desired Bf in the OBCs medium were quantified according to protocol us of Roca *et a*l. [279]. The amount of UCB necessary for the experiment was dissolved in DMSO at the final concentration of 5.0 mM and then diluted to the desired concentration in the medium. The highest concentration of 4µM UCB in the culture medium was determined using the spectrophotometer with an absorbance of 0.190. The final concentrations of 0.5µM, 1µM, and 2µM

UCB were reached by following dilutions from 4μM UCB, then Rot was added to perform co-treatments. All selected UCB concentrations corresponded to Bf < 4 nM and considered as non-toxic concentrations [287].

c. N-acetyl-cysteine (NAC)

We applied a broad range of NAC concentrations based on the literatures [288], [289]. NAC (Sigma-Aldrich, St. Louis MO, USA) was dissolved in DMSO to a 125 μM concentration, then diluted to the final concentrations (from 10μM to 15mM) in the OBC-SN medium. Rot was finally added to perform co-treatments.

d. Tumor necrosis factor alpha (TNF-α)

TNF-α (Peprotech, London, United Kingdom) was diluted directly in the OBC-SN medium at three increasing concentrations (20 ng/mL, 40 ng/mL, and 60 ng/mL), in the absence of Rot. After starting with TNF-α concentration suggested by literature [290], we increase the range until replicating the DOPAn loss observed as in the Rot treatment.

e. Infliximab

Infliximab (Flixabi®, Biogen, Hillerod, Denmark), a TNF-α neutralizing antibody, has been diluted in the OBC-SN medium at the final concentration of 41 μg/mL (275 nM) and was chosen based on available published data [291], then Rot was added to perform the co-treatments.

f. Control slices were exposed to the same final concentration of DMSO needed to dissolve the compounds (<0.05%).

3.2.2.2. PCR Primers

The previously genes reported were selected as markers to evaluate the effect of UCB in the ex vivo model of PD [135], Primers were designed using the Beacon Designer 4.2 Software (Premie Biosoft International, Palo Alto, CA, USA) based on rat sequence available in GenBank (Table 1). Quantitative real-time PCR (qPCR) was performed in an iQ5 Bio-Rad thermal cycler (BioRad Laboratories, Hercules, CA, USA). Briefly, 25 ng of cDNA and the corresponding gene-specific sense/antisense primers (250 nM each, except Cox2, 500 nM) were diluted in the Sso Advanced SYBER green supermix (Bio-Rad Laboratories, Hercules, CA, USA). The genes of interest were analyzed by performing the qPCR as follows: 95 °C for 3 min; a 40 times repetition of 95 °C for 20 s, 60 °C for 20 s, and 72 °C for 30 s. Finally, the reaction was stopped by an additional step at 72 °C for 5 min. The specificity of the amplification was verified by a melting-curve analysis, and non-specific products of PCR were not found in any case. The relative quantification was made using the iCycleriQ software, version 3.1 (Bio-Rad Laboratories, Hercules, CA, USA) by the ΔΔCt method, taking into account the efficiencies of the individual genes and normalizing the results to the housekeeping genes (TATA-binding protein: *Tbp* and Glyceraldehyde 3-phosphate dehydrogenase: *Gapdh*)[284], [285]. RTqPCR was performed as described in Dal Ben *et al*. [135].

Table 3.3. Primers used to analyze gene expression of selected genes

Gene	Accession number	Forward 5′-3′	Reverse 3′-5′
Gapdh	NM_017008.2	CTCTCTGCTCCTCCCTGTTC	CACCGACCTTCACCATCTTG
Tbp	NM_001004198.1	CAATGACTCCTATGACCCCT	TTTACAGCCAAGATTCACGG
Bdnf	NM_012513.4	GGACATATCCATGACCAGAA	GGCAACAAACCACAACAT
Hmox1	NM_012580.2	GGTGATGGCCTCCTTGTA	ATAGACTGGGTTCTGCTTGT
Srxn1	NM_001047858.3	AAGGCGGTGACTACTACT	TTGGCAGGAATGGTCTCT
Tnfα	NM_012675.2	CAACTACGATGCTCAGAAACAC	AGACAGCCTGATCCACTCC
Il6	NM_012589.1	GCCCACCAGGAACGAAAGTC	ATCCTCTGTGAAGTCTCCTCTCC
Cox2	NM_017232.3	CTTTCAATGTGCAAGACC	TACTGTAGGGTTAATGTCATC

Gapdh: Glyceraldehyde 3-phosphate dehydrogenase; *Tbp*: TATA-binding protein; *Bdnf*: Brain-derived neurotrophic factor; *Hmox1*: Heme oxygenase1; *Srxn1*: Sulfiredoxin 1; *Tnfα*: Tumor necrosis factor; *Il6*: Interleukin 6; Cox2: Cyclo-oxygenase 2.

3.2.2.3. Glutathione Content Assay

Glutathione contents, both GSH (reduced) and GSSG (oxidized) were determined from the medium of OBCs-SN using a fluorometric assay. Stock standard solutions of GSH and GSSG (Sigma-Aldrich, St. Louis, MO, USA) were prepared in 10 mM solutions in 0.01 M HCO_2H. *o*-Pthaldehyde (Sigma-Aldrich, St. Louis, MO, USA) was prepared as 1 mg/mL in methanol. For GSH and GSSG assay, 100 µL of medium/protein from tissue/GSH or GSSG standard is mixed with 0.1 mL buffered formaldehyde (1:4 (v/v) 37% formalin M Na_2HPO_4) in 96 well fluorometric assay plate. After 1-5 minutes, for GSH assay, 1.0 ml of 0.1 M Sodium phosphate: 5 mM EDTA (pH 8.0) was added to each well followed by 100 µl of *o*-pthaldehyde.

Meanwhile, for the GSSG assay 0.1 M NaOH was added to conduct the reaction at pH 13. After 45 min incubation at 37^0 C, the fluorescence was measured using an EnSpire Multimode Plate Reader (PerkinElmer, Waltham, MA, USA) with the excitation wavelength of 345 nm and the fluorescent wavelength of 425 nm. GSH and GSSG levels were quantified using Curve Expert 1.38 software (Hixon, TN, USA) and were expressed as fold change compared to control slices.

3.2.3 TASK 2B: Nanobubbles as bilirubin carriers in organotypic brain cultures of substantia nigra: an initial screening step of bilirubin-delivery in Parkinson's disease (*The experiments were performed in collaboration with Department of Drug Science and Technology and Department of Neuroscience, University of Torino, Torino, Italy*)

3.2.3.1. The Nanobubbles Preparation

All nanobubbles, consist of glycol-chitosan (GC), GC-deferoxamine (GC-DFO), GC-DFO-iron (GC-DFO-Fe), and GC-DFO-superparamagnetic iron oxide nanoparticles (GC-DFO-SPIONs) and the free iron-Fe (Iron (III) reagent) were prepared by Department of Drug Science and Technology and Department of Neuroscience, University of Torino, Torino, Italy (Prof. Caterina Guiot and Prof. Roberta Cavalli).

3.2.3.2. Experimental schemes

a. Nanobubbles safety screening on healthy slices

Prior the use of NBs as bilirubin carrier in PD model, a safety screening was performed on healthy slices (OBCs-SN without Rot). DMSO and Rotenone were used as positive and negative control, respectively (**Figure 3.2**). The rational of accessing the safety of NBs on healthy slices was to see its toxicity and to prevent the use of the toxic NBs formulation and dilutions that will even induce more harm in PD model.

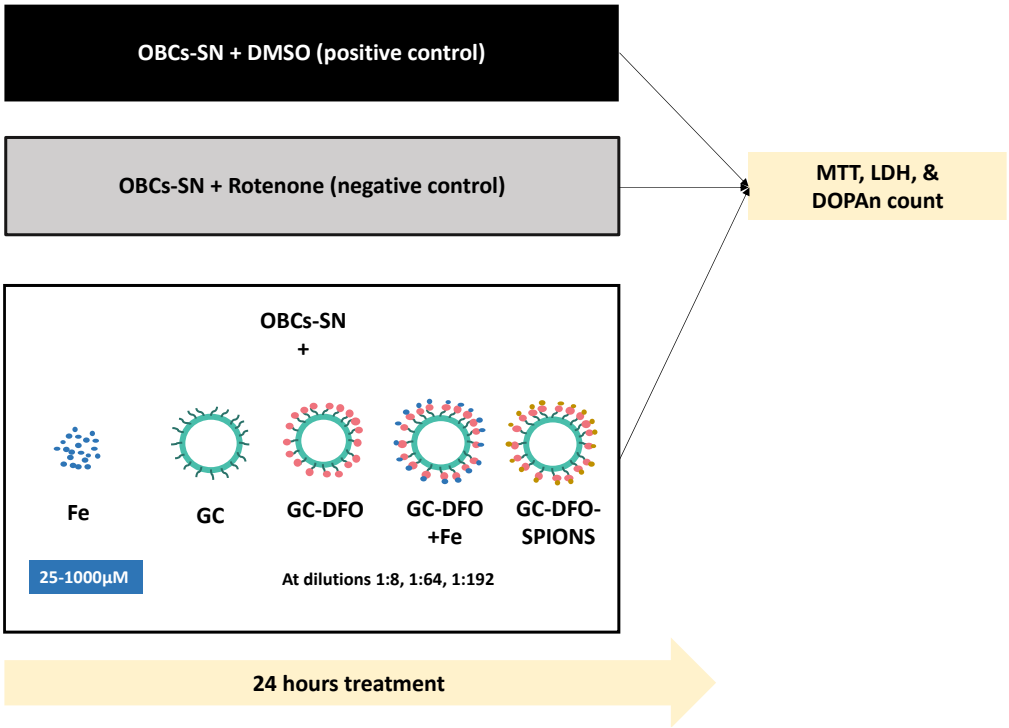

Figure 3.2. The experimental scheme of NBs and iron on healthy slices. Fe: free-iron; GC: glycol-chitosan; GC-DFO: GC-deferoxamine, GC-DFO-Fe: GC-DFO-iron and GC-DFO-SPIONs: GC-DFO-superparamagnetic iron oxide nanoparticles.

Three dilutions (1:8, 1:64, 1:192) were tested to see the viability of slices (via MTT, LDH, and DOPAn count) based on previous data published by pur collaboratos [292]. The sensitivity of the model to iron was assessed challenging the tissue with a slolution of Fe in a range of 25-1000µM. GC rappresented the skeleton NBs. Deferoxamine (DFO) was added to bind the Fe usually present in neurodegenerative diseases and responsible for enhancing the damage. The GC-DFO-Fe NBs was used to evaluate its ability to retain the loaded Fe. Finally, the addition of SIPONs (GC-DFO-SPIONs), macking the NBs paramagnetic, might allow to deliver and release in the site of lesione the drug, pick up the Fe and remove the NMS from the CNS by magnetic fields. This might be the most useful NBs

formulation in chronic diseases requiring continuous treatments.

Therefore, the goal of this safety test is to find the safe NBs to be used as bilirubin carriers in PD model itself.

b. Nanobubbles-UCB treatment on PD model

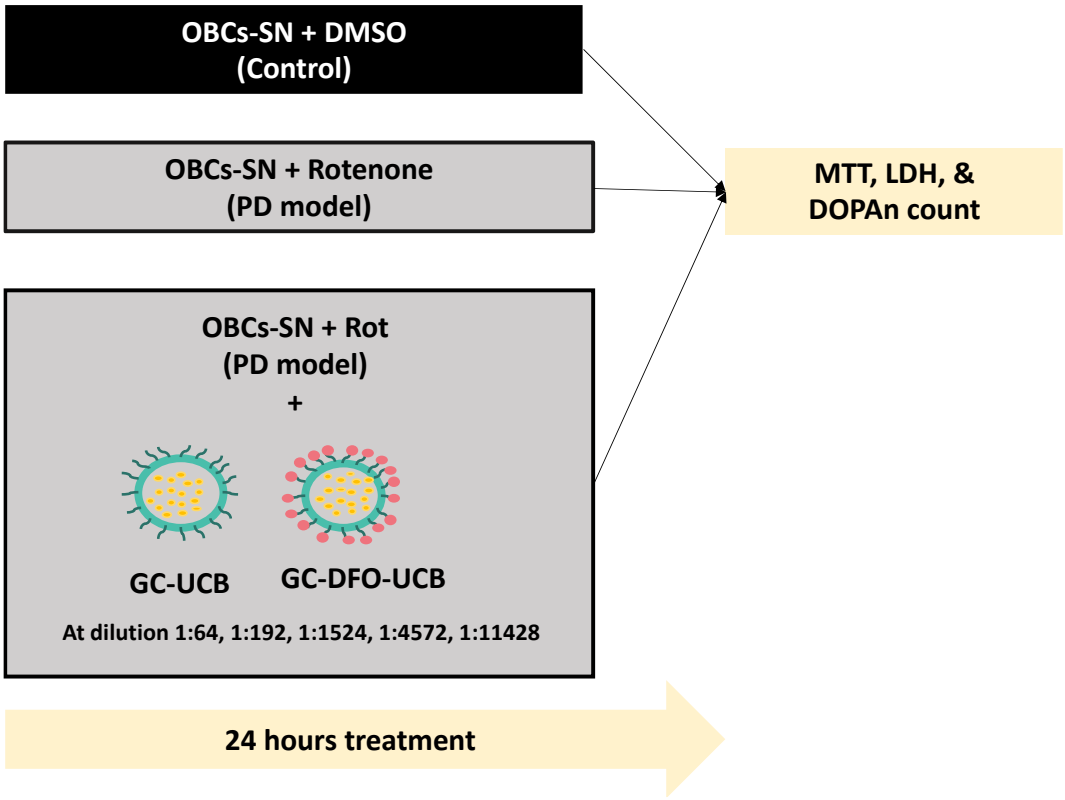

Figure 3.3. The experimental scheme of NBs-UCB on PD model.

Then the safest NBs candidates were loaded with UCB and used in PD model to assess their potential protection against DOPAn loss (**Figure 3.3.**). The range of dilutions was increased to 1:64, 1:192, 1:1524, 1:4572, and 1:11428, to supply DOPAn with the so tuned amount of UCB that is protective, without knowing how many bilirubin amounts will be released

by the NBs or how many NBs may enter the cells as bias. Again, MTT, LDH test and DOPAn count were performed to assess the potential of toxicity of NBs-UCB, which is considered as new formulation, and due to the addition of new dilutions.

3.2.3.3. The Treatments

For this experiment, OBCs-SN was used in the same preparation as described before in TASK 2 (Section **3.2.1.1 Organotypic brain cultures of substantia nigra (OBCs-SN**)). OBCs-SN was treated for 24 hours with:

a. Rotenone

   Rotenone was prepared and dissolved in the OBCs-NS medium as described in section 3.2.2.1 The treatments. It was used as reference of DOPAn loss (negative control) in the experimental scheme a (healthy slices), and as co-treatement with NBs in the PD model, to asses the potential protection conferred by the NBs loaded with UCB (experimental scheme b and c).

b. NBs

   NBs with three different polymer shells, GC, GC-DFO, and GC-DFO-SPIONs were prepared at 1:8, 1:64, and 1:192 dilutions in culture medium and used as depicted in experimental scheme a .

c. NBs-UCB

GC-UCB, GC-DFO-UCB, GC-DFO-SPIONs-UCB were prepared at 1:64, 1:192, 1:1524, 1:4572, and 1:11428 dilutions in culture medium and used as depicted in experimental scheme b and c.

d. Control slices were exposed to the same final concentration of DMSO needed to dissolve the all compounds above (<0.05%) as depicted in experimental scheme a-c.

3.2.3.4. Viability test

LDH (a metabolic enzyme present only in the cytoplasm, and its presence in the culture medium indicates the cell membrane leakage [293]) and MTT (mitochondrial activity evaluation) assays were conducted to assess the viability of OBCs-SN after challenge with DMSO, Rotenone, and different type of NBs and NBs-UCB at the end of the 24 hours treatment.

a. Lactate dehydrogenase release

The amount of total extracellular lactate dehydrogenase (LDH, marker of membrane leakage) in the medium was determined using a CytoTox-ONE™ Homogenous Membrane Integrity Assay (G7891, Promega, Madison, WI, USA) according to the manufacturer's instructions, with minor modifications. After 24 hours of treatment, the supernatant was collected, and the reaction started. The medium could be conserved also at -20°C. 100 µL of medium were incubated with 100 µL of

stop solution. The fluorescence ($560_{Ex}/590_{Em}$) was determined using an EnSpire Multimode Plate Reader (PerkinElmer, Waltham, MA, USA), and the background fluorescence, derived from the medium, subtracted. LDH in challenged slices was expressed as fold to control.

b. Mitochondrial Activity

Mitochondrial metabolic activity was assessed using a 1-(4. 5-dimethyltiazol-2-yl)-3-5-diphenylformazan (MTT) assay (Sigma-Aldrich, St.Louis, MO, USA). MTT powder was dissolved in PBS at the final concentration of 5 mg/mL. One slice for each biological repetition was incubated with 0.5 mg/mL of MTT in the medium at 37°C for 1 h, harvested, and the precipitated salt dissolved in DMSO. Absorbance was detected at 562 nm using an EnSpire Multimode Plate Reader (PerkinElmer, Waltham, MA, USA). Results were expressed as a fold of change to the control.

3.2.3.5. Dopaminergic neuron evaluation

Immunofluorescence was performed to assess and count the TH+ neuron (DOPAn) number. The procedures were performed as previously described in TASK 2 3.2.1 General Procedures, 3.2.1.4. Immunofluorescence staining and Cell counting.

3.2.4 TASK2C: Curcumin Protection in an *ex vivo* Parkinson's disease (PD) model

Taking advantage of curcumin neuroprotective effects, particularly its anti-TNF-α (see Result TASK1) and knowing the role of TNF-α in PD Model (see Result TASK2A), we continued to explore the potential protective effect of Curc in PD model.

3.2.4.1 The Treatments

For this experiment, OBCs-SN was used in the same preparation as described before in TASK 2 3.2.1. General Procedures, 3.2.1.1 3.2.1.1. Organotypic brain cultures of substantia nigra (OBCs-SN). OBCs-SN was treated for 24 hours with:

a. Rotenone

   Rotenone was prepared and dissolved in the OBCs-NS medium as described in section 3.2.2.1 The treatments

b. Curcumin

   Curcumin (Sigma-Aldrich, St. Louis MO, USA). was dissolved in DMSO and used in a final concentration of 5μM, 10μM, 20μM, and 40μM, in the culture medium

c. Control slices were exposed to the same final concentration of DMSO needed to dissolve the all compounds above (<0.05%).

3.2.4.2 Dopaminergic neuron evaluation

Immunofluorescence was performed to assess and count the TH+ neuron (DOPAn) number, as described in section in TASK 2 3.2.1 General Procedures, 3.2.1.4. Immunofluorescence staining and Cell counting.

3.2.4.3 TNF-α mRNA expression analysis

For analyzing *Tnfα* expression in PD, the previously described RT-PCR method (TASK 2 General Procedures: 3.2.1.5 RNA extraction and quantification and 3.2.1.6 Reverse Transcription PCR) and primers for housekeeping genes and *Tnfα* were used as previously described in TASK2A 3.2.2.2 PCR Primers).

CHAPTER 4
RESULTS

4.1 TASK 1 – The Effects of Curcumin in Bilirubin-induced Neurotoxicity in Severe Neonatal Hyperbilirubinemia Model

The treatment was started two days after the birth (P2: postnatal age in days), when jaundice appears in hyperbilirubinemic pups and was continued up to P17, when the cerebellar (Cll) hypoplasia, the reduced Purkinje cell number, and the reduced thickness of the external granular cell layer, reach statistical significance [12], [103], [104], [274], [276], [294]–[298]. The restoration of these landmark features of bilirubin-induced brain toxicity represents a major checkpoint and a major proof of the treatment efficacy.

4.1.1 Evaluation of the Cll Weight and Total Serum Bilirubin Level

As shown in **Figure 4.1 (a)**, in P17 hyperbilirubinemic pups (Hyper—yellow bar) the Cll weight loss reached 33% vs. the matched normobilirubinemic controls (Normo—white bar, $p < 0.001$). When Curc was administered (Hyper Curc—blue bar), complete protection against the Cll hypoplasia was observed (not statistically different from Normo; $p < 0.01$ vs. Hyper).

To assess if the efficacy of Curc in normalizing the Cll features was related to a potential decrease in the level of serum bilirubin (the stressor), we quantified the total serum bilirubin (TSB) concentration. As shown in **Figure 4.1 (b)**, Hyper pups presented 17 times higher TSB than

Normo age-matched pups ($p < 0.001$). Curc treatment did not modify the TSB (not statistically different from Hyper; $p < 0.001$ vs. Normo), indicating that the protective effect was not mediated by a reduction of the bilirubin challenging, but rather due to the in situ (Cll) interference with the main pathological mechanisms of bilirubin toxicity.

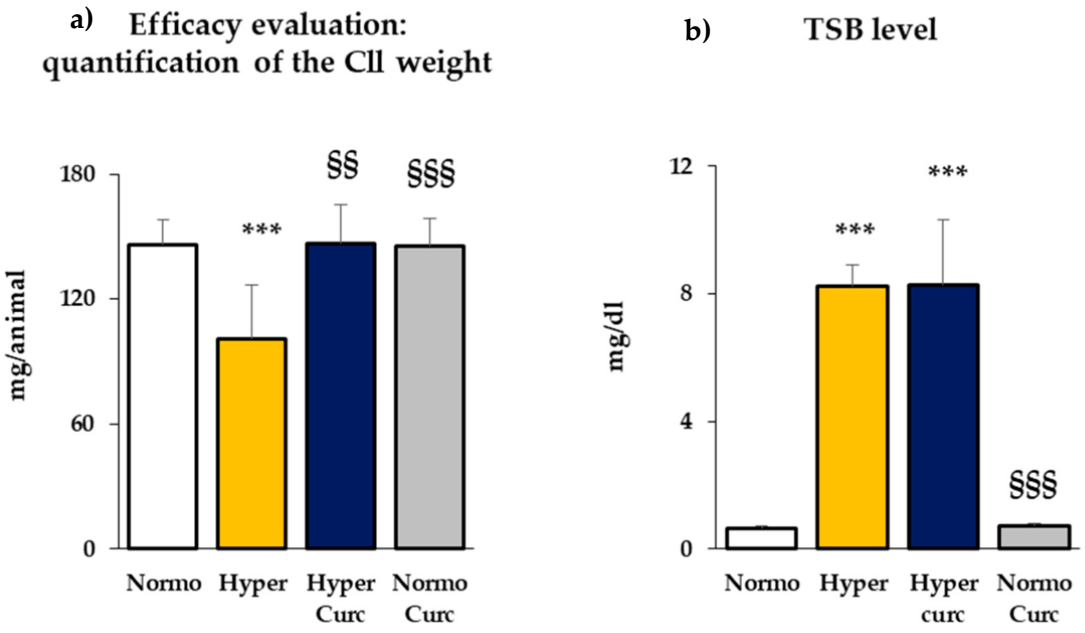

Figure 4.1. (**a**) The Cll weight (expressed in mg/animal) in P17 pups was quantified and used as a first, immediate evaluation of the efficacy of the treatment. (**b**) Total serum bilirubin (TSB in mg/dL) was quantified in each group to monitor any potential alteration due to the treatment. Both (**a**,**b**) With white bars—untreated normobilirubinemic (Normo) Gunn pups; yellow bars—untreated hyperbilirubinemic rats (Hyper); blue bars—curcumin-treated hyperbilirubinemic pups (Hyper Curc); gray bars—curcumin-treated normobilirubinemic pups (Normo Curc). Data were expressed as mean ± S.D. In each experimental group, ≥10 animals were considered. Statistical significance was evaluated by the one-way analysis of variance (ANOVA), followed by a Tukey–Kramer Multiple Comparisons Test when *p*-value < 0.05. Statistical significance: ***: p <0.001 vs. Normo pups. §§, §§§: $p < 0.01$, $p < 0.001$ vs. Hyper rats.

4.1.2 Assessment of the Histological Findings of the Cll under the Curc Treatment

To further analyze the protective effect of Curc on the Cll damage induced by bilirubin toxicity, we performed histological and morphometric analysis. The general appearance of the Cll, the number of the Purkinje neurons (PCs), as well as the thickness of the external granule cell layer (EGL), were quantified (**Figure 4.2**).

As shown in **Figure 4.2a**, 2× magnification, the reduction of the Cll volume typical of Hyper pups was fully restored in hyperbilirubinemic pups treated with Curc, in line with the restoration of the Cll weight. At higher magnification (**Figure 4.2 b** = 10× and **c** = Detail), the reversal of the reduction of the PC number is also evident (e.g., arrows) and the reversal of the EGL thickness (e.g., rectangles) in Hyper Curc pups.

As detailed by the quantification performed on the whole Cll section (**Figure 4.2d**), the PC number was reduced by about 50% in Hyper pups vs. Normo littermates ($p < 0.001$), and fully restored by Curc (not statistically significant vs. Normo; $p < 0.01$ vs. Hyper). Similarly, as detailed by the EGL thickness graph (**Figure 4.2e**) the significant reduction in Hyper animals (50%, $p < 0.05$ vs. Normo), was reversed to the physiological level represented by the Normo pups by Curc (not statistically significant vs. Normo; $p < 0.01$ vs. Hyper).

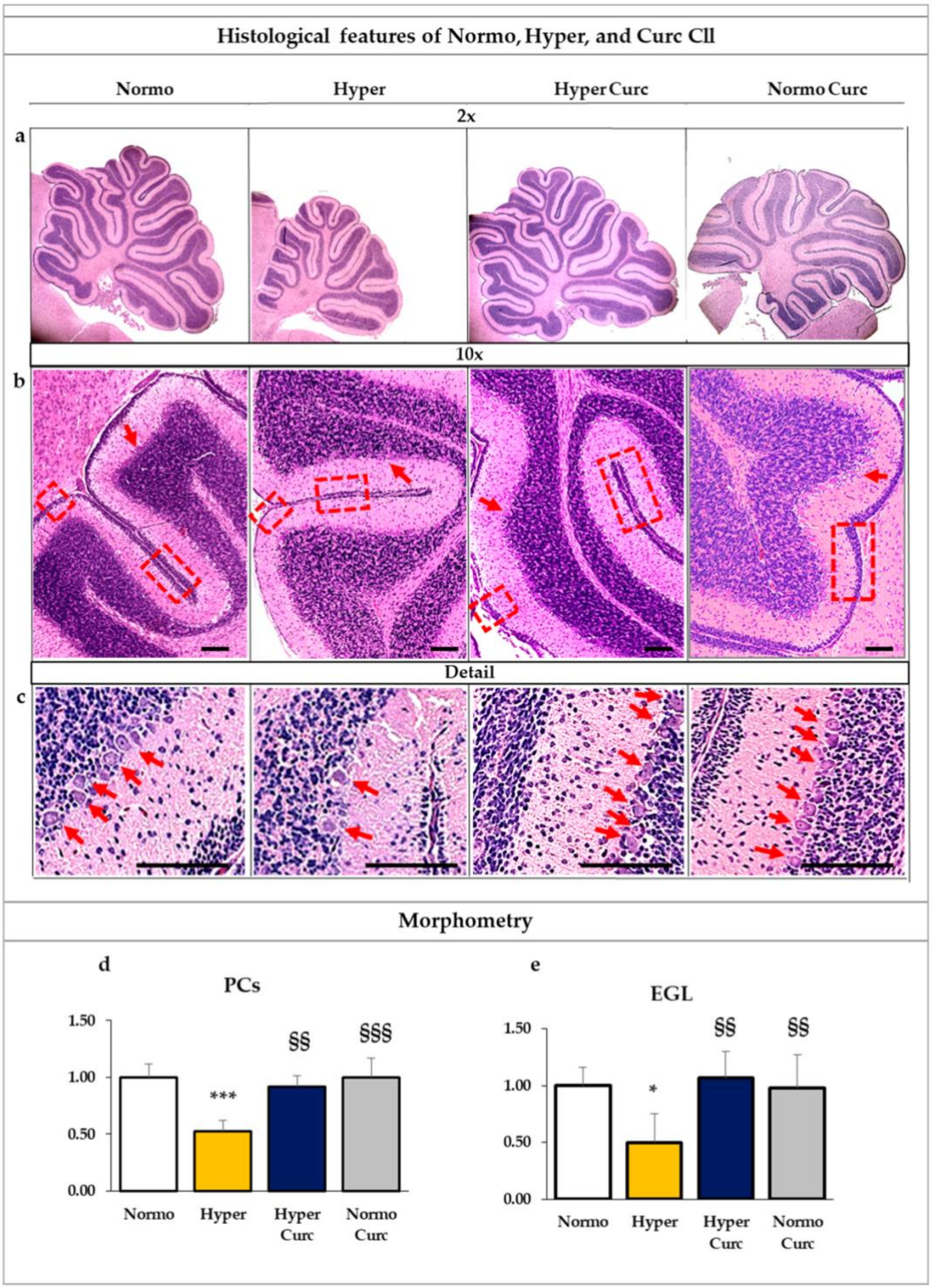

Figure 4.2. Curc prevents the alterations of the histological and morphometric features characteristic of the Hyper Gunn rat. (**a–c**) Histological features of the cerebellum (Cll) in Normo (normobilirubinemic), Hyper (hyperbilirubinemic), and curcumin (Hyper Curc and Normo Curc) treated P17 Gunn rats. Different magnifications are shown to allow appreciating the whole Cll details. (a) = 2×: Curc

fully prevents the reduction in the volume of the Cll present in the Hyper P17 pups. (**b**) = 10×: allows to better appreciate the general appearance of the external granule cell layer (EGL, e.g., squares) and the Purkinje cells (PCs, e.g., arrows), both reduced in Hyper, and reverted to the physiological features by Curc. The protective effect of Curc on PC number is even more visible in (**c**) the detailed picture (e.g., arrows). Scale bar: 200 μm. (d,e) Morphometric evaluation of the PC number (**d**) and external EGL thickness (**e**). White bars: Normo; yellow bars: Hyper; blue bars: Hyper Curc; grey bar Normo Curc. Data are in mean ± S.D. and expressed as fold vs. the Normo pups used as reference (=1). Three animals of each genotype and treatment were devoted to this goal. Statistical significance was evaluated by the one-way analysis of variance (ANOVA), followed by a Tukey–Kramer Multiple Comparisons Test when p-value < 0.05. Statistical significance: */***: $p < 0.05$, $p < 0.001$ vs. Normo age-matched pups. §§/§§§: $p < 0.01$, $p < 0.01$ vs. Hyper age-matched pups.

4.1.3 Behavioral Tests

As conclusive evidence of the protection from brain damage conferred by the molecule, we evaluated the behavior of the pups (**Figure 4.3**) by two tests: the righting reflex, and negative geotaxis (see detail on the material and method section).

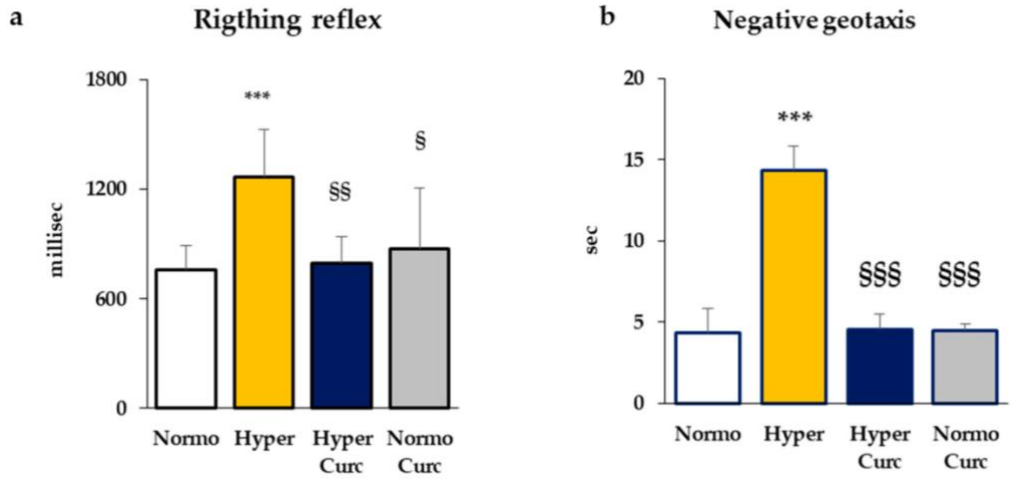

Figure 4.3. Curc restores the motor abilities of Hyper Gunn rats. The righting reflex (**a**) and the negative geotaxis (**b**) were selected as optimal tests for assessing the motor and coordination abilities of Gun rat pups. With white bars—untreated

normobilirubinemic (Normo) Gunn pups; yellow bars—untreated hyperbilirubinemic rats (Hyper); blue bars—curcumin-treated hyperbilirubinemic pups (Hyper Curc); gray bars—curcumin-treated normobilirubinemic pups (Normo Curc). Data are in mean ± S.D., and in milliseconds (millisec) for the righting reflex and in seconds (sec) in the negative geotaxis test. In each experimental group, ≥3 animals were studied. Statistical significance was evaluated by the one-way analysis of variance (ANOVA), followed by a Tukey–Kramer Multiple Comparisons Test when p-value < 0.05. Statistical significance: ***: $p < 0.001$ vs. Normo pups. §; §§, §§§: $p < 0.05$, $p < 0.01$, $p < 0.001$ vs. Hyper rats.

As shown in **Figure 4.3**, Hyper pups needed a significantly longer time for finishing both the tests. In the righting reflex test (**Figure 4.3a**), while Normo pups rapidly regained the correct position, Hyper pups required about 1.7-fold more time ($p < 0.001$ vs. Normo). Hyper Curc performed as the controls (not statistically different from Normo; $p < 0.01$ vs. Hyper).

Similarly, Hyper rats were statistically less skilled ($p < 0.001$) compared to Normo littermates in the negative geotaxis test (**Figure 4.3b**). Also, in this test, the performance of Hyper pups was fully restored by Curc treatment (Hyper Curc, not statistically different from Normo; $p < 0.001$ vs. Hyper).

4.1.4 Monitoring of the Side Effects of the Treatment

In the end, 14 Hyper pups and 12 Normo littermates as controls were treated with Curc. No distress at the daily monitoring[275], no decreased Cll weight (**Figure 4.1a)**, no changed TSB (**Figure 4.1b**), no abnormal morphometric features (**Figure 4.2**), no abnormal behavior (**Figure 4.3**), no decreased body weight (**Figure 4.4**), no deaths were

observed, indicating the absence of side effects for this formulation of Curc in this model.

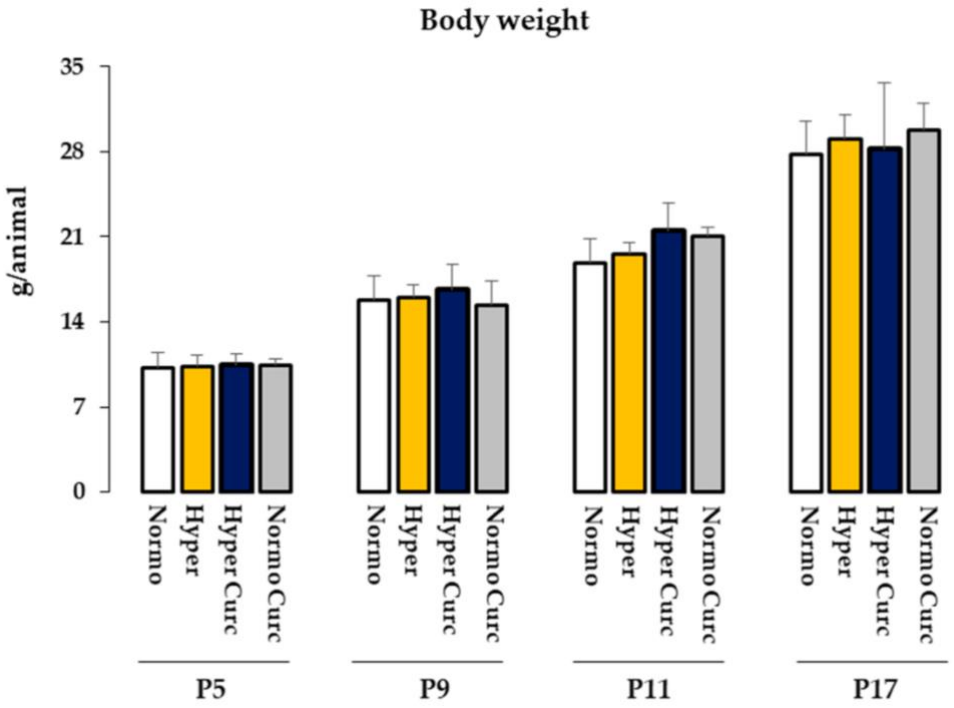

Figure 4.4. Bodyweight recording. Bodyweight in developing Gunn rats is expressed as mean ± S.D., and as g/animal. P: post-natal age in days. With white bars—untreated normobilirubinemic (Normo) Gunn pups; yellow bars—untreated hyperbilirubinemic rats (Hyper); blue bars—curcumin treated hyperbilirubinemic pups (Hyper Curc), grey bars—Curc treated Normo rats (Normo Curc). In each experimental group, ≥10 animals were studied. No statistical differences were noticed.

4.1.5 Effects of Curcumin on the Main Molecular Effectors Involved in Bilirubin Brain Damage

To substantiate the ability of Curc in preventing bilirubin-induced Cll damage, we explored the modulation of selected markers of inflammation, redox imbalance, as well as glutamate release [9]–[11][64],

[65], [76], [84], [87], [202], [209], [276], [278], [299]–[309] both at gene and protein level.

4.1.5.1 Evaluation of the Effect of Curcumin on the Inflammatory Markers

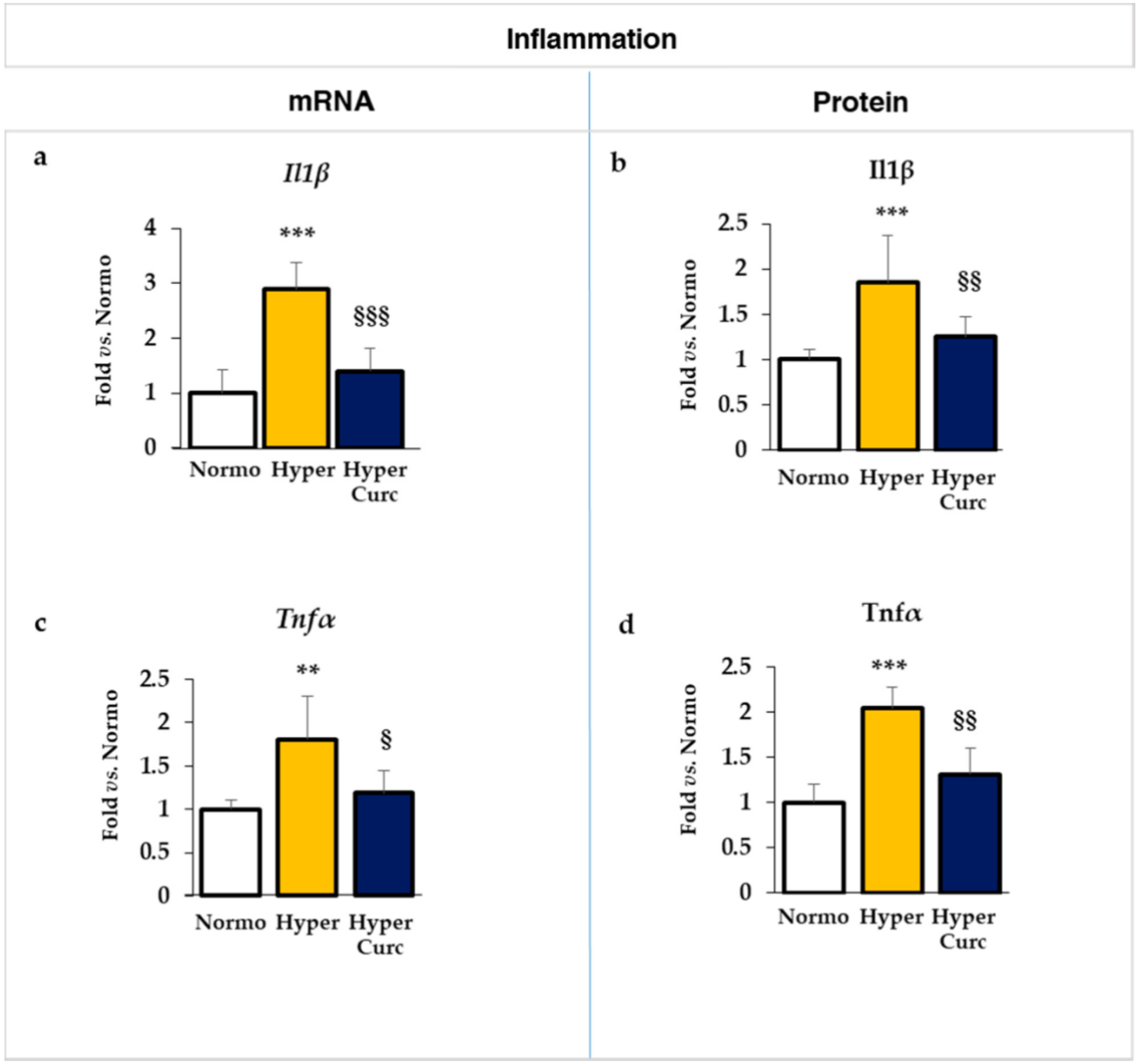

Figure 4.5. Curc prevents the induction of inflammation in the Hyper Gunn rat. The effect of Curc on the mRNA (**a,c**) and protein (**b,d**) level of *Il1β*/Il1β (interleukin 1beta—**a,b**) and *Tnfα*/Tnfα (tumor necrosis factor-alpha, **c,d**) were evaluated by RTqPCR and ELISA, respectively. With white bars—untreated normobilirubinemic (Normo) Gunn pups; yellow bars—untreated hyperbilirubinemic rats (Hyper); blue bars—curcumin-treated hyperbilirubinemic pups (Hyper Curc). Data are in mean ± S.D. and expressed as fold vs. the Normo

pups used as reference (=1). In each experimental group, ≥6 animals were studied. Statistical significance was evaluated by the one-way analysis of variance (ANOVA), followed by a Tukey–Kramer Multiple Comparisons Test when p-value < 0.05. Statistical significance: **, ***: $p < 0.01$ and $p < 0.001$ vs. Normo pups. §; §§, §§§: $p < 0.05$, $p < 0.01$, $p < 0.001$ vs. Hyper rats.

As reported in **Figure 4.5** the mRNA (italicized) expression of both *Il1β* (interleukin-1 beta, **Figure 4.5a**) and *Tnfα* (tumor necrosis factor-alpha, **Figure 4.5c**) was significantly increased in Hyper vs. Normo pups ($p < 0.001$ and $p < 0.01$, respectively). In hyperbilirubinemic rats treated with Curc, the expression of both cytokines decreased to levels comparable to the Normo controls (both not significantly different vs. Normo. *Il1β* $p < 0.001$ and *Tnfα* $p < 0.05$ vs. Hyper).

The same pattern was found at the level of the proteins (**Figure 4.5b–d**, not italicized), where the two times up-regulation present in Hyper pups for both Il1β and Tnfα (both $p < 0.001$), was reversed by Curc to a level comparable with the Normo rats (1.25-fold and 1.31-fold, respectively, both not statistically significant vs. Normo. Both $p < 0.01$ vs. Hyper).

4.1.5.2 Evaluation of the Effect of Curcumin on the Glutamate Cll Content

As shown in **Figure 4.6**, the 1.5 times increase of the glutamate (Glut) content in the Cll of Hyper rats ($p < 0.01$), responsible for glutamate neurotoxicity, was also restored by Curc to levels found in the Normo animals (not statistically different from Normo; $p < 0.05$ vs. Hyper).

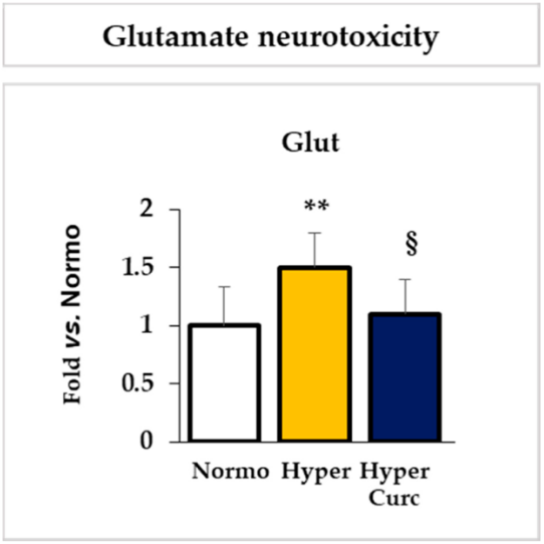

Figure 4.6. Curc prevents the increase of glutamate in the Hyper Gunn rat. The effect of Curc on the glutamate content in the Cll of hyperbilirubinemic pups was quantified by an enzymatic test. With white bars—untreated normobilirubinemic (Normo) Gunn pups; yellow bars—untreated hyperbilirubinemic rats (Hyper); blue bars—curcumin-treated hyperbilirubinemic pups (Hyper Curc). Data are in mean ± S.D. and expressed as fold vs. the Normo pups used as reference (=1). In each experimental group, ≥6 animals were studied. Statistical significance was evaluated by the one-way analysis of variance (ANOVA), followed by a Tukey–Kramer Multiple Comparisons Test when p-value < 0.05. Statistical significance: **: $p < 0.01$ vs. Normo pups. § $p < 0.05$ vs. Hyper rats.

4.1.5.3 Evaluation of the Effect of Curcumin on the Redox Markers

Similar to cytokines, the mRNA expression of *Hmox1* (Heme oxygenase 1, **Figure 4.7a**), a redox sensor, was significantly up-regulated in Hyper pups ($p < 0.05$), and reverted in Hyper rats treated with Curc. At the level of the protein (**Figure 4.7b**), despite no statistical significance, a trend toward induction in Hyper pups, again, reverted by Curc was observed.

Collectively, these data support the conclusion that Curc interferes with the main pathological mechanisms undergoing bilirubin brain toxicity [278] preventing brain damage and restoring brain functions in Hyper Gunn pups.

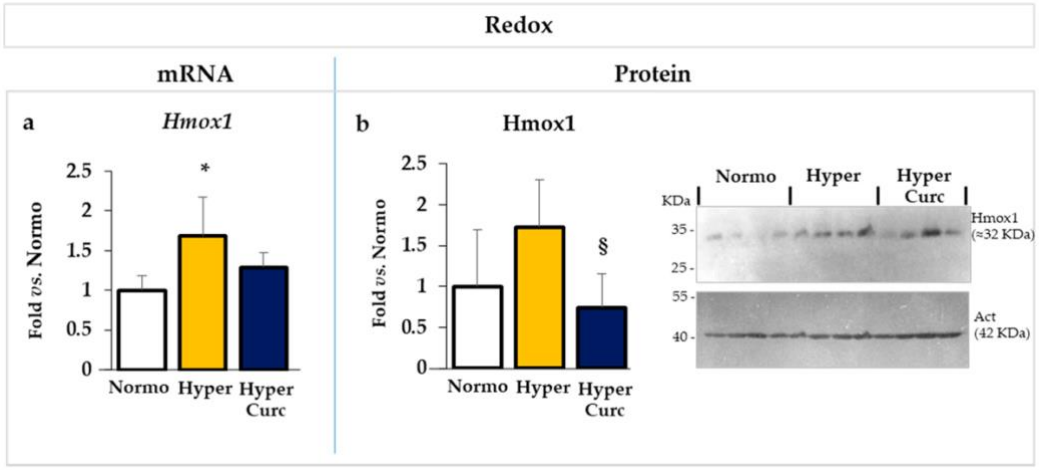

Figure 4.7. Curc prevents the increase in the redox stress in the Hyper Gunn rat. The effect of Curc on the mRNA (**a**) and protein (**b**) level of *Hmox1*/Hmox1 (heme oxygenase 1), a redox sensor, was evaluated by RTqPCR and Western blot, respectively. With white bars—untreated normobilirubinemic (Normo) Gunn pups; yellow bars—untreated hyperbilirubinemic rats (Hyper); blue bars—curcumin-treated hyperbilirubinemic pups (Hyper Curc). Data are in mean ± S.D. and expressed as fold vs. the Normo pups used as reference (=1). In each experimental group, ≥6 animals were studied. Statistical significance was evaluated by the one-way analysis of variance (ANOVA), followed by a Tukey–Kramer Multiple Comparisons Test when p-value < 0.05. Statistical significance: *: $p < 0.05$ vs. Normo pups. § $p < 0.05$ vs. Hyper rats.

4.1.6. Additional Evaluation of Curcumin Protection: Selected Markers of Brain Development

To further explore the efficacy of Curc protection, we monitored selected genes/proteins involved in brain development and maturation, whose alterations in Hyper Gunn rats have been recently suggested to participate in the progression of cerebellar hypoplasia, and that we know to be altered at P17 in Hyper pups [274].

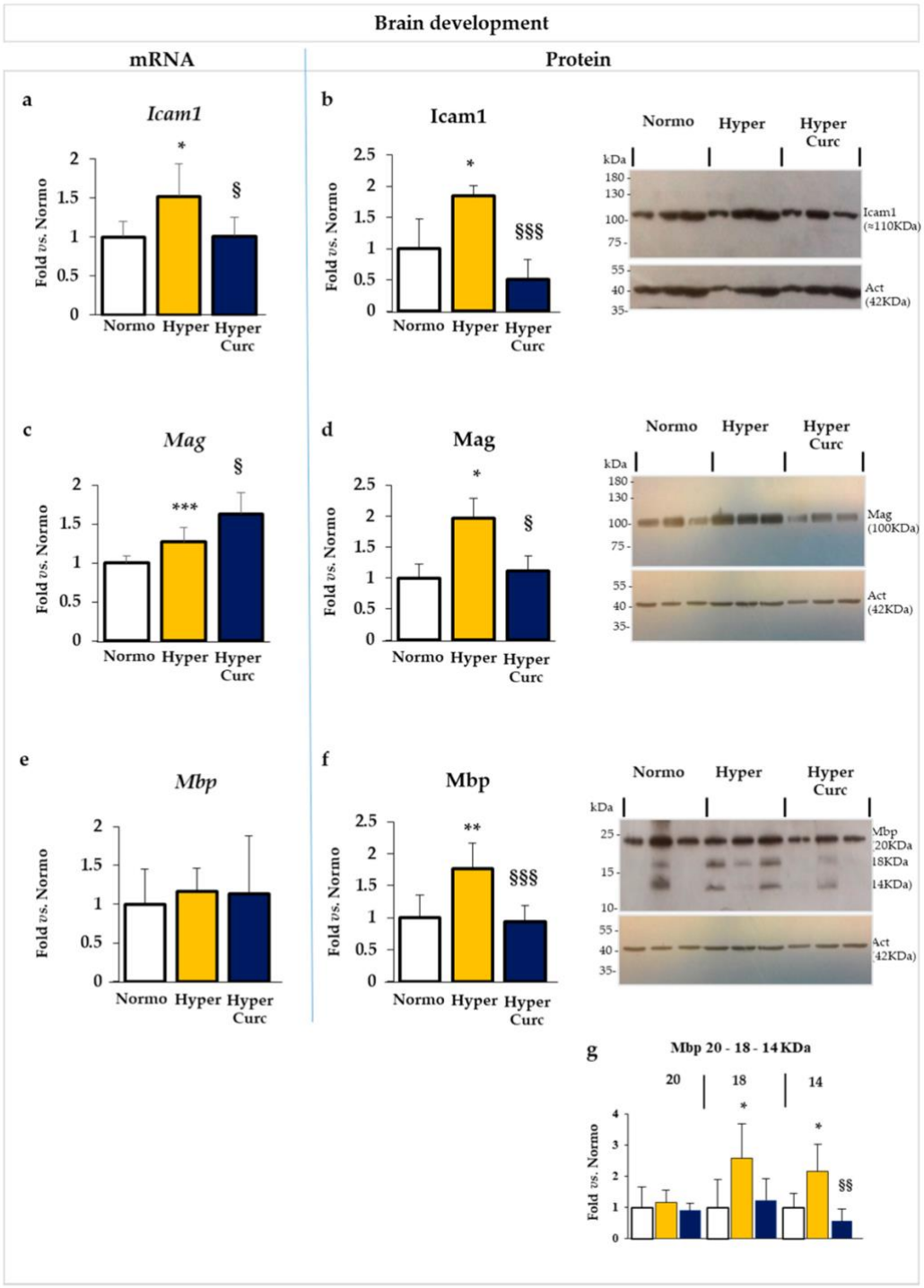

Figure 4.8. Curc normalizes the level of selected markers of brain development in the Hyper Gunn rat. The effect of Curc on the mRNA (**a**,**c**,**e**) and protein (**b**,**d**,**f**,**g**) level of *Icam1*/Icam1 (intercellular adhesion molecule 1,**a** ,**b**), *Mag*/Mag (myelin-associated glycoprotein, **c**,**d**), and *Mbp*/Mbp (myelin basic protein, **e**,**f**,**g**), known to be altered in P17 Hyper pups, were evaluated by RTqPCR and Western blot, respectively. With white bars—untreated normobilirubinemic (Normo) Gunn

pups; yellow bars—untreated hyperbilirubinemic rats (Hyper); blue bars—curcumin-treated hyperbilirubinemic pups (Hyper Curc). Data are in mean ± S.D. and expressed as fold vs. the Normo pups used as reference (=1). In each experimental group, ≥6 animals were studied. Statistical significance was evaluated by the one-way analysis of variance (ANOVA), followed by a Tukey–Kramer Multiple Comparisons Test when p-value < 0.05. Statistical significance: *, **, ***: $p < 0.05$, $p < 0.01$, $p < 0.001$: vs. Normo pups. §, §§, §§§: $p < 0.05$, $p < 0.01$, $p < 0.001$ vs. Hyper rats.

As shown in **Figure 4.8a**,**b**, *Icam1*/Icam1 (intercellular adhesion molecule 1—involved in brain maturation and morphogenesis [274]) mRNA (**Figure 4.8a**) and protein (**Figure 4.8b**) levels were both significantly increased in Hyper pups (both $p < 0.05$ vs. Normo) reverting to a level comparable to controls in Curc rats.

Mag (myelin-associated glycoprotein: myelination, dendritogenesis, cell projection organization [274]) mRNA (**Figure 4.8c**); was only marginally increased in Hyper, but was significantly upregulated in Hyper pups treated with Curc ($p < 0.001$ vs. Normo; $p < 0.05$ vs. Hyper). Conversely, the protein level of Mag (**Figure 4.8d**) was significantly induced in Hyper pups ($p < 0.05$), fully reversing to the physiological level in rats treated with the molecule.

No relevant mRNA modulation of *Mbp* (**Figure 4.8e**) myelin basic protein: stabilization of myelin [310]) was detected neither in Hyper nor Hyper Curc rats with respect to Normo littermates. At the protein level (**Figure 4.8f**), similarly to Mag, Mbp was induced in Hyper ($p < 0.01$ vs. Normo) and restored to the physiological level by Curc (no statistical difference vs. Normo; $p < 0.001$ vs. Hyper). The up-regulation (and normalization under Curc treatment) in the protein level of Mbp in Hyper pups was due to an increase of the 18 and 14KDa bands (both $p < 0.05$ vs.

Normo), while the 20KDa protein was not significantly different from Normo or Hyper Curc samples (**Figure 4.8g**: detail on Mbp quantification).

The high molecular weight (MW) isoform of Mbp is known to control the proliferation of the oligodendrocytes, while the two lower bands represent the mature myelin strongly expressed by mature oligodendrocytes in rodents [310], [311]. Interesting is the good agreement with the increased level of Mag in Hyper pups, with Mag involved in myelin stabilization and repair after demyelinating injuries [312]. In this paper, we are not focusing on the mechanisms of bilirubin brain damage, nevertheless, the data support our previous hypothesis [274] that Hyper pups at P17 try to react to the insult of bilirubin occurred in the post-natal development by increasing myelination. By preventing the bilirubin brain damage, Curc may not be associated with the hyper-activation of Mag and Mbp. The alteration (perturbation and recovery) of myelin production in the developing hyperbilirubinemic Gunn rat, is an interesting point that should be better addressed in the future by a devoted study.

4.2 TASK 2 – Bilirubin Neuroprotection in an *ex vivo* Parkinson's disease model

4.2.1 TASK2A: Bilirubin reverses the dopaminergic neuron demise in an *ex vivo* Parkinson's disease (PD) model

4.2.1.1 Safety test of UCB in the OBCs-SN

As shown by panel **Figure 4.9a**, all UCB concentrations used in the experiment have been calculated for having free bilirubin (Bf) lower than 4 nM, physiological concentrations, or Gilbert-like conditions [287], [313] that also has been demonstrated as non-toxic concentrations based on preliminary data. Based on the safety test all the selected UCB concentrations alone (no co-treatment with Rot) were not toxic to the slices (**Figure 4.9b**).

As depicted in **Figure 4.10**, the number of DOPAn under Rot challenge was reduced by 40% (Rot = black bar; $p \leq 0.01$ *vs.* Ctrl = blue bar), in line with the clinical scenario of motor PD at diagnosis [314], [315]. 0.5μM and 1μM UCB (yellow bars, corresponding to a Bf lower than 1nM – **Figure 4.9a**) in co-treatment with Rot, fully reversed the DOPAn demise ($p < 0.05$ *vs.* Rot). The protective effect was lost at higher UCB concentrations (2μM and 4μM, both corresponding to a Bf higher than 1.5nM – **Figure 4.9a**).

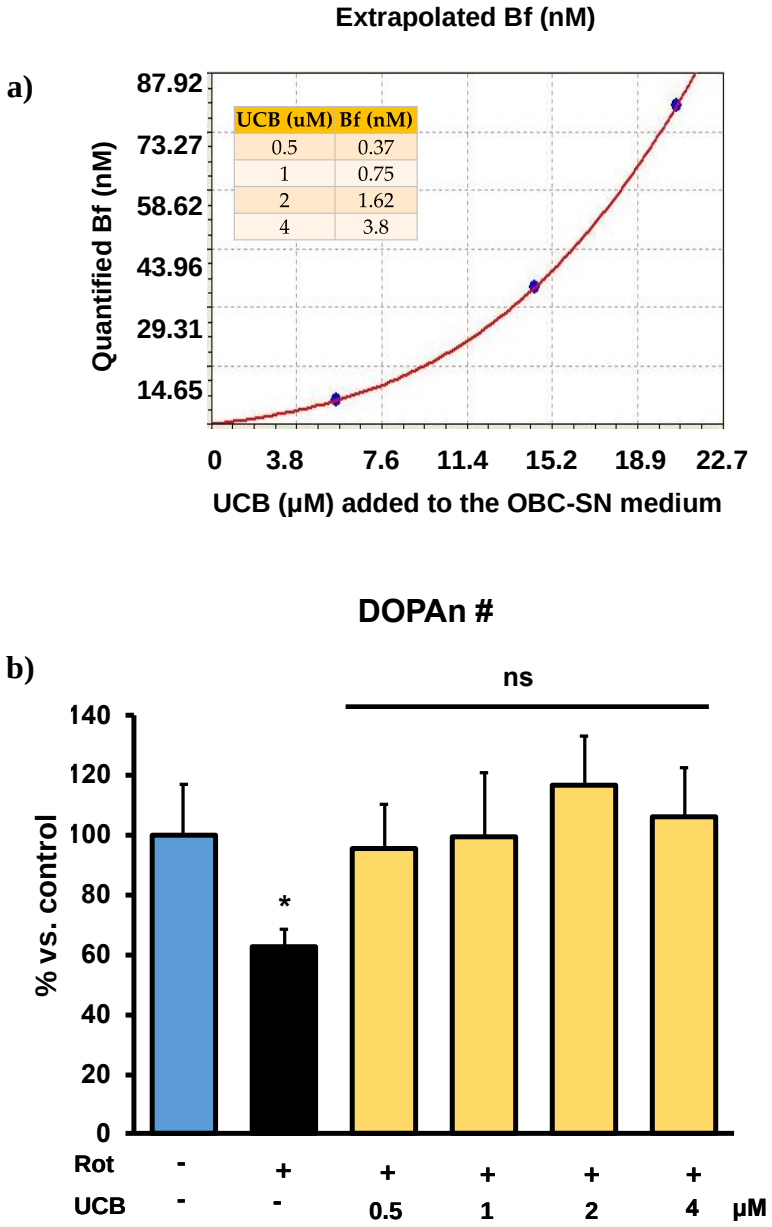

Figure 4.9. Bf (free bilirubin) calculation and UCB safety test. a) Extrapolated free bilirubin (Bf) in the OBCs-SN media. In culture media containing albumin (carried by FBS) the moiety of bilirubin able to enter the cells is limited to the albumin-unbound UCB, named free bilirubin (Bf). **b)** Counting of the DOPAn number in OBCs-SN slices exposed to UCB alone. Data are expressed as % *vs.* control and as mean ± S.D. of at least 4 independent repetitions. Statistical significance: *vs.* Control ** $p < 0.01$, ns: non significant.

4.2.1.2 Low levels of UCB protect from the DOPAn loss in the OBCs-SN model of PD

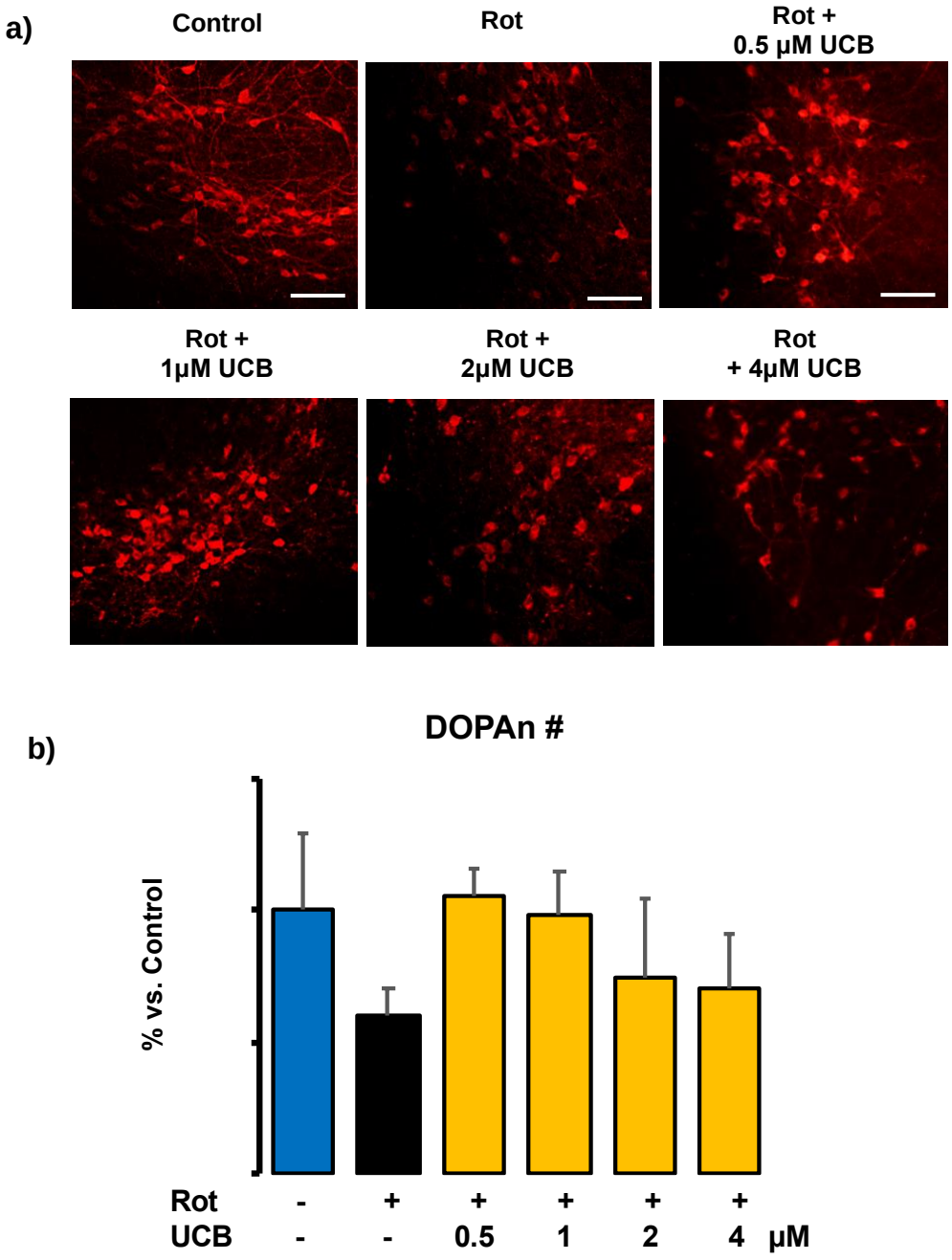

Figure 4.10. Dopaminergic neurons (DOPAn) number in bilirubin treated slices. To assess the effect of rotenone (Rot) challenging and unconjugated bilirubin (UCB) protection, dopaminergic neurons (DOPAn) numbers were counted in each treatment. **a)** Representative pictures of tyrosine hydroxylase (TH+) DOPAn

immunofluorescence (red signal). Scale bar 100 μm. **b)** Percentage of DOPAn number under Rot challenging (black bar) and UCB-Rot co-treatment (yellow bars) vs. controls (DMSO, blue bar). Data are expressed as % *vs.* control and as mean ± S.D. of at least 4 independent repetitions. Statistical significance: *vs.* Control ** $p < 0.01$; *vs.* Rot § $p < 0.05$.

4.2.1.3 Screening for the molecular mechanisms of protection

To understand the molecular mechanisms involved in UCB protection at 0.5 and 1uM, we investigated the early potential triggers of DOPAn demise previously identified [135].

Because UCB is a well-known antioxidant [316]–[319], at first we assessed the mRNA expression of *Hmox1* (heme oxygenase 1, redox sensor) and *Srxn1* (sulfiredoxin 1, belonging to the battery of adaptive to redox stress genes, and known to be induced by Hmox1 [320], [321]. Rot treatment significantly up-regulated *Hmox1* expression *vs.* ctrl (**Figure 4.11a**, Rot: black bar, Ctrl: blue bar, $p < 0.05$). Despite the lack of a statistical significance, a trend in reduction of *Hmox1* level was observed with 0.5μM and 1μM UCB (yellow bars), whereas 2μM and 4μM UCB (yellow bars) were not able to down-regulate the expression of the redox sensor.

Rot treatment increased *Srxn1* level compared to control (**Figure 4.11b**, $p < 0.05$), with all the UCB treatments unable to normalize its

expression, or even increased it at a level higher than in the PD model (4µM UCB, $p < 0.001$ *vs.* Ctrl).

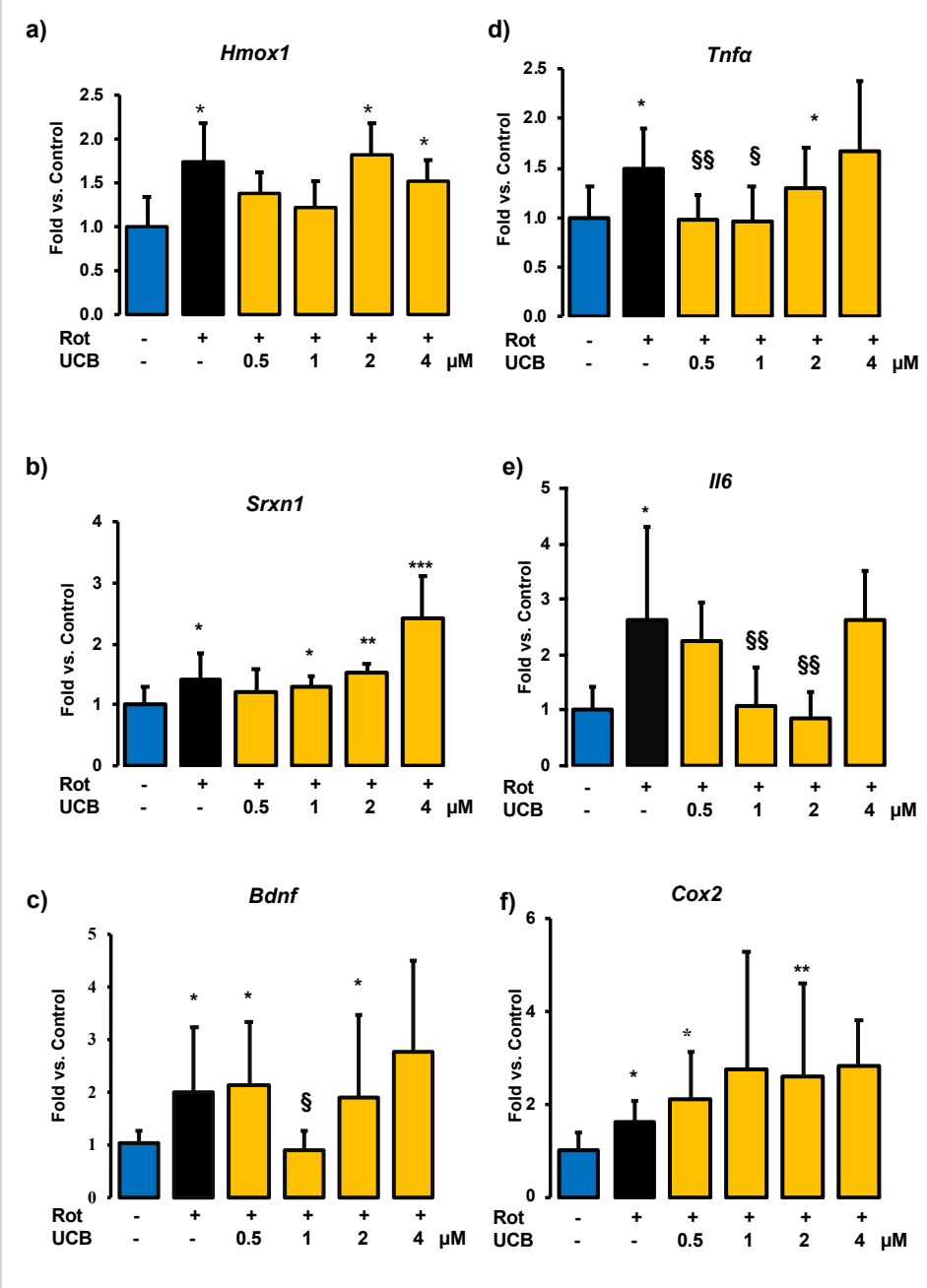

Figure 4.11. Evaluation of the changes in the early potential mechanisms of DOPAn loss. To evaluate the potential molecular mechanisms involved in UCB protection, we assessed the expression of the previously identified early molecular markers of DOPAn demise: *Hmox1*: heme-oxygenase 1 and *Srxn1*: sulfiredoxin 1

for redox stress; *Bdnf:* brain derived neurotrophic factor and *Tnf-α*: tumour necrosis factor alpha, *Il6*: interleukin 6; *Cox2*: cyclooxygenase 2 for inflammation. Blue bar: controls; black bar: rotenone (Rot); yellow bars: co-treatment Rot +UCB from 0.5μM to 4μM. Data (mRNA expression) are expressed as fold vs. controls, and as mean ± SD of at least 3 independent repetitions. Statistical significance: vs. control * $p < 0.05$, ** $p < 0.01$, ***$p < 0.001$. Vs. Rot § $p < 0.05$, §§ $p < 0.01$.

The expression of brain-derived neurotrophic factor (*Bdnf)*, altered both in PD patients and in our model [322]–[325], was significantly increased after Rot exposure (**Figure 4.11c**, $p < 0.05$). 0.5μM, 2μM, and 4μM UCB did not change it. 1μM was the only UCB concentration able to revert the *Bdnf* expression to the control level ($p < 0.05$).

Rot treatment also significantly increased the level of the inflammatory markers: tumor necrosis factor-α (*Tnfα*, **Figure 4.11d**), interleukin 6 (*Il6*, **Figure 4.11e**), and cyclooxygenase 2 (*Cox2*, **Figure 4.11f**), all $p < 0.05$). 0.5μM and 1μM UCB treatment reduced the *Tnfα* expression to the control level ($p < 0.01$ and $p < 0.05$ *vs.* Rot, respectively), while at 2μM and 4μM the effect was lost (**Figure 4.11d**). UCB induced a "U-shape" normalization of the *Il6* up-regulation present (**Figure 4.11e**) in the Rot challenged slices. 0.5μM UCB exhibited minimal normalizing effect, 1μM and 2μM UCB fully reversed the *Il6* expression (both $p < 0.01$ *vs.* Rot), with the effect lost at 4μM UCB. No reduction effect was observed in *Cox2* levels (**Figure 4.11f**) at all tested UCB concentrations to Rot.

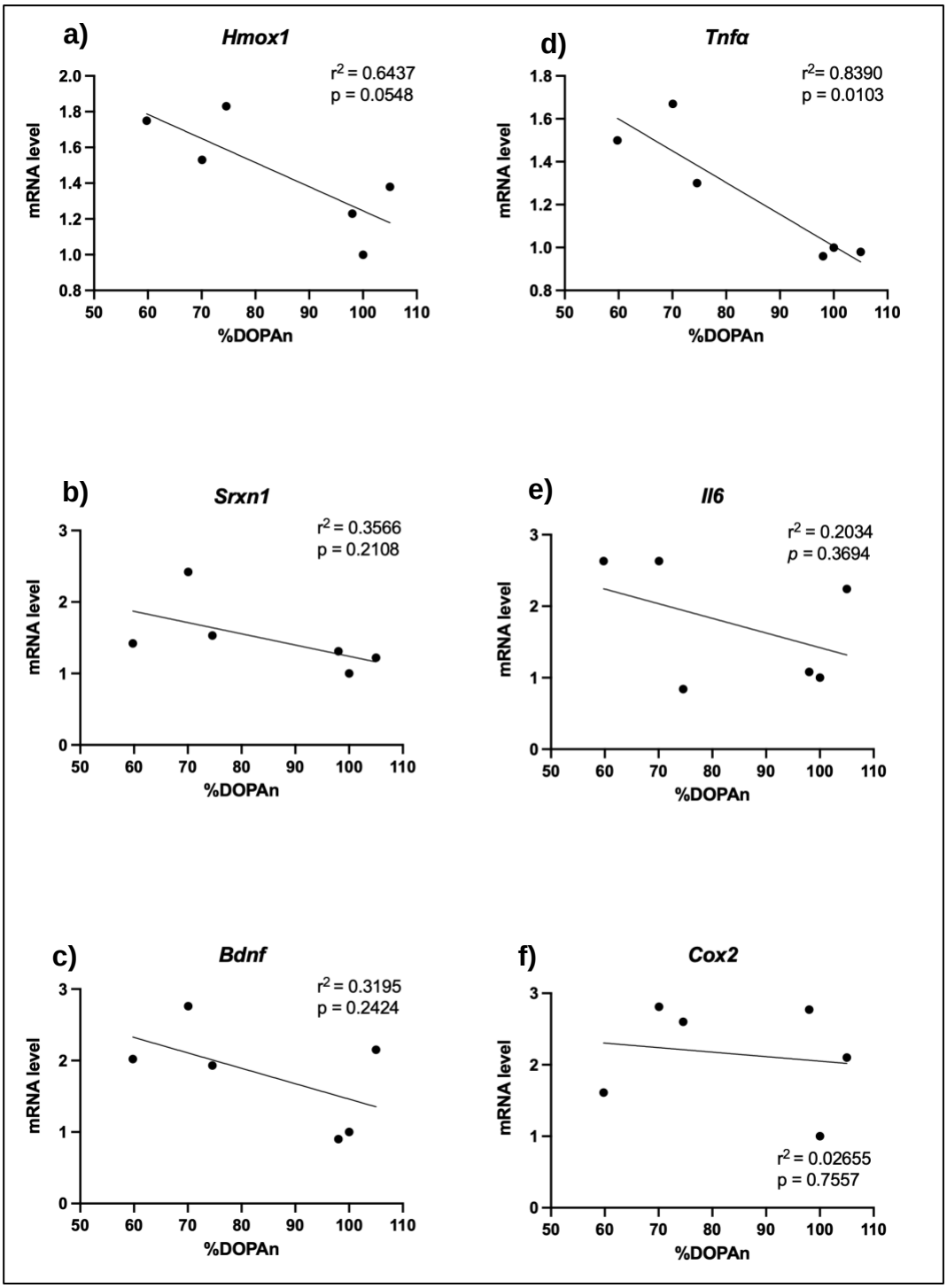

Figure 4.12. Correlation between DOPAn percentage and gene expression of inflammation, oxidative stress, and neurotrophic growth factor markers. *Hmox1*: heme-oxygenase 1 and *Srxn1*: sulfiredoxin 1 for redox stress; *Bdnf:* brain-derived neurotrophic factor and *Tnf-α*: tumor necrosis factor-alpha, *Il6*: interleukin 6; *Cox2*: cyclooxygenase 2 for inflammation. Lines represent linear regression.

A correlation analysis was performed to analyse the relationship between DOPAn number and each molecular mechanism. As depicted in **Figure 4.12**, among all markers only *Tnfα* significantly correlated with the percentage of DOPAn. From this result, we hypothesized that *Tnfα* may play a significant role in DOPAn demise and UCB protection.

4.2.1.4 Unraveling the role of redox imbalance in the model

Although the correlation analysis between *Hmox1* and DOPAn percentage was insignificant (**Figure 4.12a**), the decreasing trend of *Hmox1* after 0.5μM and 1μM UCB treatment in PD model **(Figure 4.11a)**, as well as the fact of UCB as powerful antioxidant [8], [326] brought us to the curiosity about the redox status in our model. Therefore, we deeply investigated not only the involvement of the redox stress but also the absence of a role of redox stress in UCB protection on the early mechanisms triggering DOPAn loss in our model by adding two sets of experiments.

At first, we investigated the glutathione content in our cultures medium (**Figure 4.13**), then, to further clarify the role of oxidative imbalance on DOPAn demise, slices were co-exposed to Rot and a wide range of concentrations of N-acetyl cysteine (NAC, from 10 to 15,000μM, **Figure 4.14**), a powerful antioxidant[327]. Because the induction of the redox stress is known to act quickly, we performed a time course from 5 minutes after Rot exposure up to the ending of the experimental time (24 hours).

a. Evaluation of the GSH/GSSG ratio, GSH, and GSSG along the experimental time

As shown in **Figure 4.13a**, the GSH/GSSG ratio in culture medium was significantly reduced shortly after Rot challenge (5 min, black bar, $p <$

0.05), demonstrating the expected induction of oxidative stress by the pesticide [328], [329]. The reduction of GSH/GSSG ratio was not reverted by 0.5μM UCB exposure ($p < 0.05$ *vs*. DMSO). Meanwhile, the level of GSH/GSSG was unchanged at 1μM and 2μM UCB treatment (not significant *vs.* Ctrl and Rot). Only 4μM UCB treatment was able to revert the change of GSH/GSSG ratio ($p < 0.01$ *vs.* Rot). This result indicates that the protective effect of UCB against Rot-induced DOPAn loss is independent of its antioxidant effect.

The previously indicated redox stress (the reduction of the GSH/GSSG ratio) under 5 minutes of Rot exposure was solely due to a significant decrease of the reduced glutathione (GSH, $p < 0.01$ **Figure 4.13b**) as no changes were observed in the oxidized form (GSSG) level (**Figure 4.13c**). No changes of GSH at 5 minutes (**Figure 4.13b)** were observed in any concentrations of UCB, except for 4μM UCB showing a significant increase of GSH ($p < 0.05$ *vs.* Rot). Meanwhile, the decrease of glutathione ratio at 0.5μM UCB (**Figure 4.13a**) was caused by the increase of GSSG ($p < 0.05$ *vs* DMSO), indicative of redox stress.

After 20 minutes, no differences in the GSH/GSSG ratio (**Figure 4.13a**), or GSH (**Figure 4.13b**) and GSSG (**Figure 4.13c**) content between controls, Rot, and UCB samples were observable.

The GSH/GSSG ratio significantly increased under the Rot challenge at 1 hours (**Figure 4.13a**, $p < 0.01$ *vs.* Ctrl) as well as 0.5μM UCB (**Figure 4.13a**, $p<0.001$ *vs.* Ctrl), 1μM UCB and 2μM UCB (**Figure 4.13a**, $p < 0.01$ *vs.* Ctrl), while 4μM UCB stayed unchanged. The GSH/GSSG ratio under Rot treatment was found even higher at 3 hours (**Figure 4.13a**, $p < 0.001$ *vs.* Ctrl). This was in agreement with other models using low amounts

of Rot, describing a late tentative reaction to the redox imbalance induced by the pesticide [330]. The change in the GSH/GSSG ratio under Rot treatment was driven by the reduced form of glutathione (GSH, the "protective one"), reaching a significant up-modulation at 3 hours (Rot, **Figure 4.13b**, $p < 0.05$ vs. control), while no changes in the oxidized glutathione (GSSG) were observed (Rot, **Figure 4.13c**). At that time (3h), co-exposing the slices to Rot and UCB avoided the potentially protective increase of both GSH/GSSG ratio and GSH content (3h, **Figure 4.13a and Figure 4.13b,** respectively).

At 24 hours, in GSH/GSSG ratio or GSH level in medium, no statistical differences among Ctrl and Rot were found, but significant reduction was detected in 0.5μM UCB and 4μM UCB (24h **Figure 4.13a and Figure 4.13b).**

We also evaluated the glutathione from OBCs-SN tissue. There was no significant change of both reduced and oxidized glutathione after Rot exposure at all the timing under analysis (**Figure 4.14**), indicating that glutathione level in tissue is less sensitive to use as a redox sensor than in medium. Differently, a decreasing trend of GSSG under all the UCB treatments was observed. This led only to a significant increase in the GSH/GSSG ratio under 0.5μM and 4μM UCB UCB treatment (**Figure 4.14a** $p<0.05$ *vs* DMSO).

Based on this glutathione analysis in the medium, we have confirmed that redox stress is present in our PD model and indeed UCB exhibits antioxidant activity. However, UCB protection against Rot-induced DOPAn loss seems independent from its antioxidant capacity

because it is not congruent with the DOPAn protection demonstrated by the neurons counting.

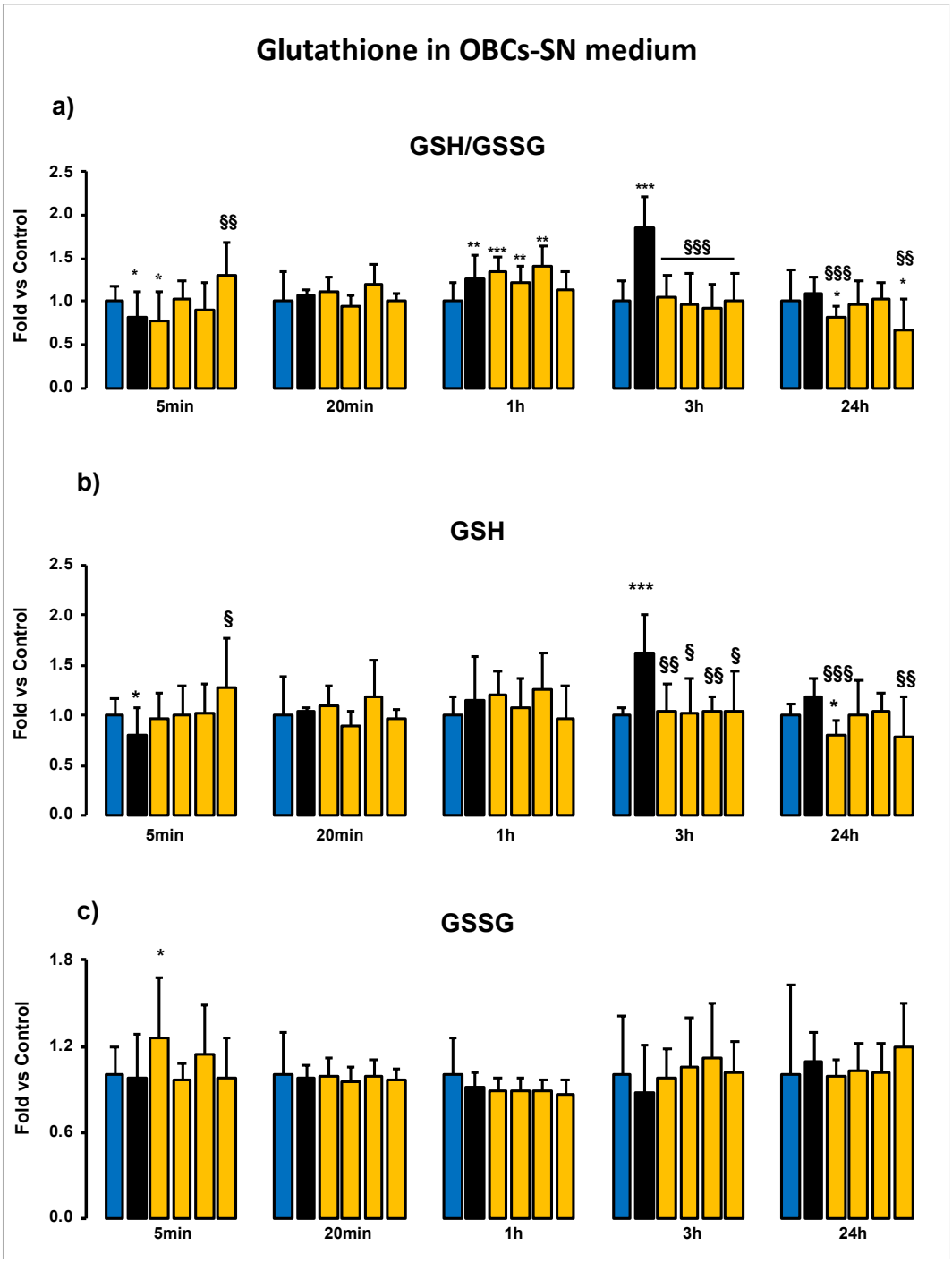

Figure 4.13 Time course of the glutathione changes in the OBCs-SN medium under Rot and UCB challenging. **a)** GSH/GSSG ratio, **b)** GSH, and **c)** GSSG. GSH: reduced glutathione; GSSG: oxidized glutathione; min: minutes. Blue bar: control; black bar: rotenone (Rot); yellow bar: co-treatment Rot +UCB

(from left to right: 0.5µM, 1µM, 2µM, and 4µM). Data are expressed as fold vs. control, and as mean ± SD of at least 4 independent repetitions. Statistical significance: vs. control * $p < 0.05$, ** $p < 0.01$; vs. Rot § $p < 0.05$.

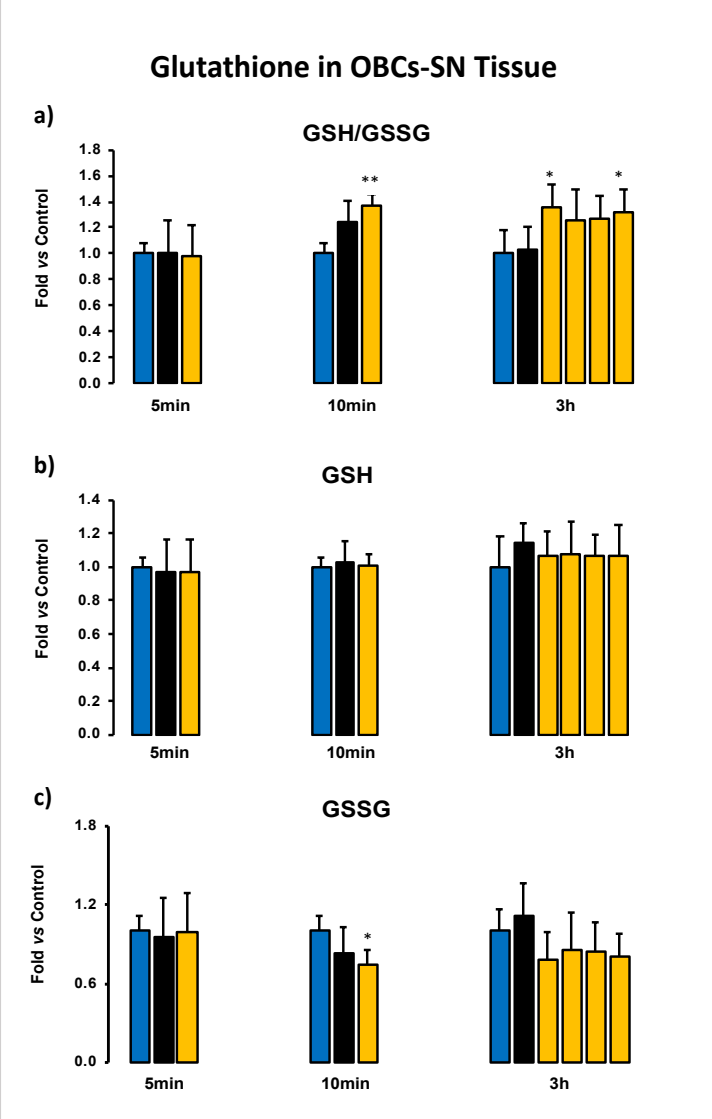

Figure 4.14 The glutathione changes in the OBCs-SN tissue under Rot and UCB challenging. **a)** GSH/GSSG ratio, **b)** GSH, and **c)** GSSG. GSH: reduced glutathione; GSSG: oxidized glutathione; min: minutes. Blue bar: control; black bar: rotenone (Rot); yellow bar: co-treatment Rot +UCB (from left to right: 0.5µM, 1µM, 2µM, and 4µM). Data are expressed as fold vs. control, and as mean ± SD of at least 3 independent repetitions. Statistical significance: vs. control * $p < 0.05$

b. NAC protection against the Rot induced redox imbalance

To rule out the protection against Rot-induced DOPAn is antioxidant dependent, we treated our model with NAC. When slices were co-exposed to Rot and NAC, a robust anti-oxidant [331], none of the concentrations of NAC used was able to increase the survival of DOPAn (**Figure 4.15**), definitively demonstrating that redox imbalance is not decisive in the DOPAn reduction as well as UCB-conferred protection.

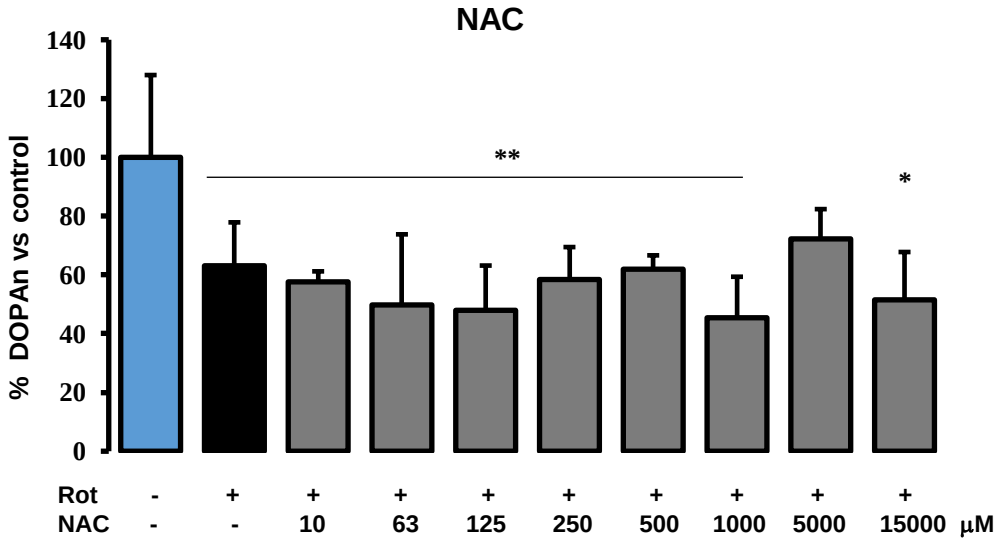

Figure 4.15. Effect of N-acetyl cysteine (NAC) treatment on DOPAn number. Blue bar: controls; black bar: rotenone (Rot); grey bars: co-treatment Rot + NAC from 10nM to 15,000nM. Data (DOPAn) are expressed as percentage (%) *vs.* control, and as mean ± SD of at least 5 independent repetitions. Statistical significance: *vs.* control * $p < 0.05$, ** $p < 0.01$, *** $p < 0.001$; *vs.* Rot § $p < 0.05$, §§ $p < 0.01$.

Altogether these data pointed out that, despite its powerful antioxidant potential, the UCB ability to rescue DOPAn from Rot toxicity was not congruent with its antioxidant effect in our OBCs-SN model of PD.

4.2.1.5 TNF-α role in DOPAn demise

We then decided to move forward with the evaluation of the other early induced mechanisms of damage involved in DOPAn loss [135], [322]–[329].

Among all the inflammatory mediators modulated by Rot in our model, only TNF-α modulation is correlated with DOPAn count (**Figure 4.12d**). Based on this finding, we hypothesized a major role for TNF-α in the induction of DOPAn loss (under Rot) and protection (under Rot and UCB co-treatment) in our PD model. To demonstrate our hypothesis, we used two opposite approaches (**Figure 4.16**). First, we treated the OBCs-SN with TNF-α alone (pink bars, in absence of Rot) and, as the second approach, we co-treated OBCs-SN with Rot and Infliximab, a monoclonal antibody neutralizing TNF-α (green bar)[291], [340], [341]. As usual, the count of TH+ DOPAn number was used to assess the results of the two experimental settings.

Challenging OBCs-SN with TNF-α induced a concentration-dependent decrease of the DOPAn number, with 60ng/mL TNF-α replicating the dopaminergic loss observed in the PD model (**Figure 4.16a**, TNF-α: pink bars, 40%, $p < 0.05$ *vs.* Ctrl: blue bar; compare with black bar: Rot). As counterprove, Infliximab co-treatment with the pesticide fully protected DOPAn toward Rot-induced death (**Figure 4.16b**, Infliximab: green bar *vs.* Ctrl: blue bar).

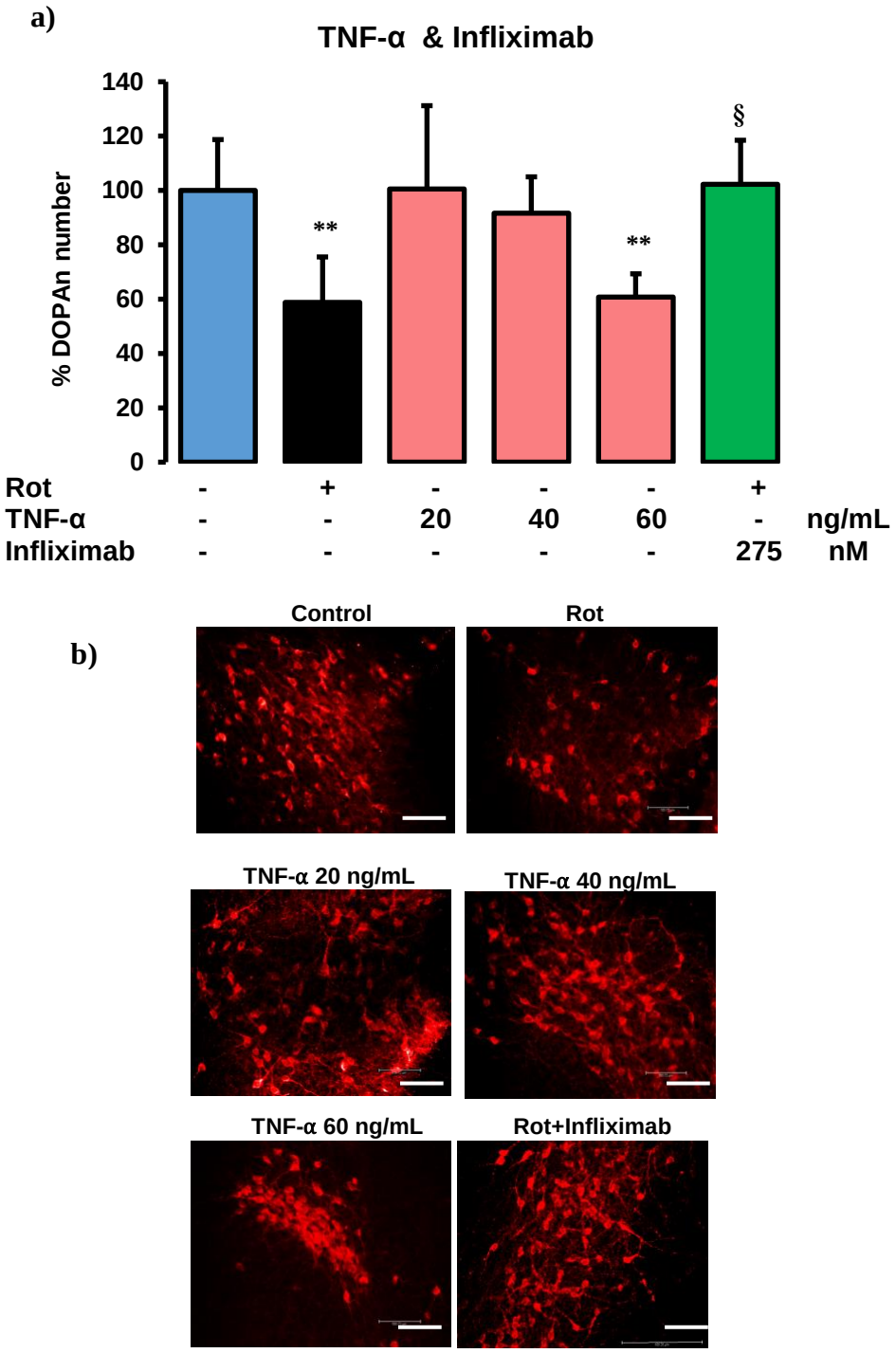

Figure 4.16. Demonstration of the TNF-α role in the DOPAn demise. **a)** Percentage of DOPAn count. Blue bar: controls; black bar: rotenone (Rot); pink bars: TNF-α from 20ng/mL to 60ng/mL, green bar: infliximab (anti TNF- α). Data (DOPAn) are expressed as percentage (%) *vs.* control, and as mean ± SD of at least 3 independent repetitions. Statistical significance: *vs.* control ** $p < 0.01$; *vs.* Rot § $p < 0.05$. **b)** Representative pictures of tyrosine hydroxylase (TH+) DOPAn immunofluorescence (red signal). Scale bar 100 μm.

The data confirmed that TNF-α is the key player in DOPAn loss in the model and that UCB conferred protection by acting through TNF-α normalization.

4.2.2 TASK2B: Nanobubbles as bilirubin carriers in organotypic brain cultures of substantia nigra: an initial screening step of bilirubin-delivery in Parkinson's disease (*The experiments were performed in collaboration with Department of Drug Science and Technology and Department of Neuroscience, University of Torino, Torino, Italy*)

We have shown that unconjugated bilirubin (UCB) at specific concentrations (0.5μM and 1μM) prevents dopaminergic neuron (DOPAn) loss in the *ex vivo* (organotypic brain cultures of substantia nigra - OBCs-SN) model of PD.

Despite the modulation of UCB through its enzymatic machinery (HMOX1—heme oxygenase 1 and BVLR—biliverdin reductase) production is possible, the consequence of the increase of other heme catabolism products (Fe and CO)[234], [237], [342] that potentially harm in excessive amount will also follow. Moreover, as HMOX1 increase has been reported to increase in the PD brain along with iron *in situ* deposition[234], [237], [342], its further induction will lead even to further damage. Due to these reasons, we have shifted from our initial plan to work on UCB modulation to UCB delivery in the brain. For reaching a so-tuned concentration in the CNS, a carrier (nanovectors) looks to be the best solution.

Thus, we tested different polymeric shells of nanobubbles (NBs, **Figure 4.17**), consisting of glycol-chitosan (GC), GC-deferoxamine (GC-

DFO), and the magnetic NBs, GC-DFO-iron (GC-DFO-Fe) and GC-DFO-superparamagnetic iron oxide nanoparticles (GC-DFO-SPIONs), as potential UCB carriers in the OBCs-SN (for experimental schemes see Chapter 3 Materials and Methods, Section 3.2.3.2 Experimental schemes)

4.2.2.1 Nanobubbles physicochemical characterization

The physicochemical characterizations of each NBs formulation, including size, pH, viscosity, osmolarity, and zeta potential, have been assessed by Dr. Shoeb Ansari and Dr. Eleonora Ficiarà (Department of Drug Science and Technology and Department of Neuroscience, University of Torino, Torino, Italy) in their thesis.

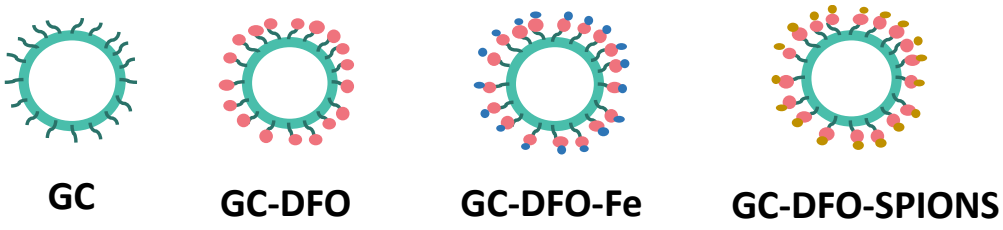

Figure 4.17. The nanobubble schematic graphs and its polymer shell structure. GC: glycol-chitosan; GC-DFO: GC-deferoxamine, GC-DFO-Fe: GC-DFO-iron and GC-DFO-SPIONs: GC-DFO-superparamagnetic iron oxide nanoparticles.

4.2.2.2 Nanobubbles safety test on OBCs-SN (healthy slices)

Before the use of UCB-loaded nanobubbles in our PD model, safety tests of these NBs formulations were performed in OBCs-SN (healthy slices, without rotenone) after 24 hours of treatment. The test was conducted in the healthy slices to see if the NBs itself will be toxic or not to OBCs-SN. Different ranges of dilutions (1:8, 1:64, 1:192) of NBs were tested as well as

free iron (Fe) (see the rationale of the treatment in Chapter 3 Materials and Methods, Section 3.2.3.2 Experimental schemes, part a). Rot challenging was used alone as negative control (reference to the DOPAn demise on the PD model), while the positive control was DMSO. The safety tests included MTT (mitochondrial activity), LDH (lactate dehydrogenase, marker of membrane leakage), and dopaminergic neuron (DOPAn) count.

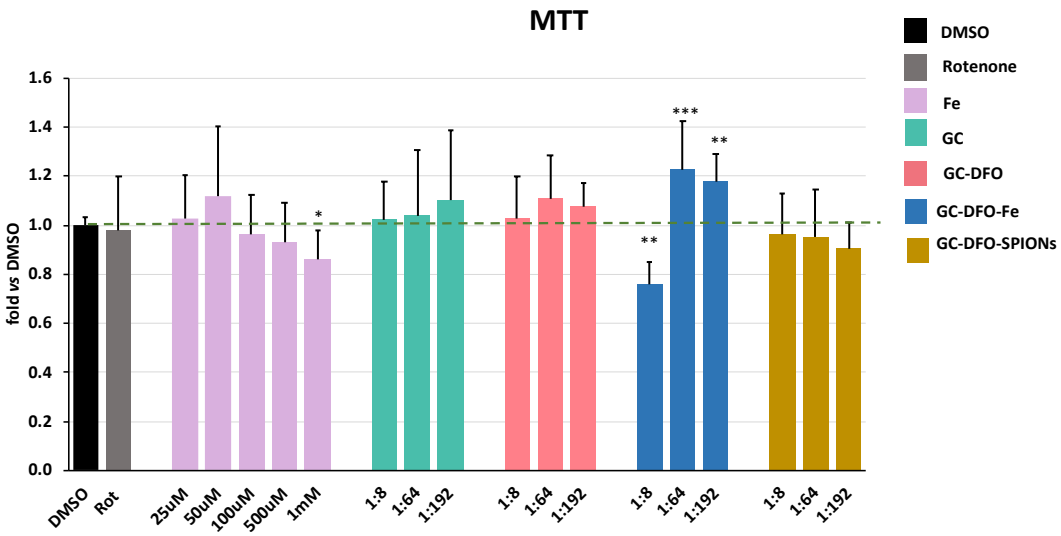

Figure 4.18. MTT assay of different NBs formulation on OBCs-SN. Data are expressed as fold of change *vs.* control, and as mean ± SD of at least 4 independent repetitions. No statistical significance was found. Statistical significance: no statistical significance is found.

The MTT results showed that GC-DFO-Fe was toxic at 1:8 dilution, while none of the other NBs formulations in different dilutions induced mitochondrial toxicity (**Figure 4.18**). Meanwhile, 1mM iron exposure induced toxicity.

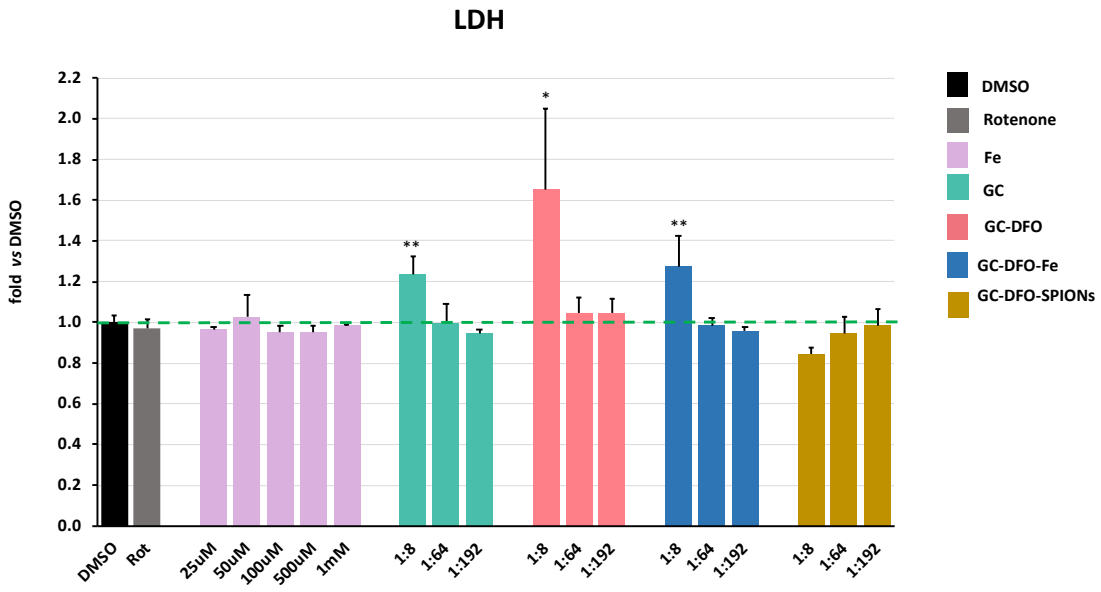

Figure 4.19. LDH test of different NBs formulations on OBCs-SN. Data are expressed as fold of change *vs.* control, and as mean ± SD of at least 4 independent repetitions. Statistical significance: *vs.* control * $p < 0.05$, ** $p < 0.01$.

Based on LDH test, GC, GC-DFO, and GC-DFO-Fe were toxic at 1:8 dilution by increasing LDH release 1.24-fold (p<0.01), 1.65-fold (p<0.05), and 1.27-fold (p<0.01) *vs*. DMSO, respectively (**Figure 4.19**). While Fe showed no increase in LDH level at all concentrations tested.

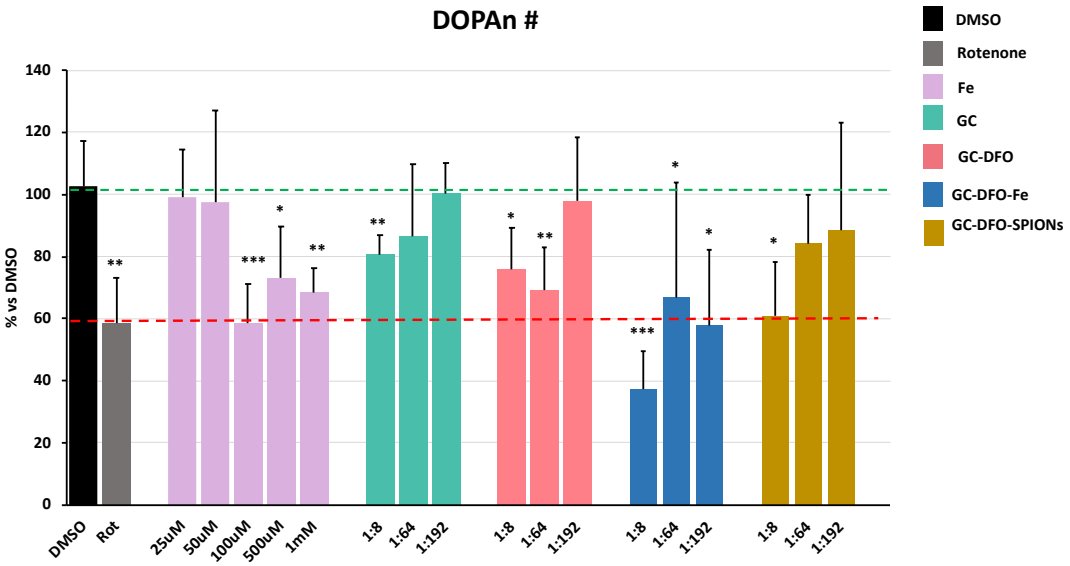

Figure 4.20. DOPAn number of different NBs formulation on OBCs-SN. Data (DOPAn) are expressed as percentage (%) *vs.* control, and as mean ± SD of at least 4 independent repetitions. Statistical significance: *vs.* control * $p < 0.05$, ** $p < 0.01$, *** $p < 0.001$.

Because DOPAn may have different sensitivity with respect to the other cells composing the tissue, and most importantly, they are our main target, we counted DOPAn to deeply assess the safety of the NBs formulations (**Figure 4.20**). The toxicity was found in GC at 1:8 dilution ($p<0.05$ *vs*. DMSO), GC-DFO at 1:8 and 1:64 dilutions ($p<0.01$ *vs*. DMSO), GC-DFO-Fe at all dilutions, and GC-DFO SPIONs was toxic only at 1:8 dilution. Unlikely, we found agglomeration of GC-DFO-SPIONs under the immunofluorescence assays (**Figure 4.21**) marked the instability of GC-DFO-SPIONs. Therefore, we exclude the GC-DFO-SPIONs from the further experiment. Meanwhile, Fe showed concentration-dependent toxicity at 100μM and higher concentrations, indicating that the toxicity of GC-DFO-Fe might be due to the presence of iron in this formulation.

Combining the knowledge of the cellular heterogenicity of OBCs-SN, MTT, and LDH tests as viability assays of the whole tissue viability, the result from DOPAn evaluation confirms that DOPAn is a selectively vulnerable cell in substantia nigra [343].

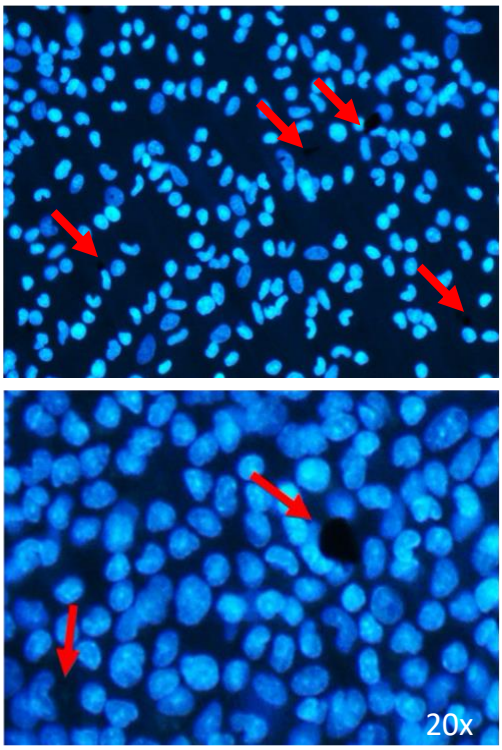

Figure 4.21. Agglomeration event of GC-DFO-SPIONs. Agglomeration was depicted as the black dots and emphasized with the red arrows under Hoechst staining in immunofluorescence.

Summarizing the safety test results altogether, the safest candidate for NBs are the GC and GC DFO at ≥ 1:192 dilutions. GC-DFO-Fe is toxic for OBCs-SN possibly releasing Fe and GC-DFO-SPIONs was excluded from the experiment due to its agglomeration event.

4.2.2.3 Nanobubbles on OBCs-SN model of Parkinson's Disease

Based on the prior NBs safety test, the selected NBs were GC and GC-DFO. As the main goal of this task is to use the NB as a bilirubin-delivery system, both NBs were loaded with UCB to further use in the OBCs-SN PD model (with Rotenone). In this test, the range of dilutions was increased to 1:64, 1:192, 1:1524, 1:4572, and 1:11428 (see the rationale of the treatment in Chapter 3 Materials and Methods, Section 3.2.3.2 Experimental schemes, part c).

a. Bilirubin concentration in NBs

Based on the safety test we select the GC and GC-DFO as candidates for bilirubin carrier. Based on HPLC quantification of UCB content performed by our collaborators at the University of Torino, the concentration of UCB in NBs was as in **Table 4.1**.

Table 4.1. Bilirubin concentration in NBs.

	GC+UCB	**GC-DFO + UCB**
Bilirubin concentrations (μM)	32.3	33.75

b. Viability test of NBs-UCB in PD model

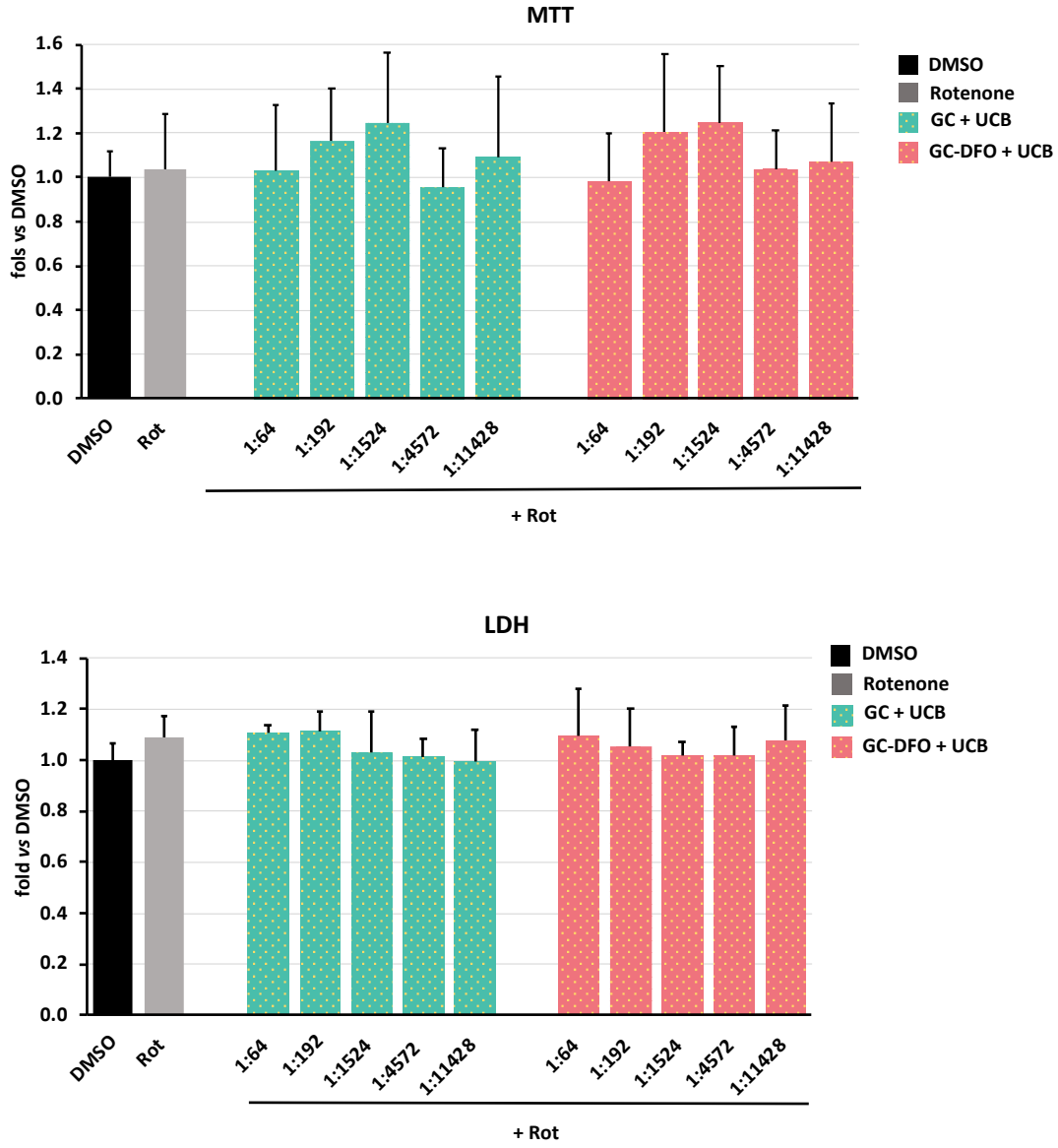

Figure 4.22. MTT and LDH assay of GC-UCB and GC-DFO-UCB on PD model. Data are expressed as fold of change *vs.* control, and as mean ± SD of at least 4 independent repetitions. No statistical significance was found.

Both MTT and LDH assays (**Figure 4.22**) showed no sign of toxicity for GC-UCB and GC-DFO-UCB in all ranges of dilution co-treatment with rotenone, confirming the safety test previously performed in healthy slices has allowed us to choose the non-toxic formulations and dilutions of NBs.

c. NBs-UCB protection toward rotenone-induced dopaminergic neuron loss in PD model

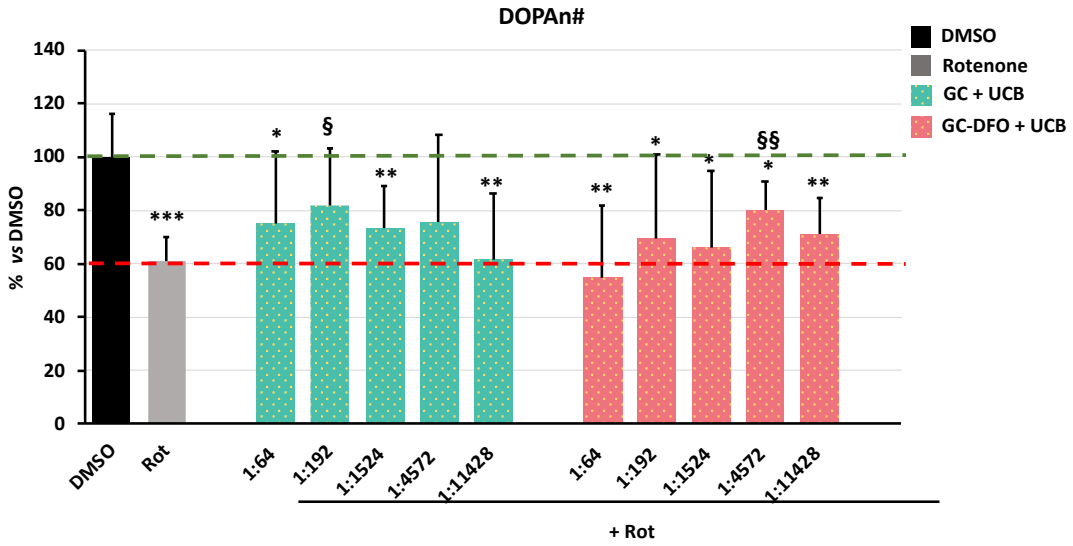

Figure 4.23. DOPAn number of different NBs formulation on OBCs-SN. Data (DOPAn) are expressed as percentage (%) *vs.* control, and as mean ± SD of at least 4 independent repetitions. Statistical significance: *vs.* DMSO * $p < 0.05$, ** $p < 0.01$, *** $p < 0.001$; *vs.* Rot § $p < 0.05$, §§ $p < 0.01$.

As shown in **Figure 4.23**, Rot alone induced the expected reduction of DOPAn number (-40%, $p<0.001$, [135]). In this set of experiments (PD model, co-challenging of Rot with NBs), the increase in DOPAn number in respect to Rot, represents the protection conferred by the NBs-UCB. Although it did not offer full protection, GC-UCB at 1:192 dilution and GC-DFO-UCB at 1:4572 dilution offer the highest protection, 82% ($p<0.05$) and 80% ($p<0.01$), respectively.

Though the protection of the two formulations is almost similar, their different dilutions indicate that GC-DFO-UCB is protective at a lower concentration compared to GC-UCB. Thinking of clinical use, needing

fewer NBs for carrying enough UCB may be a pro, thus GC-DFO-UCB looks to be a good candidate. Indeed, the presence of DFO, the iron chelator, might also explain the achieved result (cooperative action of UCB and Iron chelation). Therefore, we selected the GC-DFO-UCB as the best formulation.

Table 4.2. Summary of viability results of selected-NBs on healthy slices

	Healthy slices		**PD model**	
	GC	**GC-DFO**	**GC-UCB**	**GC-DFO-UCB**
MTT				
1:64	1.04±0.27	1.11±0.18	1.16±0.24	0.98±0.21
1:192	1.10±0.29	1.08±0.09	1.25±0.32	1.20±0.36
LDH				
1:64	0.99±0.10	1.05±0.07	1.11±0.03	1.10±0.18
1:192	0.95±0.02	1.04±0.07	1.11±0.08	1.06±0.15
DOPAn				
1:64	86.42±23.22	69.04±13.96**	75.12±27*	54.73±27.9**
1:192	100.08±10.02	98.02±20.41	81.91±21.55§	69.34±31.45*

Data of MTT and LDH are presented as mean of fold change ± S.D. *vs.* DMSO. Data of DOPAn is expressed as percentage (%) ± S.D. *vs*. DMSO. Statistical significance: *vs.* DMSO * $p < 0.05$, ** $p < 0.01$, *** $p < 0.001$, *vs.* Rot § $p < 0.05$

Based on the MTT and LDH results of selected NBs in healthy slices and NBs-UCB in PD, all selected NBs showed no toxicity for both healthy and PD model slices. Meanwhile, by comparing the result of DOPAn count in healthy and PD model slices (summarized in **Table 4.2)** it looks like the selected NBs formulations confirm their fate (or even be protective) also in the PD tissue. After finding the most promising and protective NBs (in the

specific formulation and dilution), the future goal is to optimize its protection (increasing 20% from the current protection) by loading different concentrations of UCB in NBs to be used at the same protective dilutions of the NBs-UCB found in this task **(Figure 4.24)**.

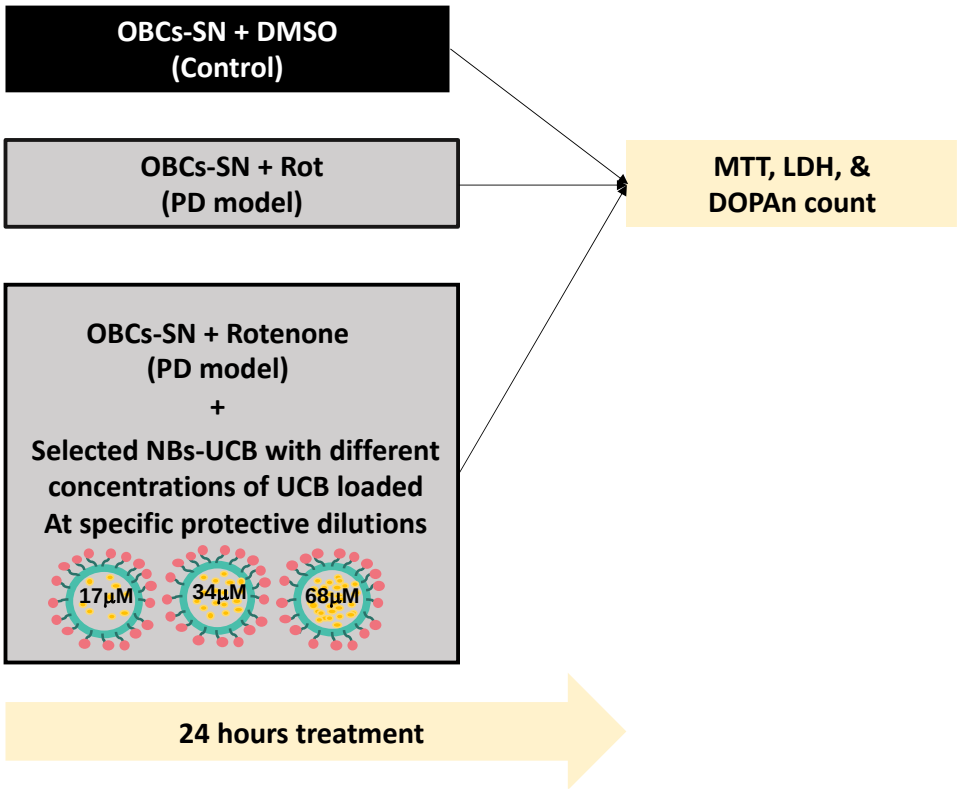

Figure 4.24 Future experimental scheme of selected-condition NBs on PD model

Future works will also consist of the exploration of NBs efficiency in UCB delivery, release and enter the cells. Therefore, we plan: (1) repeating the same experiment NBs dilution loaded with coumarin, a fluorescence agent [344], which allow us to visualize and quantify NBs inside the cells; (2) performing UCB quantification in the medium and the tissue of PD model treated with NBs-UCB to allow us understand where

UCB is released; and (3) exploring the DFO capacity as chelator in PD model, by quantifying the amount of iron in the tissue.

4.2.3 TASK2C: Curcumin Protection in an *ex vivo* Parkinson's disease (PD) model

Knowing the main challenge of PD management is its late diagnosis and having a prior demonstration (TASK1) about the pleiotropic effect of curcumin (a widely available nutraceutical compound) not only as an anti-oxidant but also anti-inflammation (including anti-TNF-α, Figure **4.5c**). We expanded our project to investigate the Curcumin neuroprotection effect in an *ex vivo* model of PD.

4.2.3.1. Low concentrations of Curcumin protect from rotenone-induced DOPAn demise in *ex vivo* model of PD

We used 5-40μM Curc and co-treat with Rot for 24 hours. Among the range concentrations of Curc tested (**Figure 4.25**), 5 μM Curc fully protected DOPAn (112%, $p<0.001$ *vs.*Rot) against rotenone toxicity (-50%, $p<0.01$ *vs.* Control). Meanwhile, 10μM Curc offered around 90% protection ($p<0.01$ *vs.* Rot) and the protection was lost at higher Curc concentrations (20μM and 40μM).

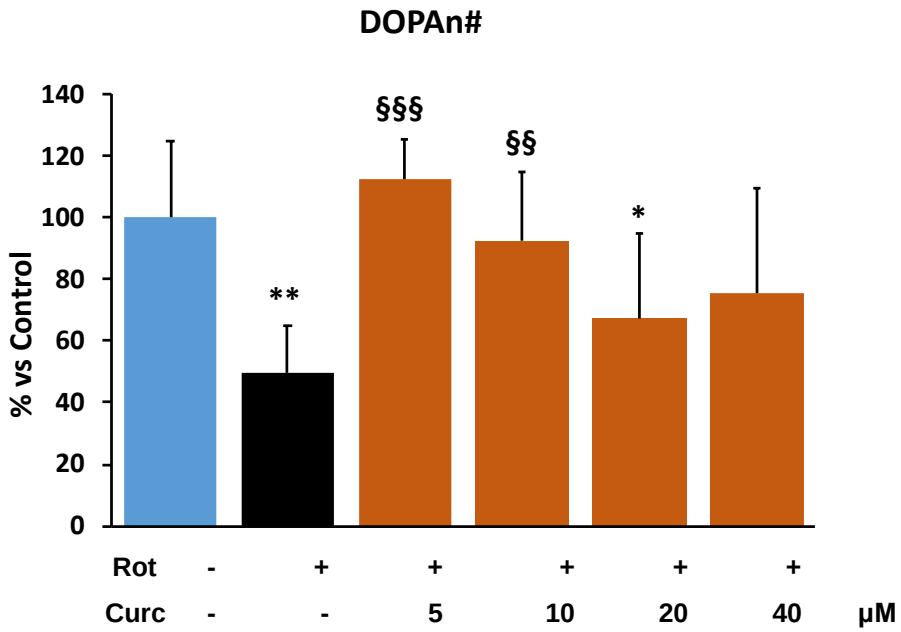

Figure 4.25. Dopaminergic neurons (DOPAn) number in Curc treated slices. <control and as mean ± S.D. of at least 3 independent repetitions. Statistical significance: *vs.* Control *p<0.05, ** $p < 0.01$; *vs.* Rot §§ $p < 0.01$, §§§ $p < 0.001$.

4.2.3.2. Curcumin action toward TNF-α in *ex vivo* model of PD

Initially, we used only 10µM Curc and we collected samples for RTqPCr analysis. Even though the data is still preliminary, the results support the idea that Curc is protecting from DOPAn loss by normalizing TNF-α (**Figure 4.24)**. Now we will repeat the analyses at 5µM.

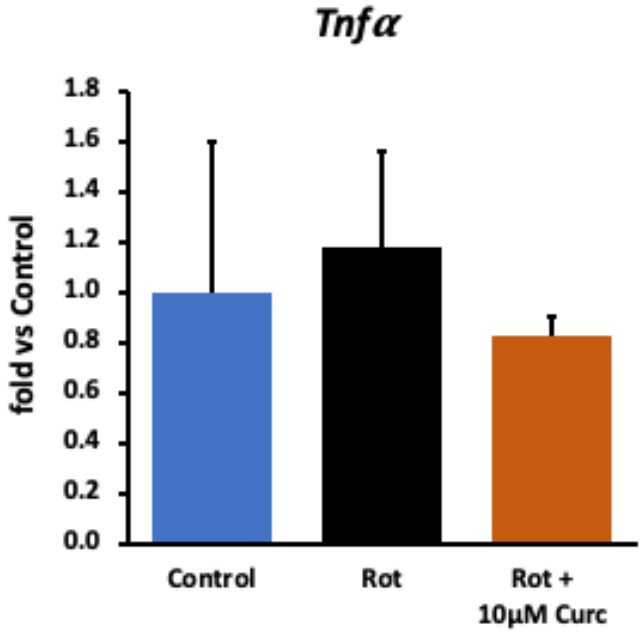

Figure 4.26. Effect of Curc treatment on *Tnfα*. *Tnfα*.: tumor necrosis factor α. Blue bar: control; black bar: rotenone (Rot); orange bar: co-treatment Rot and 10µM Curc. Data (mRNA expression) are expressed as fold vs. control, and as mean ± SD of 2 independent repetitions.

Additional experiments are still needed to unravel the mechanism of protection, particularly its effect on TNF-α in all concentrations of Curc. Then we aim in identifying the cells secreting TNF-α (DOPAn, astrocytes, microglia, etc.). We suggest reaching the goal by double immunofluorescences on PD slices (Ab anti-TNF-α, in co-stain with markers of that different cell families).

CHAPTER 5

DISCUSSIONS

5.1 TASK 1 – The Effects of Curcumin in Bilirubin-induced Neurotoxicity in Severe Neonatal Hyperbilirubinemia Model

The need to increase the therapeutic approaches to kernicterus spectrum disorder (KSD), as well as to find supportive solutions when adequate medical care is not available, prompted us to evaluate a novel pharmacological approach aimed to counteract directly the main molecular mechanisms of bilirubin-induced brain damage, without necessarily decreasing total serum bilirubin (TSB).

A similar approach was used in the past in the Gunn rat by the administration of minocycline [65], [103], [104]. Despite the drug being fully effective in protecting the rat brain from neurological damage, the side effects of minocycline prevented its clinical use [98], [277]. Analogs with less/no side effects have been developed and tested, but unfortunately, the loss of toxicity of the new molecules was accompanied by the loss of the protective effect [65]. Indeed single anti-oxidant, anti-inflammatory, and glutamate channel antagonist principles alone were not, or only partly, able to restore damage [65], [87], [105], suggesting that none of these mechanisms alone was determinant. In line with this conclusion, in preliminary work we reported that only treatment with a cocktail of anti-inflammatory and anti-oxidant drugs together with a glutamate channel blocker almost fully reverted the damage in an ex vivo setting, suggesting

that bilirubin toxicity was due to a synergistic effect of different mechanisms [278].

Based on that, and to accelerate the possible clinical application to newborns, we used Curc because the molecule is already used in other diseases and can enter and accumulate into the brain [345]–[348], and because it is reported to be able to counteract all the main pathological mechanisms undergoing KSD [345], [349]–[359].

The data we collected support rather strongly the efficacy of the Curc formulation we used in preventing cerebellar damage (weight—**Figure 4.1a**; volume, EGL, PCs: **Figure 4.2a-e**) typical of the Hyper Gunn rats [12], [103], [104], [274], [276], [294]–[296]. The protection was not mediated by lowering serum bilirubin level (**Figure 4.1b**), but rather to a direct effect on the damaging mechanisms (inflammation, glutamate excitotoxicity, and redox state—**Figure 4.5, Figure 4.6, Figure 4.7**), with the normalization of the behavior in Hyper Curc pups **(Figure 4.3**) representing a convincing proof of the efficacy of Curc.

The results may be explained by the multiple functions of Curc, a pleiotropic capability that the molecule shares with minocycline[360]. In addition to anti-oxidant effect (e.g., on HMOX1 [351]), curcumin possesses anti-inflammatory (on IL6, COX2, TNFα, IL1β), anti-apoptotic, anti-tumorigenic effect, and acts on numerous signaling pathways [345], [351]–[358]. The modulatory and protective effects of curcumin against glutamate neurotoxicity have also been previously reported [349], [350], [358].

Mhillaj *et al.* reviewed that Curc confers protection in wide array of diseases by acting as Hmox1 inducer [361], meanwhile in our model the curcumin confer protection by normalizing the Hmox1 in gene and protein

level. The discrepancy of this curcumin action can be explained by the difference of the experimental setting/model and also the studied disease as well. Most of the models reviewed are non-CNS diseases where the downregulated Hmox1 considered as the lack of antioxidant activity. Meanwhile, the hyperactivity of Hmox1 in the brain can be both neuroprotective as well as neurodystrophic [362]. The upregulation of Hmox1 in our study also supported by bilirubin neurotoxicity study in *ex vivo* model [278], supporting that hyperbilirubinemia conditions increase the Hmox1 in mRNA and protein level. Therefore, curcumin ability to reverted the level of Hmox1 is considered as neuroprotective effect. Nevertheless, the curcumin action toward Hmox1 in severe neonatal hyperbilirubinemia is still need to be elucidated.

Curc is mainly used in cancer therapy. It can suppress cancer growth by interfering with cell division [353], [355], but the reported side effects (diarrhea, headache, rash, yellow stool, nausea, increased serum alkaline phosphatase and lactate dehydrogenase, abdominal pain; are usually reported at very high dosage and long exposition) call for precaution [351], [357], [363]. On the other side, Curc consumption of up to 2–2.5 g/day (about 40 mg/kg) is part of the culture in Nepal and India, where it is used in the traditional Indian Ayurveda medicine (reviewed in [364]). Curc is a "generally recognized as safe" (GRAS) compound (EMA and FDA) with no demonstrated side effects even at high dosages[255]. The typical dosage in adults is about 4–8 g/day (about 60–114 mg/kg), and dosages up to 12 g/day (about 170 mg/kg) for several months have been reported[351], [357], with minor side effects. Beneficial effects of Curc administration in infants for bowel disease are reported[364]–[367], and in

pediatric cancer, 400 mg/day of Curc orally administered for nine months to a six-month-old baby with infantile hemangioendothelioma, has been reported as improving body weight gain, reducing liver dimensions with no evidence of residual hepatic lesions, and without reporting side effects[365]. This suggests that Curc administration in neonatal hyperbilirubinemia (for 24 h in case of PT; or 10–20 days in case of spontaneous normalization of blood bilirubin levels in absence of PT [368], [369]) might be, in principle, feasible.

Recent studies on the accumulation of Curc in the rodent brain indicate that the molecule enters rapidly and accumulates into CNS, especially when administered for a long period (chronic assumption) [346]. Importantly, no significant differences between oral vs. i.p. administration have been reported. The extrapolation of what was observed in the experimental model to the newborn still needs to be demonstrated [346].

The daily administration of the drug as soon as jaundice appeared, possibly interfering promptly with the damage, might be an additive reason for the success of the work. In this respect, we believe our experimental scheme may well reproduce the clinical scenario of a severely hyperbilirubinemic infant not treated with PT.

The dose we used (10 mg/kg) is below the posology reported in clinical trials (see above) and lower also in respect of other works in rodent models of CNS diseases [370]–[372]. This suggests that small amounts of the molecule might be effective in counteracting KSD.

Our data (**Figure 4.1a,b** Cll weight and TSB; **Figure 4.2** histology and morphometry; **Figure 4.3** behavior, and **Figure 4.4** bodyweight) also agree with previous works, where benefits and no side effects of the

molecule have been documented [370]–[372]. Nevertheless, independent confirmations of our results with different doses and different timing of treatment in animal models are required before suggesting Curc in the clinical setting. Efficacy/safety evaluation in the human is, in any case, an obligated step, considering a possible species-specific different sensitivity to the principle.

In conclusion, these data indicate the ability of the formulation of Curc we used in preventing the bilirubin brain-induced damage in the Gunn rat model of neonatal hyperbilirubinemia. We need to confirm these data before curcumin might be considered to be administered to the jaundiced newborns. If successful, the possibility to deliver the principle diluted in the baby bottle may become a feasible alternative/complementary approach to PT where this is not easily available.

5.2.TASK 2 – Bilirubin Neuroprotection in an *ex vivo* Parkinson's disease model

5.2.1 TASK 2A: Bilirubin reverses the dopaminergic neuron demise in an *ex vivo* Parkinson's disease (PD) model

Therapy for delaying or stopping PD evolution is still an unmet medical need. Redox imbalance, and most recently inflammation, are two discussed hits [373]–[375] in DOPAn demise in PD patients and models [373], [376], [377]. UCB possesses both anti-oxidant and anti-inflammatory properties, with demonstrated beneficial epidemiological effects in extra-CNS diseases [317], [378], [379]. In this work, we demonstrated that low concentrations of UCB (0.5μM and 1μM, corresponding to a free bilirubin—

Bf lower than 1nM) may protect from the 40% DOPAn loss quantified in our *ex vivo* chronic model of PD (**Figure 4.10**). First, we focused our attention on the anti-oxidant capability of UCB. As testified by the GSH and GSSG evaluation (**Figure 4.13)**, low doses of Rot induced the expected early increase of the pro-oxidant status of the cultures [380], supported by the up-regulation of both *Homx1* (a redox sensor [64], a transcription factor of the battery of anti-oxidant genes [321], as well as the key enzyme in UCB production [2]), and *Srxn1* (belonging to the anti-oxidant response mechanism - [321]) (**Figure 4.11a-b**). In agreement, an up-regulation of Hmox1 and an increased level of UCB in the serum have been reported in the early clinical stages of PD (Hoehn & Yahr Stage ≤3) [381]–[383] turning upside down with the progression of the severity of disease in the clinical setting. It was hypothesized that this double-sided trend represented an initial tentative reaction to the ongoing damage by increasing the *in situ* (CNS) production of bilirubin, failing later on with the progression of the disease [342]. In our model, the addition of exogenous UCB to the cultures, possibly overcomes the need for *Hmox1* induction, conferring protection.

The longstanding *Srnx1* up-regulation (up 24 hours, **Figure 4.11b**), the glutathione level alteration in the medium after rotenone exposure (5 min and 3h, **Figure 4.13a)** and in both medium (5 min, 3h, and 24h **Figure 4.13a)** and tissue (**Figure 4.14)** after UCB treatment, marking the presence of oxidative stress in the model as well as confirming UCB acted as an antioxidant. However, the antioxidant activity of UCB is not congruent with UCB protective effect against DOPAn loss in PD model (**Figure 4.10**), indicating that UCB protection in PD model is independent of its antioxidant capacity.

Supporting the previous findings, the NAC experiment (**Figure 4.15**) is unable to normalize the DOPAn counting in our model despite the wide spectra of concentrations used indicating oxidative stress is not the key player in our PD model. This point might appears in disagreement with different models of PD, where NAC has been reported partially restoring DOPAn demise [384]. The different results might be due to the model (we: OBCs-SN, others: animals and cell lines). Or, in our opinion, the disagreement was mainly attributable to the kind of PD model we developed. Usually, high doses of Rot have been used to develop an acute model of the disease [380], [385]. Differently, we used a slowly progressing model of the disease, better reproducing the clinical scenario of a slow, chronic condition that requires decades to develop, and allowing us to discriminate the early from the late mechanisms involved in the DOPAn demise [135]. Thus, the severity of the mechanism of induction might affect the results.

Bdnf, another potential contributor of DOPAn demise in models [135], [314], [315], [375], [376] as well as in the clinical setting [322], [323], was normalized only by 1μM UCB (**Figure 4.11c**), disagreeing with the protection form DOPAn observed in (**Figure 4.10**). Similarly happened with *Il6*, with a maximally normalized at 2μM UCB(**Figure 4.11e**), where UCB protection is lost (**Figure 4.10**), and *Cox2*, never restored by UCB treatments (**Figure 4.11f**). The experimental data we report in our model agrees with different models of PD and the clinic, where all these markers have been reported to be altered [135], [325]–[329]. Multiple trials to normalize these factors, or evaluate their correlation with PD have been reported. Bdnf administration in PD models failed in diminishing DOPAn loss [389]–[391].

Despite some controversy [392], the intake of the non-steroid anti-inflammation drugs (NSAIDs, the COX2 inhibitors) by patients with chronic pro-inflammatory diseases different from PD was not associated with a reduced risk of PD [393], [394]. Finally, the correlation between IL6 genetic polymorphisms increasing cytokine production and the risk of PD is unclear, keeping open the question about the relevance of this cytokine in PD onset [395], [396].

Recently, Tnf-α as a key contributor to PD onset and DOPAn loss is gaining more and more attention [290], [333], [397]–[404], but still strong proof of its relevance is missing. Indeed, up to now, no efficient drugs (in this work we used bilirubin as a drug [405]) to reverse its expression and restore the DOPAn number have been found. TNF-α modulation has been reported in patients [332]–[334], and is associated with a rapid motor decline [332]. Data have been replicated in models [135], [325], with increased apoptosis [406] and DOPAn death [407]. Experimental data obtained by neutralizing TNF-α resulted in a partial (50%) rescue from DOPAn loss [290]. Similarly, a small reduction in the incidence of PD has been reported in patients with inflammatory bowel disease exposed to Infliximab [408], possibly because of the limited ability of the drug in crossing the blood-brain barrier[409].

We fully documented that Tnf-α is the determinant of DOPAn demise and UCB protection in the model. The correlation analysis performed between DOPAn and early potential mechanisms marker (**Figure 4.12**) showed that among all the markers only *Tnfα* was significantly correlated with DOPAn number (**Figure 4.12d**). Furthermore, the addition of purified Tnf-α well reproducing the neuronal loss, and the full protection

obtained by Infliximab are indisputable pieces of evidence of its key role (**Figure 4.16**).

Clinical studies evaluating the incidence of PD in the Gilbert population are so far not available but are required in the light of our data. Notably, and differently from the limited bioavailability of Infliximab in the CNS, free bilirubin (Bf), the UCB moiety not bound to serum albumin, may quickly diffuse across the blood-brain barriers and the cells [410] carrying out its biological functions. Nevertheless, translating the use of UCB as a drug in the clinic is not so easy. Despite modulating the systemic level of UCB being feasible [238], reaching a so-tuned amount of bilirubin in the substantia nigra of PD patients is a challenge. Delivery by nano-vehicles carried with UCB could be the most feasible way [5], [411]–[413]. Weak points of this approach as therapy are the delayed diagnosis, usually occurring when the 40% of DOPAn are already lost, and the concerns in the possible needing for repeated administration of the UCB-loaded nano-vehicles, despite slowing or stopping the progression of the disease is a great goal. Further experimental work will be needed to translate the use of UCB finding into clinical settings. Nevertheless, the finding reported in this paper is greatly useful for searching for new (prophylactic) therapeutic approaches able to target specifically TNF-α to prevent PD, and potentially other neurodegenerative diseases sharing TNF-α as a contributor to neurodegenerative progression. Research is ongoing.

5.2.2 TASK2B: Nanobubbles as bilirubin carriers in organotypic brain cultures of substantia nigra: an initial screening step of bilirubin-delivery in Parkinson's disease (*The experiments were performed in collaboration with Department of Drug Science and Technology and Department of Neuroscience, University of Torino, Torino, Italy*)

UCB at specific concentrations has been demonstrated to prevent DOPAn loss in the *ex vivo* (OBCs-SN) model of PD (TASK 2A). However, this finding is challenged by the main question: how it can be modulated in the brain?

(a) A pharmacological approach targeted in a systemic (whole-body) modulation of the yellow players (part of enzymatic machinery of bilirubin production) seems to be the most obvious and is already primarily evaluated in extra-CNS diseases [226], [239], [245] by inducing HMOX1 and increasing TSB.

(b) Nowadays, all types of cells have been known to possess the enzymatic machinery (HMOX1 and BLVR) for producing bilirubin [5], [8]. A second approach might consist of modulating HMOX1 or BLVR directly in the CNS. Nevertheless, it has to be mentioned that inducing even more HMOX1 will possibly enhance the side effects and accelerate the disease progression. As reported in a human study, HMOX1 has been reported to increase in the serum [382]and in the brain of PD subjects [383], where it is supposed to enhance the toxicity by deposition of iron, one of its products[207], [241], [414]

(c) A third exciting alternative is the use of nanoparticles. Nanoparticles designed explicitly for brain delivery (of mRNA, small peptides, chemotherapeutic agents, etc.) are under evaluation [243], [244], [246]–

[248] and are of routine clinical use as agents in magnetic resonance, magnetic-field-directed drug targeting to tumors across the blood-brain interfaces (BBIs), and for direct anti-tumor treatment by magnetic hyperthermia [244], [246]–[250].

In the context of PD studies (animal models), nanoparticle delivery of dopamine and levodopa, ropinirole and apomorphine (dopaminergic agonists), and growth factors (NGF, GDNF) have been tested, reporting positive results in terms of reaching the target, the release of the content, good efficacy, and tolerance [246]. Hence, the basis for developing UCB-loaded nanoparticles becomes an option to optimize its tuned delivery *in vivo*. For this reason, we have collaborated with University of Torino which priorly developed the so-called nanobubbles (NBs), as multi-compound carriers [415], [416].

The different polymeric shells of nanobubbles (NBs), consisting of glycol-chitosan (GC), GC-deferoxamine (GC-DFO), GC-DFO-Iron (GC-DFO-Fe), and GC-DFO-superparamagnetic iron oxide nanoparticles (GC-DFO-SPIONs), (**Figure 4.17**), as potential UCB carriers in the OBCs-SN model, were used as bilirubin carrier candidates.

In this study, the viability of OBCs-SN (healthy slice, see the rationale of the treatment in Chapter 3 Materials and Methods, Section 3.2.3.2 Experimental schemes, part a) exposed to NBs only was examined. Although the magnetic nanoparticle is very sophisticated in medical applications due to its possibility to achieve a targeted site by a harmless remote magnetic field [118],[119], unlikely, that GC-DFO-Fe was found to be toxic to DOPAn at all dilutions in healthy slices (**Figure 4.20**). This suggests that the NBS may release part of the Fe, inducing damage at least

to the most sensitive cells composing the tissue (DOPAn). This hypothesis fits with the result of Fe treatment alone showing dose-dependent toxicity at 100μM and higher concentrations (**Figure 4.20**). The iron ability to induce neurotoxicity and its correlation with several neurodegenerative diseases has been frequently reported [414], [417]–[421]. Thus, the ability of CG-DFO NBs to firmly retain the Fe concentrations possibly present in the site of lesion of neurodegenerative disease is a critical step to evaluate.

Meanwhile, GC and GC-DFO were demonstrated to be safe for OBCs-SN **at ≥ 1:192 (Figure 4.20)**.

Gaining the crucial information about the safest NBs candidate, the experiment was continued by loading UCB into the selected NBs (GC and GC DFO) and the dilutions were increased from 1:192 to 1:11428. A wide range of dilutions was used to increase the possibility of delivering the protective concentration of UCB to DOPAn in PD model (0.5-1uM UCB in medium, corresponding to less than 1nM Bf), with the lack of knowledge about UCB amount that could enter the cell as a bias.

Furthermore, despite it is not full protection, GC-UCB at 1:192 dilution and GC-DFO-UCB at 1:4572 dilution were found able to counteract Rot-induced DOPAn death, by restoring around 80% of DOPAn (**Figure 4.23**).

The protection exhibited by the two NBs in different dilutions indicates the difference in both formulations. The presence of DFO (deferoxamine), an iron chelator, in GC-DFO-UCB might be explained the protective effect even in the lower dilution than GC-UCB. Since iron was also found to increase in human and PD models [422]–[424], the use of DFO was found to be protective against Rot-induced DOPAn loss [424].

GC-DFO-SPIONs was found to be toxic at 1:8 (**Figure 4.20**). Moreover, agglomeration events were found in the OBC-SN slices under GC-DFO-SPIONs challenge (**Figure 4.21**), a common event that usually limits the use of magnetic nanoparticles[425], [426]. The change of nanoparticle physicochemical behavior due to its interaction with culture media components (e.g protein) is considered one of the co-factors in nanoparticle aggregation [427]. Due to this physio-chemical instability, we decided to exclude the GC-DFO-SPIONs in the following experiment.

As the results with GC-UCB at 1:192 dilution and GC-DFO-UCB at 1:4572 bring us closer to the potential of UCB delivery in substantia nigra of PD, further investigation to maximize the protection by loading different concentrations of UCB as well as exploration of the potential combined-protection effect of DFO compound in GC-DFO-UCB are needed before expanding NBs application as bilirubin delivery system in *in vivo* model.

5.2.3 TASK2C: Curcumin Protection in an ex vivo Parkinson's disease (PD) model

The major clinical challenge in PD is the late diagnosis, occurring when the 40-50% of DOPAn has been already lost [5]. While the administration of UCB-loaded NBs at diagnosis to stop the progression of DOPAn loss is rational, it will neither revert nor prevent the already occurred damage, as well as a repeated delivery of NBs-UCB to the CNS is not a suitable possibility. Moreover, while PD has been known as a progressive disease, only in the last years it has been suggested that the hits to PD might be a chronic (lifelong) exposure to stressor stimuli (inflammation, redox, pollution, environment, intestine derived, etc.) [373],

[421], [428]. This strengthened the basis of suggesting a prophylactic treatment may have a place before the excessive damage of DOPAn.

Therefore, we took advantage of two important results obtained in this Ph.D. work. The major result of the thesis was demonstrating that TNF-α is the crucial player in DOPAn loss (TASK 2A). We have noticed in TASK 1 that curcumin (Curc) protects the Gunn rat brain against the toxicity of very high UCB levels also by normalizing TNF-α [273]. Considering Curc worldwide availability as a nutraceutical compound will lead us to an easy way to address it as PD prophylaxis treatment in the future, we have begun to explore its effect in our ex vivo PD model.

From the DOPAn evaluation, we demonstrated that Curc protection in *ex vivo* PD model is dose-dependent and Curc gave protection at 10μM (**Figure 4.25)**, the initial concentration used in this experiment. Due to the dose-response trend of Curc observed in DOPAn protection, we added 5μM Curc to be tested. While DOPAn count is conclusive (from at least 3 biological repetions), we have to confirm the protective effect shown by 5μM Curc **(Figure 4.26**), is due to its anti-TNF-α capacity. The experiment to unravel the protective mechanism focusing on Curc anti-TNF-α capacity in all concentrations of Curc used is still ongoing.

Several studies have demonstrated the protective effect of Curc in *in vivo* and *in vitro* models of PD. Curc is found able to restore behavioral impairments, reduce oxidative stress, restore mitochondrial deficits, counteract neuroinflammation and prevent cell apoptosis [429]–[434]. Curc anti-TNF-α capacity also has been demonstrated in other models of PD [435]–[437]. The therapeutic potential of Curc is supported by its ability to cross the blood-brain barrier (BBB) *in vivo* [438].

A small clinical trial of 9 months Curc administration (80 mg/daily) in PD patients failed to show Curc efficacy in alleviating clinical symptoms and quality of life of PD patients [439]. On contrary, the clinical trial using Curc (2g/daily) for 12 months in PD showed the improvement of Curc-treated patients not only in clinical symptoms but also decrease p-syn deposits (a pathological form of α-Syn in skin nerves) compare to untreated patients[440]. Moreover, this study also included the proof of Curc present in the cerebrospinal fluid suggesting that Curc able to cross BBB in human [440].

The fact that the first-mentioned trial was performed in younger PD patients (first trial: 58.2 ± 11.2 years, second trial: 72 ± 2 years) that usually have the more progressive type of PD, and the second trial administered a higher dose of Curc for longer periods may explain the dissimilarity outcome among the two trials. Also considering the heterogeneity of PD, the Curc efficacy at the severe stage (around half of DOPAn populations or more are already irreversibly damaged) will be challenged.

Nevertheless, as the incidence of PD in India is reported as the lowest all over the world (70 per 100,000 normal populations) [441], it brings to the hypothesis that the high consumption of Curc among Indians (not only as a dietary spice but also a herbal medicine [442]) may work as a prophylactic medicine in PD. Therefore, the main goal of our project is to introduce Curc as a prophylactic treatment of PD. However, more investigations (preclinical and clinical) are required to complete the story.

CHAPTER 6

CONCLUSION

6.1. TASK 1 – The Effects of Curcumin in Bilirubin-induced Neurotoxicity in Severe Neonatal Hyperbilirubinemia Model

In this project we have demonstrated that curcumin fully effective in restoring bilirubin-induced neurotoxicity in Gunn rats with its pleiotropic effect as anti-oxidant, anti-inflammation, anti-glutamate neurotoxicity and normalizer of brain development marker. The ability of curcumin counteracted bilirubin-induced neurotoxicity without reducing the total serum bilirubin level indicates its therapeutical capacity *in situ*. The wide world availability of curcumin brings us to a future perspective for curcumin application as an alternative, non-invasive therapeutical approach that can be complementary to current standard treatments (e.g. phototherapy and exchange transfusion). These data are needed to be confirmed before curcumin might be considered to be administered to the jaundiced newborns. Morever, the curcumin administration in the later age of Gunn rats as well as different experimental models are needed to mimic the clinical challenge in hyperbilirubinemia management.

6.2. TASK 2 – Bilirubin Neuroprotection in An *Ex Vivo* Parkinson's disease Model

From this task, we have reached not only a new perspective about the therapeutical potential of low concentration of UCB toward dopaminergic neuron loss in *ex vivo* model of PD but also a proof concept of the major role of TNF-α in dopaminergic neuron demise and protection.

Nanobubbles as UCB carrier seems a promising delivery system. The screening of nanobubbles in OBCs-SN has shown that GC and GC-DFO as the safest UCB carrier candidates, reaching up to now 80% of protection. Further studies to optimize the protectivity are needed.

An extended project by using curcumin and PD model also brings a new insight. Low concentration of curcumin was protective in *ex vivo* PD model and preliminary data shows its protection potentially comes from its anti-TNFα effect. The use of curcumin as a nutraceutical-prophylactic compound for PD will be an interesting story needed to be completed.

SCIENTIFIC PUBLICATIONS

A. Published Papers

1. **Jayanti S**, Moretti R, Tiribelli C, Gazzin S. Bilirubin: A Promising Therapy for Parkinson's Disease. International Journal of Molecular Sciences. 2021; 22(12):6223. Https://Doi.Org/10.3390/Ijms22126223
2. **Jayanti S**, Ghersi-Egea Jf, Strazielle N, Tiribelli C, Gazzin S. Severe Neonatal Hyperbilirubinemia and The Brain: The Old But Still Evolving Story. Pediatr Med 2021;4:37. Doi: 10.21037/Pm-21-5
3. Gazzin S, Dal Ben M, Montrone M**, Jayanti S**, Lorenzon A, Bramante A, Bottin C, Moretti R, Tiribelli C. Curcumin Prevents Cerebellar Hypoplasia and Restores the Behavior in Hyperbilirubinemic Gunn Rat By A Pleiotropic Effect On The Molecular Effectors Of Brain Damage. International Journal of Molecular Sciences. 2021; 22(1):299. Https://Doi.Org/10.3390/Ijms22010299
4. **Jayanti S**, Moretti R, Tiribelli C, Gazzin S. Bilirubin and Inflammation in Neurodegenerative And Other Neurological Diseases. Neuroimmunol Neuroinflammation 2020;7:[Online First]. Http://Dx.Doi.Org/10.20517/2347-8659.2019.14
5. **Jayanti** S, Vítek L, Tiribelli C, Gazzin S. The Role of Bilirubin and The Other "Yellow Players" In Neurodegenerative Diseases. Antioxidants. 2020; 9(9):900. Https://Doi.Org/10.3390/Antiox9090900

B. Submitted Paper

1. Gazzin S**, Jayanti S**, Tiribelli C,. Models Of Neonatal Bind and Kernicterus: What We Learned from and The New Challenges. Pediatric Research.

2. **Jayanti S**, Moretti R, Tiribelli C, Gazzin S. Bilirubin Reverses The Dopaminergic Neuron Demise In The Ex Vivo Parkinson's Disease Model. Biochemical Pharmacology.

C. Congresses/Conferences Publication (Abstracts)

1. **Jayanti S**, Moretti R, Tiribelli C, Gazzin S. (2021) Curcumin In Neuroprotection: From Kernicterus To Parkinson's Disease J Neurosurg Imaging Techniques, 6(S1): 17. Https://Www.Scitcentral.Com/Article/38/2237/Curcumin-In-Neuroprotection:-From-Kernicterus-To-Parkinson%E2%80%99s-Disease
2. **Jayanti S**, Moretti R, Tiribelli C, Gazzin S. Low Concentrations of Bilirubin Protect from Dopaminergic Neuron Loss In An Ex Vivo Model Of Parkinson's Disease. Journal of the Neurological Sciences. Doi:10.1016/J.Jns.2021.119566
3. **Jayanti S**, Gerotto C, Tiribelli C, Gazzin S. Protective Effects of Bilirubin Toward Dopaminergic Neuron Sufferance In An Ex Vivo Model For Parkinson's Diseases. European Journal Of Neurology, 2020, 27 (Suppl.1), 523-769. Https://Doi.Org/10.1111/Ene.14308. (Bursary Granted)

D. Oral Presentations at International Conferences

1. Jayanti S, Moretti R, Tiribelli C, Gazzin S. Curcumin in Neuroprotection: From Kernicterus to Parkinson's Disease. 17th International Conference on Neurology and Spine Disorders. Virtual. 23 April 2021.

2. Jayanti S, Gazzin S, Dal Ben M, Montrone M, Lorenzon A, Bramante A, Bottin C, Moretti R, Tiribelli C. Curcumin Prevents Cerebellar Hypoplasia and Restores the Behavior in Hyperbilirubinemic Gunn Rat by A Pleiotropic Effect on The Molecular Effectors Of Brain Damage. Oral Presentation at Don Ostrow Yellow Retreat (Dotyr) 2019 - Trieste (Italy)

ACKNOWLEDGEMENT

This thesis is a story of my journey not only in research but also in part of my life, and along this road, I never walk alone.

It's a genuine pleasure to express my gratitude to Prof. Claudio Tiribelli, my supervisor, for his outstanding support in giving me space and opportunity to grow not only as a scientist but also as a person. My sincere gratitude also to Dr. Silvia Gazzin, my co-supervisor, for her long-lasting support for these past four years, a major catalyst of my scientific growth both in skills and way of thinking, as well as my source of admiration for persistence and hardworking. I thank also Prof. Nasrum Massi for his sincerity in helping me for having this chance to pursue my PhD.

Special acknowledgment to Indonesia Endowment Fund for Education for the financial support allowing me to have my precious Ph.D. experience.

I thank Prof. Caterina Guiot, Prof. Roberta Cavalli, Dr. Shoeb Ansari, and Dr. EleonoraFiciarà from University of Torino for their collaboration in the work of this thesis.

I would like also to acknowledge all staff in Animal Facility of University of Trieste for their helping hands during my 'stabulario' day.

I thank my teammate John Paul, Emanuela Fioritti, and Clodia Gerotto for sharing not only the works but also the laughs in the lab.

I owe deep sense of gratitude also for all my colleagues and friends in Fondazione Italiana Fegato, for making our institution like a home from day one I arrived. Special thanks to Lorraine Kay Cabral, Noel Salvoza, Luca Grisetti, Chiara Andolfi, and Inah Mari Aquino for sharing the joys and griefs (and foods!), in all we learn a lot as a human being.

My special gratitude to Muhammad Yogi Pratama, my best friend, for making my first two years here much easier, his constant presence and support till now even though we are on the different edges of time zone, and for being a source of optimism. A special thanks to Nuranindia Endah Arum, for her drama-free sisterhood, her shareable beautiful knowledge, and for being my important support system regardless the distance.

To all my family and friends in Indonesia for their constant support.

My forever gratitude for Mama, Bapak, Asrul and Wandi, my oasis of infinite and eternal love, whenever and wherever they are. This work is dedicated to you.

Ultimately, to Cabenge—a place where I was born and grew up as a curious girl, and to Trieste—a place that I have called home for the past four years, a city where I found a better version of myself, I gratefully thank you.

Summer dawn, on June 30, 2022

Sincerely

Sri Jayanti

REFERENCES

[1] Libor Vitek and J. Donald Ostrow, 'Bilirubin Chemistry and Metabolism; Harmful and Protective Aspects', *Current Pharmaceutical Design*, Aug. 31, 2009. https://www.eurekaselect.com/69920/article (accessed Jul. 27, 2020).

[2] S. Gazzin, L. Vitek, J. Watchko, S. M. Shapiro, and C. Tiribelli, 'A Novel Perspective on the Biology of Bilirubin in Health and Disease', *Trends Mol Med*, vol. 22, no. 9, pp. 758–768, Sep. 2016, doi: 10.1016/j.molmed.2016.07.004.

[3] S. Gazzin, F. Masutti, L. Vítek, and C. Tiribelli, 'The molecular basis of jaundice: An old symptom revisited', *Liver International*, vol. 37, Dec. 2016, doi: 10.1111/liv.13351.

[4] L. Vítek and J. D. Ostrow, 'Bilirubin chemistry and metabolism; harmful and protective aspects', *Curr Pharm Des*, vol. 15, no. 25, pp. 2869–2883, 2009, doi: 10.2174/138161209789058237.

[5] S. Jayanti, R. Moretti, C. Tiribelli, and S. Gazzin, 'Bilirubin: A Promising Therapy for Parkinson's Disease', *International Journal of Molecular Sciences*, vol. 22, no. 12, Art. no. 12, Jan. 2021, doi: 10.3390/ijms22126223.

[6] M. Nitti, S. Piras, L. Brondolo, U. M. Marinari, M. A. Pronzato, and A. L. Furfaro, 'Heme Oxygenase 1 in the Nervous System: Does It Favor Neuronal Cell Survival or Induce Neurodegeneration?', *Int J Mol Sci*, vol. 19, no. 8, Art. no. 8, Aug. 2018, doi: 10.3390/ijms19082260.

[7] S. W. Ryter, J. Alam, and A. M. K. Choi, 'Heme oxygenase-1/carbon monoxide: from basic science to therapeutic applications', *Physiol. Rev.*, vol. 86, no. 2, Art. no. 2, Apr. 2006, doi: 10.1152/physrev.00011.2005.

[8] S. Gazzin, L. Vitek, J. Watchko, S. M. Shapiro, and C. Tiribelli, 'A Novel Perspective on the Biology of Bilirubin in Health and Disease', *Trends in Molecular Medicine*, vol. 22, no. 9, Art. no. 9, Sep. 2016, doi: 10.1016/j.molmed.2016.07.004.

[9] C. E. Ahlfors, G. D. Marshall, D. K. Wolcott, D. C. Olson, and B. Van Overmeire, 'Measurement of unbound bilirubin by the peroxidase test using Zone Fluidics', *Clinica Chimica Acta*, vol. 365, no. 1, Art. no. 1, Mar. 2006, doi: 10.1016/j.cca.2005.07.030.

[10] J. S. Hahm, J. D. Ostrow, P. Mukerjee, and L. Celic, 'Ionization and self-association of unconjugated bilirubin, determined by rapid

solvent partition from chloroform, with further studies of bilirubin solubility', *J Lipid Res*, vol. 33, no. 8, Art. no. 8, Aug. 1992.
[11] F. F. Rubaltelli, 'Bilirubin Metabolism in the Newborn', *NEO*, vol. 63, no. 3, Art. no. 3, 1993, doi: 10.1159/000243922.
[12] M. J. Daood and J. F. Watchko, 'Calculated in vivo free bilirubin levels in the central nervous system of Gunn rat pups', *Pediatr. Res.*, vol. 60, no. 1, Art. no. 1, Jul. 2006, doi: 10.1203/01.pdr.0000219561.07550.04.
[13] G. R. Gourley, 'Bilirubin metabolism and kernicterus', *Adv Pediatr*, vol. 44, pp. 173–229, 1997.
[14] J. F. Watchko and M. J. Maisels, 'Jaundice in low birthweight infants: pathobiology and outcome', *Archives of Disease in Childhood - Fetal and Neonatal Edition*, vol. 88, no. 6, Art. no. 6, Nov. 2003, doi: 10.1136/fn.88.6.F455.
[15] M. G. Mooij *et al.*, 'Ontogeny of human hepatic and intestinal transporter gene expression during childhood: age matters', *Drug Metab Dispos*, vol. 42, no. 8, Art. no. 8, Aug. 2014, doi: 10.1124/dmd.114.056929.
[16] S. Onishi, S. Itoh, N. Kawade, K. Isobe, and S. Sugiyama, 'An accurate and sensitive analysis by high-pressure liquid chromatography of conjugated and unconjugated bilirubin IX-alpha in various biological fluids.', *Biochem J*, vol. 185, no. 1, Art. no. 1, Jan. 1980, doi: 10.1042/bj1850281.
[17] E. C. Gritz and V. Bhandari, 'The Human Neonatal Gut Microbiome: A Brief Review', *Front. Pediatr.*, vol. 3, 2015, doi: 10.3389/fped.2015.00017.
[18] L. Morelli, 'Postnatal Development of Intestinal Microflora as Influenced by Infant Nutrition', *J Nutr*, vol. 138, no. 9, Art. no. 9, Sep. 2008, doi: 10.1093/jn/138.9.1791S.
[19] L. Vítek *et al.*, 'Intestinal colonization leading to fecal urobilinoid excretion may play a role in the pathogenesis of neonatal jaundice', *J Pediatr Gastroenterol Nutr*, vol. 30, no. 3, Art. no. 3, Mar. 2000, doi: 10.1097/00005176-200003000-00015.
[20] S. Gazzin and S. M. Riordan, 'Commentary on the Don Ostrow Trieste Yellow Retreat 2019: a successful biennium, what next?', *Pediatric Research*, pp. 1–2, Jan. 2020, doi: 10.1038/s41390-020-0767-z.
[21] T. W. R. Hansen, 'Pioneers in the Scientific Study of Neonatal Jaundice and Kernicterus', *Pediatrics*, vol. 106, no. 2, Art. no. 2, Aug. 2000, doi: 10.1542/peds.106.2.e15.

[22] J.-B. Le Pichon, S. M. Riordan, J. Watchko, and S. M. Shapiro, 'The Neurological Sequelae of Neonatal Hyperbilirubinemia: Definitions, Diagnosis and Treatment of the Kernicterus Spectrum Disorders (KSDs)', *Curr Pediatr Rev*, vol. 13, no. 3, Art. no. 3, 2017, doi: 10.2174/1573396313666170815100214.
[23] V. K. Bhutani and L. Johnson-Hamerman, 'The clinical syndrome of bilirubin-induced neurologic dysfunction', *Semin Fetal Neonatal Med*, vol. 20, no. 1, Art. no. 1, Feb. 2015, doi: 10.1016/j.siny.2014.12.008.
[24] T. M. Slusher *et al.*, 'Burden of severe neonatal jaundice: a systematic review and meta-analysis', *BMJ Paediatrics Open*, vol. 1, no. 1, Art. no. 1, Nov. 2017, doi: 10.1136/bmjpo-2017-000105.
[25] S. M. Shapiro, 'Definition of the Clinical Spectrum of Kernicterus and Bilirubin-Induced Neurologic Dysfunction (BIND)', *Journal of Perinatology*, p. 6.
[26] M. J. Maisels, 'Neonatal hyperbilirubinemia and kernicterus - not gone but sometimes forgotten', *Early Hum Dev*, vol. 85, no. 11, Art. no. 11, Nov. 2009, doi: 10.1016/j.earlhumdev.2009.09.003.
[27] B. O. Olusanya, S. Teeple, and N. J. Kassebaum, 'The Contribution of Neonatal Jaundice to Global Child Mortality: Findings From the GBD 2016 Study', *Pediatrics*, vol. 141, no. 2, Art. no. 2, Feb. 2018, doi: 10.1542/peds.2017-1471.
[28] V. K. Bhutani and R. J. Wong, 'Bilirubin neurotoxicity in preterm infants: Risk and prevention', *Journal of Clinical Neonatology*, vol. 2, no. 2, Art. no. 2, Jan. 2013, doi: 10.4103/2249-4847.116402.
[29] S. on Hyperbilirubinemia, 'Management of Hyperbilirubinemia in the Newborn Infant 35 or More Weeks of Gestation', *Pediatrics*, vol. 114, no. 1, Art. no. 1, Jul. 2004, doi: 10.1542/peds.114.1.297.
[30] A. Okumura *et al.*, 'Kernicterus in Preterm Infants', *Pediatrics*, May 2009, doi: 10.1542/peds.2008-2791.
[31] P. Govaert *et al.*, 'Changes in globus pallidus with (pre)term kernicterus', *Pediatrics*, vol. 112, no. 6 Pt 1, Art. no. 6 Pt 1, Dec. 2003, doi: 10.1542/peds.112.6.1256.
[32] A. Kamei, M. Sasaki, M. Akasaka, N. Soga, K. Kudo, and S. Chida, 'Proton Magnetic Resonance Spectroscopic Images in Preterm Infants with Bilirubin Encephalopathy', *The Journal of Pediatrics*, vol. 160, no. 2, Art. no. 2, Feb. 2012, doi: 10.1016/j.jpeds.2011.09.036.
[33] J. F. Watchko and M. Jeffrey Maisels, 'The enigma of low bilirubin kernicterus in premature infants: Why does it still occur, and is it

preventable?', *Seminars in Perinatology*, vol. 38, no. 7, Art. no. 7, Nov. 2014, doi: 10.1053/j.semperi.2014.08.002.
[34] I. Morioka *et al.*, 'Serum unbound bilirubin as a predictor for clinical kernicterus in extremely low birth weight infants at a late age in the neonatal intensive care unit', *Brain and Development*, vol. 37, no. 8, Art. no. 8, Sep. 2015, doi: 10.1016/j.braindev.2015.01.001.
[35] S. B. Amin, C. Ahlfors, M. S. Orlando, L. E. Dalzell, K. S. Merle, and R. Guillet, 'Bilirubin and serial auditory brainstem responses in premature infants', *Pediatrics*, vol. 107, no. 4, Art. no. 4, Apr. 2001, doi: 10.1542/peds.107.4.664.
[36] H. Nakamura, M. Yonetani, Y. Uetani, M. Funato, and Y. Lee, 'Determination of serum unbound bilirubin for prediction of kernicterus in low birthweight infants', *Acta Paediatr Jpn*, vol. 34, no. 6, Art. no. 6, Dec. 1992, doi: 10.1111/j.1442-200x.1992.tb01024.x.
[37] C. E. Ahlfors, S. B. Amin, and A. E. Parker, 'Unbound bilirubin predicts abnormal automated auditory brainstem response in a diverse newborn population', *J Perinatol*, vol. 29, no. 4, Art. no. 4, Apr. 2009, doi: 10.1038/jp.2008.199.
[38] S. B. Amin *et al.*, 'Auditory toxicity in late preterm and term neonates with severe jaundice', *Dev Med Child Neurol*, vol. 59, no. 3, Art. no. 3, Mar. 2017, doi: 10.1111/dmcn.13284.
[39] S. B. Amin, H. Wang, N. Laroia, and M. Orlando, 'Unbound Bilirubin and Auditory Neuropathy Spectrum Disorder in Late Preterm and Term Infants with Severe Jaundice', *The Journal of Pediatrics*, vol. 173, pp. 84–89, Jun. 2016, doi: 10.1016/j.jpeds.2016.02.024.
[40] S. B. Amin *et al.*, 'Chronic Auditory Toxicity in Late Preterm and Term Infants With Significant Hyperbilirubinemia', *Pediatrics*, vol. 140, no. 4, Art. no. 4, Oct. 2017, doi: 10.1542/peds.2016-4009.
[41] S. B. Amin and H. Wang, 'Unbound unconjugated hyperbilirubinemia is associated with central apnea in premature infants', *J Pediatr*, vol. 166, no. 3, Art. no. 3, Mar. 2015, doi: 10.1016/j.jpeds.2014.12.003.
[42] S. B. Amin, L. Charafeddine, and R. Guillet, 'Transient bilirubin encephalopathy and apnea of prematurity in 28 to 32 weeks gestational age infants', *J Perinatol*, vol. 25, no. 6, Art. no. 6, Jun. 2005, doi: 10.1038/sj.jp.7211295.
[43] H. Ye *et al.*, 'Bilirubin-induced neurotoxic and ototoxic effects in rat cochlear and vestibular organotypic cultures', *Neurotoxicology*, vol. 71, pp. 75–86, Mar. 2019, doi: 10.1016/j.neuro.2018.12.004.

[44] W. T. Shaia, S. M. Shapiro, and R. F. Spencer, 'The jaundiced gunn rat model of auditory neuropathy/dyssynchrony', *Laryngoscope*, vol. 115, no. 12, Art. no. 12, Dec. 2005, doi: 10.1097/01.MLG.0000181501.80291.05.

[45] F. Usman, U. Diala, S. Shapiro, J.-B. LePichon, and T. Slusher, 'Acute bilirubin encephalopathy and its progression to kernicterus: current perspectives', *Research and Reports in Neonatology*, vol. 8, pp. 33–44, Mar. 2018.

[46] J. F. Watchko, 'Bilirubin-Induced Neurotoxicity in the Preterm Neonate', *Clin Perinatol*, vol. 43, no. 2, Art. no. 2, Jun. 2016, doi: 10.1016/j.clp.2016.01.007.

[47] K. A. Jangaard, D. B. Fell, L. Dodds, and A. C. Allen, 'Outcomes in a Population of Healthy Term and Near-Term Infants With Serum Bilirubin Levels of ≥325 μmol/L (≥19 mg/dL) Who Were Born in Nova Scotia, Canada, Between 1994 and 2000', *Pediatrics*, vol. 122, no. 1, pp. 119–124, Jul. 2008, doi: 10.1542/peds.2007-0967.

[48] L. Hokkanen, J. Launes, and K. Michelsson, 'Adult neurobehavioral outcome of hyperbilirubinemia in full term neonates—a 30 year prospective follow-up study', *PeerJ*, vol. 2, p. e294, Mar. 2014, doi: 10.7717/peerj.294.

[49] R. D. Maimburg, M. Væth, D. E. Schendel, B. H. Bech, J. Olsen, and P. Thorsen, 'Neonatal jaundice: a risk factor for infantile autism?', *Paediatric and Perinatal Epidemiology*, vol. 22, no. 6, pp. 562–568, 2008, doi: 10.1111/j.1365-3016.2008.00973.x.

[50] R. D. Maimburg, B. H. Bech, M. Væth, B. Møller-Madsen, and J. Olsen, 'Neonatal Jaundice, Autism, and Other Disorders of Psychological Development', *Pediatrics*, vol. 126, no. 5, pp. 872–878, Nov. 2010, doi: 10.1542/peds.2010-0052.

[51] G.-S. Nam, S. H. Kwak, S. H. Bae, S. H. Kim, J. Jung, and J. Y. Choi, 'Hyperbilirubinemia and Follow-up Auditory Brainstem Responses in Preterm Infants', *Clin Exp Otorhinolaryngol*, vol. 12, no. 2, Art. no. 2, May 2019, doi: 10.21053/ceo.2018.00899.

[52] D. H. Adamkin, 'Late preterm infants: severe hyperbilirubinemia and postnatal glucose homeostasis', *Journal of Perinatology*, vol. 29, no. 2, Art. no. 2, May 2009, doi: 10.1038/jp.2009.41.

[53] K. Gkoltsiou, M. Tzoufi, S. Counsell, M. Rutherford, and F. Cowan, 'Serial brain MRI and ultrasound findings: Relation to gestational age, bilirubin level, neonatal neurologic status and neurodevelopmental outcome in infants at risk of kernicterus', *Early*

Human Development, vol. 84, no. 12, Art. no. 12, Dec. 2008, doi: 10.1016/j.earlhumdev.2008.09.008.

[54] J. F. Watchko, 'Kernicterus and the molecular mechanisms of bilirubin-induced CNS injury in newborns', *Neuromolecular Med*, vol. 8, no. 4, Art. no. 4, 2006, doi: 10.1385/NMM:8:4:513.

[55] S. M. Shapiro, 'Bilirubin toxicity in the developing nervous system', *Pediatric Neurology*, vol. 29, no. 5, Art. no. 5, Nov. 2003, doi: 10.1016/j.pediatrneurol.2003.09.011.

[56] E. Hankø, T. W. R. Hansen, R. Almaas, J. Lindstad, and T. Rootwelt, 'Bilirubin induces apoptosis and necrosis in human NT2-N neurons', *Pediatr Res*, vol. 57, no. 2, Art. no. 2, Feb. 2005, doi: 10.1203/01.PDR.0000148711.11519.A5.

[57] D. Brites, 'The evolving landscape of neurotoxicity by unconjugated bilirubin: role of glial cells and inflammation', *Front Pharmacol*, vol. 3, p. 88, 2012, doi: 10.3389/fphar.2012.00088.

[58] J. F. Watchko and C. Tiribelli, 'Bilirubin-Induced Neurologic Damage — Mechanisms and Management Approaches', *New England Journal of Medicine*, vol. 369, no. 21, Art. no. 21, Nov. 2013, doi: 10.1056/NEJMra1308124.

[59] C. M. P. Rodrigues, S. Solá, R. E. Castro, P. A. Laires, D. Brites, and J. J. G. Moura, 'Perturbation of membrane dynamics in nerve cells as an early event during bilirubin-induced apoptosis', *J Lipid Res*, vol. 43, no. 6, Art. no. 6, Jun. 2002.

[60] J. D. Ostrow, L. Pascolo, D. Brites, and C. Tiribelli, 'Molecular basis of bilirubin-induced neurotoxicity', *Trends in Molecular Medicine*, vol. 10, no. 2, pp. 65–70, Feb. 2004, doi: 10.1016/j.molmed.2003.12.003.

[61] C. M. P. Rodrigues, S. Solá, M. A. Brito, D. Brites, and J. J. G. Moura, 'Bilirubin directly disrupts membrane lipid polarity and fluidity, protein order, and redox status in rat mitochondria', *Journal of Hepatology*, vol. 36, no. 3, Art. no. 3, Mar. 2002, doi: 10.1016/S0168-8278(01)00279-3.

[62] M. A. Brito *et al.*, 'Bilirubin injury to neurons: contribution of oxidative stress and rescue by glycoursodeoxycholic acid', *Neurotoxicology*, vol. 29, no. 2, Art. no. 2, Mar. 2008, doi: 10.1016/j.neuro.2007.11.002.

[63] L. Cesaratto *et al.*, 'Bilirubin-induced cell toxicity involves PTEN activation through an APE1/Ref-1-dependent pathway', *J Mol Med (Berl)*, vol. 85, no. 10, pp. 1099–1112, Oct. 2007, doi: 10.1007/s00109-007-0204-3.

[64] M. Qaisiya, C. D. Coda Zabetta, C. Bellarosa, and C. Tiribelli, 'Bilirubin mediated oxidative stress involves antioxidant response activation via Nrf2 pathway', *Cellular Signalling*, vol. 26, no. 3, pp. 512–520, Mar. 2014, doi: 10.1016/j.cellsig.2013.11.029.
[65] M. J. Daood, M. Hoyson, and J. F. Watchko, 'Lipid peroxidation is not the primary mechanism of bilirubin-induced neurologic dysfunction in jaundiced Gunn rat pups', *Pediatr. Res.*, vol. 72, no. 5, Art. no. 5, Nov. 2012, doi: 10.1038/pr.2012.111.
[66] M. Dal Ben, C. Bottin, F. Zanconati, C. Tiribelli, and S. Gazzin, 'Evaluation of region selective bilirubin-induced brain damage as a basis for a pharmacological treatment', *Sci Rep*, vol. 7, p. 41032, Jan. 2017, doi: 10.1038/srep41032.
[67] V. Rawat, G. Bortolussi, S. Gazzin, C. Tiribelli, and A. F. Muro, 'Bilirubin-Induced Oxidative Stress Leads to DNA Damage in the Cerebellum of Hyperbilirubinemic Neonatal Mice and Activates DNA Double-Strand Break Repair Pathways in Human Cells', *Oxid Med Cell Longev*, vol. 2018, Nov. 2018, doi: 10.1155/2018/1801243.
[68] G. Bortolussi *et al.*, 'Impairment of enzymatic antioxidant defenses is associated with bilirubin-induced neuronal cell death in the cerebellum of Ugt1 KO mice', *Cell Death Dis*, vol. 6, p. e1739, May 2015, doi: 10.1038/cddis.2015.113.
[69] M. Davutoglu *et al.*, 'Oxidative stress and antioxidant status in neonatal hyperbilirubinemia', *Saudi Med J*, vol. 29, no. 12, pp. 1743–1748, Dec. 2008.
[70] D. Sarici *et al.*, 'Investigation on malondialdehyde, S100B, and advanced oxidation protein product levels in significant hyperbilirubinemia and the effect of intensive phototherapy on these parameters', *Pediatr Neonatol*, vol. 56, no. 2, pp. 95–100, Apr. 2015, doi: 10.1016/j.pedneo.2014.06.006.
[71] A. S. Falcão, A. Fernandes, M. A. Brito, R. F. M. Silva, and D. Brites, 'Bilirubin-induced inflammatory response, glutamate release, and cell death in rat cortical astrocytes are enhanced in younger cells', *Neurobiology of Disease*, vol. 20, no. 2, Art. no. 2, Nov. 2005, doi: 10.1016/j.nbd.2005.03.001.
[72] A. M. Connolly and J. J. Volpe, 'Clinical Features of Bilirubin Encephalopathy', *Clinics in Perinatology*, vol. 17, no. 2, pp. 371–379, Jun. 1990, doi: 10.1016/S0095-5108(18)30573-6.
[73] K. Liaury *et al.*, 'Morphological features of microglial cells in the hippocampal dentate gyrus of Gunn rat: a possible schizophrenia

animal model', *Journal of Neuroinflammation*, vol. 9, no. 1, Art. no. 1, Mar. 2012, doi: 10.1186/1742-2094-9-56.
[74] K. Liaury *et al.*, 'Minocycline improves recognition memory and attenuates microglial activation in Gunn rat: A possible hyperbilirubinemia-induced animal model of schizophrenia', *Progress in Neuro-Psychopharmacology and Biological Psychiatry*, vol. 50, pp. 184–190, Apr. 2014, doi: 10.1016/j.pnpbp.2013.12.017.
[75] A. Fernandes, A. S. Falcão, R. F. M. Silva, M. A. Brito, and D. Brites, 'MAPKs are key players in mediating cytokine release and cell death induced by unconjugated bilirubin in cultured rat cortical astrocytes', *European Journal of Neuroscience*, vol. 25, no. 4, Art. no. 4, 2007, doi: 10.1111/j.1460-9568.2007.05340.x.
[76] A. Fernandes *et al.*, 'Inflammatory signalling pathways involved in astroglial activation by unconjugated bilirubin', *J. Neurochem.*, vol. 96, no. 6, Art. no. 6, Mar. 2006, doi: 10.1111/j.1471-4159.2006.03680.x.
[77] D. Brites and M. A. Brito, 'Chapter 7. Bilirubin Toxicity', in *Care of the Jaundiced Neonate*, D. K. Stevenson, M. J. Maisels, and J. F. Watchko, Eds. New York, NY: The McGraw-Hill Companies, 2012. Accessed: Jun. 25, 2022. [Online]. Available: accesspediatrics.mhmedical.com/content.aspx?aid=56322515
[78] S. Vodret, G. Bortolussi, J. Jašprová, L. Vitek, and A. F. Muro, 'Inflammatory signature of cerebellar neurodegeneration during neonatal hyperbilirubinemia in Ugt1 (-/-) mouse model', *J Neuroinflammation*, vol. 14, no. 1, Art. no. 1, Mar. 2017, doi: 10.1186/s12974-017-0838-1.
[79] M. V. Sofroniew and H. V. Vinters, 'Astrocytes: biology and pathology', *Acta Neuropathol*, vol. 119, no. 1, pp. 7–35, Jan. 2010, doi: 10.1007/s00401-009-0619-8.
[80] A. Nair, T. J. Frederick, and S. D. Miller, 'Astrocytes in multiple sclerosis: A product of their environment', *Cell. Mol. Life Sci.*, vol. 65, no. 17, p. 2702, Jun. 2008, doi: 10.1007/s00018-008-8059-5.
[81] W. Liu, Y. Tang, and J. Feng, 'Cross talk between activation of microglia and astrocytes in pathological conditions in the central nervous system', *Life Sciences*, vol. 89, no. 5, pp. 141–146, Aug. 2011, doi: 10.1016/j.lfs.2011.05.011.
[82] M. D. Haustein, D. J. Read, J. R. Steinert, N. Pilati, D. Dinsdale, and I. D. Forsythe, 'Acute hyperbilirubinaemia induces presynaptic neurodegeneration at a central glutamatergic synapse', *The Journal of*

Physiology, vol. 588, no. 23, pp. 4683–4693, 2010, doi: 10.1113/jphysiol.2010.199778.

[83] D. J. Hoffman, S. A. Zanelli, J. Kubin, O. P. Mishra, and M. Delivoria-Papadopoulos, 'The in Vivo Effect of Bilirubin on the N-Methyl-D-Aspartate Receptor/Ion Channel Complex in the Brains of Newborn Piglets', *Pediatr Res*, vol. 40, no. 6, Art. no. 6, Dec. 1996, doi: 10.1203/00006450-199612000-00005.

[84] S. Grojean, V. Koziel, P. Vert, and J. L. Daval, 'Bilirubin induces apoptosis via activation of NMDA receptors in developing rat brain neurons', *Exp. Neurol.*, vol. 166, no. 2, Art. no. 2, Dec. 2000, doi: 10.1006/exnr.2000.7518.

[85] R. Silva, L. R. Mata, S. Gulbenkian, M. A. Brito, C. Tiribelli, and D. Brites, 'Inhibition of Glutamate Uptake by Unconjugated Bilirubin in Cultured Cortical Rat Astrocytes: Role of Concentration and pH', *Biochemical and Biophysical Research Communications*, vol. 265, no. 1, pp. 67–72, Nov. 1999, doi: 10.1006/bbrc.1999.1646.

[86] S. Grojean, V. Lievre, V. Koziel, P. Vert, and J. L. Daval, 'Bilirubin exerts additional toxic effects in hypoxic cultured neurons from the developing rat brain by the recruitment of glutamate neurotoxicity', *Pediatr. Res.*, vol. 49, no. 4, Art. no. 4, Apr. 2001, doi: 10.1203/00006450-200104000-00012.

[87] J. W. McDonald, S. M. Shapiro, F. S. Silverstein, and M. V. Johnston, 'Role of glutamate receptor-mediated excitotoxicity in bilirubin-induced brain injury in the Gunn rat model', *Exp. Neurol.*, vol. 150, no. 1, Art. no. 1, Mar. 1998, doi: 10.1006/exnr.1997.6762.

[88] M. P. Mattson, 'Excitotoxic and excitoprotective mechanisms', *Neuromol Med*, vol. 3, no. 2, pp. 65–94, Apr. 2003, doi: 10.1385/NMM:3:2:65.

[89] M. J. Maisels and A. F. McDonagh, 'Phototherapy for neonatal jaundice', *N. Engl. J. Med.*, vol. 358, no. 9, Art. no. 9, Feb. 2008, doi: 10.1056/NEJMct0708376.

[90] M. J. Maisels, J. F. Watchko, V. K. Bhutani, and D. K. Stevenson, 'An approach to the management of hyperbilirubinemia in the preterm infant less than 35 weeks of gestation', *Journal of Perinatology*, vol. 32, no. 9, Art. no. 9, Sep. 2012, doi: 10.1038/jp.2012.71.

[91] M. A. Nizam, A. S. Alvi, M. M. Hamdani, A. S. Lalani, S. A. Sibtain, and N. A. Bhangar, 'Efficacy of double versus single phototherapy in treatment of neonatal jaundice: a meta-analysis', *Eur J Pediatr*, vol. 179, no. 6, Art. no. 6, Jun. 2020, doi: 10.1007/s00431-020-03583-x.

[92] M. Yurdakök, 'Phototherapy in the newborn: what's new?', *J Ped Neonat Individual Med*, vol. 4, no. 2, Art. no. 2, Oct. 2015, doi: 10.7363/040255.
[93] J. E. Tyson *et al.*, 'Does aggressive phototherapy increase mortality while decreasing profound impairment among the smallest and sickest newborns?', *Journal of Perinatology*, vol. 32, no. 9, Art. no. 9, Sep. 2012, doi: 10.1038/jp.2012.64.
[94] C. Arnold, C. Pedroza, and J. E. Tyson, 'Phototherapy in ELBW newborns: Does it work? Is it safe? The evidence from randomized clinical trials', *Seminars in Perinatology*, vol. 38, no. 7, Art. no. 7, Nov. 2014, doi: 10.1053/j.semperi.2014.08.008.
[95] C. Greco *et al.*, 'Neonatal Jaundice in Low- and Middle-Income Countries: Lessons and Future Directions from the 2015 Don Ostrow Trieste Yellow Retreat', *Neonatology*, vol. 110, no. 3, Art. no. 3, 2016, doi: 10.1159/000445708.
[96] B. O. Olusanya, T. A. Ogunlesi, and T. M. Slusher, 'Why is kernicterus still a major cause of death and disability in low-income and middle-income countries?', *Arch Dis Child*, vol. 99, no. 12, Art. no. 12, Dec. 2014, doi: 10.1136/archdischild-2013-305506.
[97] A. R. Borden *et al.*, 'Variation in the Phototherapy Practices and Irradiance of Devices in a Major Metropolitan Area', *Neonatology*, vol. 113, no. 3, Art. no. 3, 2018, doi: 10.1159/000485369.
[98] S. M. Shapiro and S. M. Riordan, 'Review of bilirubin neurotoxicity II: preventing and treating acute bilirubin encephalopathy and kernicterus spectrum disorders', *Pediatr. Res.*, Oct. 2019, doi: 10.1038/s41390-019-0603-5.
[99] V. J. Flaherman, M. W. Kuzniewicz, G. J. Escobar, and T. B. Newman, 'Total Serum Bilirubin Exceeding Exchange Transfusion Thresholds in the Setting of Universal Screening', *The Journal of Pediatrics*, vol. 160, no. 5, Art. no. 5, May 2012, doi: 10.1016/j.jpeds.2011.09.063.
[100] M. F. Wolf *et al.*, 'Exchange transfusion safety and outcomes in neonatal hyperbilirubinemia', *Journal of Perinatology*, vol. 40, no. 10, Art. no. 10, Oct. 2020, doi: 10.1038/s41372-020-0642-0.
[101] S. Murki and P. Kumar, 'Blood exchange transfusion for infants with severe neonatal hyperbilirubinemia', *Semin Perinatol*, vol. 35, no. 3, Art. no. 3, Jun. 2011, doi: 10.1053/j.semperi.2011.02.013.
[102] M. K. Sabzehei, B. Basiri, M. Shokouhi, and S. Torabian, 'Complications of exchange transfusion in hospitalized neonates in two neonatal centers in Hamadan, a five-year experience', *Journal of*

Comprehensive Pediatrics, vol. 6, no. 2, Art. no. 2, 2015, Accessed: Nov. 13, 2020. [Online]. Available: https://www.scopus.com/inward/record.uri?eid=2-s2.0-84959039061&doi=10.17795%2fcomperped-20587&partnerID=40&md5=3edaa319948a24e1c5dff3bac4abd4f9

[103] A. S. Geiger, A. C. Rice, and S. M. Shapiro, 'Minocycline blocks acute bilirubin-induced neurological dysfunction in jaundiced Gunn rats', *Neonatology*, vol. 92, no. 4, Art. no. 4, 2007, doi: 10.1159/000103740.

[104] S. Lin *et al.*, 'Minocycline blocks bilirubin neurotoxicity and prevents hyperbilirubinemia-induced cerebellar hypoplasia in the Gunn rat', *Eur. J. Neurosci.*, vol. 22, no. 1, Art. no. 1, Jul. 2005, doi: 10.1111/j.1460-9568.2005.04182.x.

[105] S. Vodret, G. Bortolussi, A. Iaconcig, E. Martinelli, C. Tiribelli, and A. F. Muro, 'Attenuation of neuro-inflammation improves survival and neurodegeneration in a mouse model of severe neonatal hyperbilirubinemia', *Brain Behav. Immun.*, vol. 70, pp. 166–178, 2018, doi: 10.1016/j.bbi.2018.02.011.

[106] P. Reddy, S. Najundaswamy, R. Mehta, A. Petrova, and T. Hegyi, 'Tin-mesoporphyrin in the Treatment of Severe Hyperbilirubinemia in a Very-low-birth-weight Infant', *Journal of Perinatology*, vol. 23, no. 6, Art. no. 6, Sep. 2003, doi: 10.1038/sj.jp.7210943.

[107] V. K. Bhutani, R. Poland, L. D. Meloy, T. Hegyi, A. A. Fanaroff, and M. J. Maisels, 'Clinical trial of tin mesoporphyrin to prevent neonatal hyperbilirubinemia', *Journal of Perinatology*, vol. 36, no. 7, Art. no. 7, Jul. 2016, doi: 10.1038/jp.2016.22.

[108] S. Gazzin, L. Vitek, J. Watchko, S. M. Shapiro, and C. Tiribelli, 'A Novel Perspective on the Biology of Bilirubin in Health and Disease', *Trends in Molecular Medicine*, vol. 22, no. 9, pp. 758–768, Sep. 2016, doi: 10.1016/j.molmed.2016.07.004.

[109] H. M. Schipper, W. Song, A. Tavitian, and M. Cressatti, 'The sinister face of heme oxygenase-1 in brain aging and disease', *Prog Neurobiol*, vol. 172, pp. 40–70, Jan. 2019, doi: 10.1016/j.pneurobio.2018.06.008.

[110] L. Vítek, 'Bilirubin as a signaling molecule', *Medicinal Research Reviews*, vol. 40, no. 4, pp. 1335–1351, 2020, doi: https://doi.org/10.1002/med.21660.

[111] V. L. Feigin *et al.*, 'Global, regional, and national burden of neurological disorders during 1990–2015: a systematic analysis for the Global Burden of Disease Study 2015', *The Lancet Neurology*, vol.

16, no. 11, pp. 877–897, Nov. 2017, doi: 10.1016/S1474-4422(17)30299-5.
[112] E. R. Dorsey and B. R. Bloem, 'The Parkinson Pandemic-A Call to Action', *JAMA Neurol*, vol. 75, no. 1, pp. 9–10, Jan. 2018, doi: 10.1001/jamaneurol.2017.3299.
[113] W. Yang *et al.*, 'Current and projected future economic burden of Parkinson's disease in the U.S.', *npj Parkinson's Disease*, vol. 6, no. 1, Art. no. 1, Jul. 2020, doi: 10.1038/s41531-020-0117-1.
[114] A. Lee and R. M. Gilbert, 'Epidemiology of Parkinson Disease', *Neurologic Clinics*, vol. 34, no. 4, pp. 955–965, Nov. 2016, doi: 10.1016/j.ncl.2016.06.012.
[115] A. De Virgilio *et al.*, 'Parkinson's disease: Autoimmunity and neuroinflammation', *Autoimmunity Reviews*, vol. 15, no. 10, pp. 1005–1011, Oct. 2016, doi: 10.1016/j.autrev.2016.07.022.
[116] Q. Mao, W. Qin, A. Zhang, and N. Ye, 'Recent advances in dopaminergic strategies for the treatment of Parkinson's disease', *Acta Pharmacol Sin*, vol. 41, no. 4, Art. no. 4, Apr. 2020, doi: 10.1038/s41401-020-0365-y.
[117] D. Belvisi, R. Pellicciari, G. Fabbrini, M. Tinazzi, A. Berardelli, and G. Defazio, 'Modifiable risk and protective factors in disease development, progression and clinical subtypes of Parkinson's disease: What do prospective studies suggest?', *Neurobiology of Disease*, vol. 134, p. 104671, Feb. 2020, doi: 10.1016/j.nbd.2019.104671.
[118] Z. Liu and H.-H. Cheung, 'Stem Cell-Based Therapies for Parkinson Disease', *Int J Mol Sci*, vol. 21, no. 21, Oct. 2020, doi: 10.3390/ijms21218060.
[119] J. Blesa, I. Trigo-Damas, A. Quiroga-Varela, and V. R. Jackson-Lewis, 'Oxidative stress and Parkinson's disease', *Front. Neuroanat.*, vol. 9, 2015, doi: 10.3389/fnana.2015.00091.
[120] V. Calabrese *et al.*, 'Aging and Parkinson's Disease: Inflammaging, neuroinflammation and biological remodeling as key factors in pathogenesis', *Free Radical Biology and Medicine*, vol. 115, pp. 80–91, Feb. 2018, doi: 10.1016/j.freeradbiomed.2017.10.379.
[121] D. J. Surmeier, 'Determinants of dopaminergic neuron loss in Parkinson's disease', *The FEBS Journal*, vol. 285, no. 19, pp. 3657–3668, 2018, doi: https://doi.org/10.1111/febs.14607.
[122] W. M. Johnson, A. L. Wilson-Delfosse, and J. J. Mieyal, 'Dysregulation of Glutathione Homeostasis in Neurodegenerative

Diseases', *Nutrients*, vol. 4, no. 10, Art. no. 10, Oct. 2012, doi: 10.3390/nu4101399.
[123] L. Puspita, S. Y. Chung, and J. Shim, 'Oxidative stress and cellular pathologies in Parkinson's disease', *Molecular Brain*, vol. 10, no. 1, p. 53, Nov. 2017, doi: 10.1186/s13041-017-0340-9.
[124] P. Jenner, 'Oxidative stress in Parkinson's disease', *Ann Neurol*, vol. 53 Suppl 3, pp. S26-36; discussion S36-38, 2003, doi: 10.1002/ana.10483.
[125] C. Zhou, Y. Huang, and S. Przedborski, 'Oxidative Stress in Parkinson's Disease', *Annals of the New York Academy of Sciences*, vol. 1147, no. 1, pp. 93–104, 2008, doi: https://doi.org/10.1196/annals.1427.023.
[126] Z. Wei, X. Li, X. Li, Q. Liu, and Y. Cheng, 'Oxidative Stress in Parkinson's Disease: A Systematic Review and Meta-Analysis', *Front. Mol. Neurosci.*, vol. 11, 2018, doi: 10.3389/fnmol.2018.00236.
[127] H. E. Moon and S. H. Paek, 'Mitochondrial Dysfunction in Parkinson's Disease', *Exp Neurobiol*, vol. 24, no. 2, pp. 103–116, Jun. 2015, doi: 10.5607/en.2015.24.2.103.
[128] K.-H. Chang and C.-M. Chen, 'The Role of Oxidative Stress in Parkinson's Disease', *Antioxidants*, vol. 9, no. 7, Art. no. 7, Jul. 2020, doi: 10.3390/antiox9070597.
[129] A. H. V. Schapira, J. M. Cooper, D. Dexter, J. B. Clark, P. Jenner, and C. D. Marsden, 'Mitochondrial Complex I Deficiency in Parkinson's Disease', *Journal of Neurochemistry*, vol. 54, no. 3, pp. 823–827, 1990, doi: https://doi.org/10.1111/j.1471-4159.1990.tb02325.x.
[130] C. M. Tanner *et al.*, 'Rotenone, Paraquat, and Parkinson's Disease', *Environ Health Perspect*, vol. 119, no. 6, Art. no. 6, Jun. 2011, doi: 10.1289/ehp.1002839.
[131] E. K. Pissadaki and J. P. Bolam, 'The energy cost of action potential propagation in dopamine neurons: clues to susceptibility in Parkinson's disease', *Front. Comput. Neurosci.*, vol. 7, 2013, doi: 10.3389/fncom.2013.00013.
[132] B. G. Trist, D. J. Hare, and K. L. Double, 'Oxidative stress in the aging substantia nigra and the etiology of Parkinson's disease', *Aging Cell*, vol. 18, no. 6, p. e13031, 2019, doi: https://doi.org/10.1111/acel.13031.
[133] G. T. Kannarkat, J. M. Boss, and M. G. Tansey, 'The Role of Innate and Adaptive Immunity in Parkinson's Disease', *Journal of*

Parkinson's Disease, vol. 3, no. 4, pp. 493–514, Jan. 2013, doi: 10.3233/JPD-130250.

[134] S. Jayanti, R. Moretti, C. Tiribelli, and S. Gazzin, 'Bilirubin and inflammation in neurodegenerative and other neurological diseases', *Neuroimmunology and Neuroinflammation*, vol. 7, no. 2, pp. 92–108, May 2020, doi: 10.20517/2347-8659.2019.14.

[135] M. Dal Ben *et al.*, 'Earliest Mechanisms of Dopaminergic Neurons Sufferance in a Novel Slow Progressing Ex Vivo Model of Parkinson Disease in Rat Organotypic Cultures of Substantia Nigra', *International Journal of Molecular Sciences*, vol. 20, no. 9, Art. no. 9, Jan. 2019, doi: 10.3390/ijms20092224.

[136] S. A. Ferreira and M. Romero-Ramos, 'Microglia Response During Parkinson's Disease: Alpha-Synuclein Intervention', *Front Cell Neurosci*, vol. 12, p. 247, 2018, doi: 10.3389/fncel.2018.00247.

[137] F. Novellino *et al.*, 'Innate Immunity: A Common Denominator between Neurodegenerative and Neuropsychiatric Diseases', *International Journal of Molecular Sciences*, vol. 21, no. 3, Art. no. 3, Jan. 2020, doi: 10.3390/ijms21031115.

[138] M. G. Tansey and M. Romero-Ramos, 'Immune system responses in Parkinson's disease: Early and dynamic', *European Journal of Neuroscience*, vol. 49, no. 3, pp. 364–383, 2019, doi: https://doi.org/10.1111/ejn.14290.

[139] X. Su, K. A. Maguire-Zeiss, R. Giuliano, L. Prifti, K. Venkatesh, and H. J. Federoff, 'Synuclein activates microglia in a model of Parkinson's disease', *Neurobiology of Aging*, vol. 29, no. 11, pp. 1690–1701, Nov. 2008, doi: 10.1016/j.neurobiolaging.2007.04.006.

[140] E. C. Hirsch and D. G. Standaert, 'Ten Unsolved Questions About Neuroinflammation in Parkinson's Disease', *Movement Disorders*, vol. 36, no. 1, pp. 16–24, 2021, doi: https://doi.org/10.1002/mds.28075.

[141] S. Ojha, H. Javed, S. Azimullah, and M. E. Haque, 'β-Caryophyllene, a phytocannabinoid attenuates oxidative stress, neuroinflammation, glial activation, and salvages dopaminergic neurons in a rat model of Parkinson disease', *Mol Cell Biochem*, vol. 418, no. 1, pp. 59–70, Jul. 2016, doi: 10.1007/s11010-016-2733-y.

[142] L.-H. Bao *et al.*, 'Urate inhibits microglia activation to protect neurons in an LPS-induced model of Parkinson's disease', *Journal of Neuroinflammation*, vol. 15, no. 1, p. 131, May 2018, doi: 10.1186/s12974-018-1175-8.

[143] K. Hassanzadeh and A. Rahimmi, 'Oxidative stress and neuroinflammation in the story of Parkinson's disease: Could targeting these pathways write a good ending?', *Journal of Cellular Physiology*, vol. 234, no. 1, pp. 23–32, 2019, doi: https://doi.org/10.1002/jcp.26865.
[144] S. J. Chinta, C. A. Lieu, M. DeMaria, R.-M. Laberge, J. Campisi, and J. K. Andersen, 'Environmental stress, ageing and glial cell senescence: a novel mechanistic link to Parkinson's disease?', *Journal of Internal Medicine*, vol. 273, no. 5, pp. 429–436, May 2013, doi: 10.1111/joim.12029.
[145] Y. Zhang and B. A. Barres, 'Astrocyte heterogeneity: an underappreciated topic in neurobiology', *Current Opinion in Neurobiology*, vol. 20, no. 5, pp. 588–594, Oct. 2010, doi: 10.1016/j.conb.2010.06.005.
[146] V. Brochard *et al.*, 'Infiltration of $CD4^+$ lymphocytes into the brain contributes to neurodegeneration in a mouse model of Parkinson disease', *J Clin Invest*, vol. 119, no. 1, pp. 182–192, Jan. 2009, doi: 10.1172/JCI36470.
[147] D. Sulzer *et al.*, 'T cells from patients with Parkinson's disease recognize α-synuclein peptides', *Nature*, vol. 546, no. 7660, Art. no. 7660, Jun. 2017, doi: 10.1038/nature22815.
[148] C. H. Williams-Gray *et al.*, 'Serum immune markers and disease progression in an incident Parkinson's disease cohort (ICICLE-PD)', *Movement Disorders*, vol. 31, no. 7, pp. 995–1003, 2016, doi: https://doi.org/10.1002/mds.26563.
[149] C. Raza, R. Anjum, and N. ul A. Shakeel, 'Parkinson's disease: Mechanisms, translational models and management strategies', *Life Sciences*, vol. 226, pp. 77–90, Jun. 2019, doi: 10.1016/j.lfs.2019.03.057.
[150] M. Deleidi and W. Maetzler, 'Protein Clearance Mechanisms of Alpha-Synuclein and Amyloid-Beta in Lewy Body Disorders', *International Journal of Alzheimer’s Disease*, vol. 2012, p. e391438, Oct. 2012, doi: 10.1155/2012/391438.
[151] D. Ebrahimi-Fakhari, L. Wahlster, and P. J. McLean, 'Protein degradation pathways in Parkinson's disease: curse or blessing', *Acta Neuropathol*, vol. 124, no. 2, pp. 153–172, Aug. 2012, doi: 10.1007/s00401-012-1004-6.
[152] Š. Lehtonen, T.-M. Sonninen, S. Wojciechowski, G. Goldsteins, and J. Koistinaho, 'Dysfunction of Cellular Proteostasis in Parkinson's Disease', *Front. Neurosci.*, vol. 13, 2019, doi: 10.3389/fnins.2019.00457.

[153] M. Bi, X. Du, Q. Jiao, X. Chen, and H. Jiang, 'Expanding the role of proteasome homeostasis in Parkinson's disease: beyond protein breakdown', *Cell Death & Disease*, vol. 12, no. 2, Art. no. 2, Feb. 2021, doi: 10.1038/s41419-021-03441-0.
[154] Y. Furukawa *et al.*, 'Brain proteasomal function in sporadic Parkinson's disease and related disorders', *Annals of Neurology*, vol. 51, no. 6, pp. 779–782, 2002, doi: https://doi.org/10.1002/ana.10207.
[155] E. Bentea, L. Verbruggen, and A. Massie, 'The Proteasome Inhibition Model of Parkinson's Disease', *J Parkinsons Dis*, vol. 7, no. 1, pp. 31–63, 2017, doi: 10.3233/JPD-160921.
[156] C. McKinnon *et al.*, 'Early-onset impairment of the ubiquitin-proteasome system in dopaminergic neurons caused by α-synuclein', *Acta Neuropathologica Communications*, vol. 8, no. 1, p. 17, Feb. 2020, doi: 10.1186/s40478-020-0894-0.
[157] R. Balestrino and A. H. V. Schapira, 'Parkinson disease', *European Journal of Neurology*, vol. 27, no. 1, pp. 27–42, 2020, doi: https://doi.org/10.1111/ene.14108.
[158] C. Klein and A. Westenberger, 'Genetics of Parkinson's disease', *Cold Spring Harb Perspect Med*, vol. 2, no. 1, p. a008888, Jan. 2012, doi: 10.1101/cshperspect.a008888.
[159] C. Marras *et al.*, 'Nomenclature of genetic movement disorders: Recommendations of the international Parkinson and movement disorder society task force', *Mov Disord*, vol. 31, no. 4, pp. 436–457, Apr. 2016, doi: 10.1002/mds.26527.
[160] M. Bi, S. Kang, X. Du, Q. Jiao, and H. Jiang, 'Association between SNCA rs356220 polymorphism and Parkinson's disease: A meta-analysis', *Neurosci Lett*, vol. 717, p. 134703, Jan. 2020, doi: 10.1016/j.neulet.2019.134703.
[161] W. Poewe *et al.*, 'Parkinson disease', *Nature Reviews Disease Primers*, vol. 3, no. 1, Art. no. 1, Mar. 2017, doi: 10.1038/nrdp.2017.13.
[162] Z. Gan-Or, P. A. Dion, and G. A. Rouleau, 'Genetic perspective on the role of the autophagy-lysosome pathway in Parkinson disease', *Autophagy*, vol. 11, no. 9, pp. 1443–1457, Sep. 2015, doi: 10.1080/15548627.2015.1067364.
[163] J. Liu, W. Liu, R. Li, and H. Yang, 'Mitophagy in Parkinson's Disease: From Pathogenesis to Treatment', *Cells*, vol. 8, no. 7, Art. no. 7, Jul. 2019, doi: 10.3390/cells8070712.

[164] E. Tolosa, M. Vila, C. Klein, and O. Rascol, 'LRRK2 in Parkinson disease: challenges of clinical trials', *Nature Reviews Neurology*, vol. 16, no. 2, Art. no. 2, Feb. 2020, doi: 10.1038/s41582-019-0301-2.
[165] D. Berg *et al.*, 'Changing the research criteria for the diagnosis of Parkinson's disease: obstacles and opportunities', *The Lancet Neurology*, vol. 12, no. 5, pp. 514–524, May 2013, doi: 10.1016/S1474-4422(13)70047-4.
[166] M. T. Hayes, 'Parkinson's Disease and Parkinsonism', *Am J Med*, vol. 132, no. 7, pp. 802–807, Jul. 2019, doi: 10.1016/j.amjmed.2019.03.001.
[167] L. V. Kalia and A. E. Lang, 'Parkinson's disease', *Lancet*, vol. 386, no. 9996, pp. 896–912, Aug. 2015, doi: 10.1016/S0140-6736(14)61393-3.
[168] A. Tarakad and J. Jankovic, 'Diagnosis and Management of Parkinson's Disease', *Semin Neurol*, vol. 37, no. 2, pp. 118–126, Apr. 2017, doi: 10.1055/s-0037-1601888.
[169] M. J. Armstrong and M. S. Okun, 'Diagnosis and Treatment of Parkinson Disease: A Review', *JAMA*, vol. 323, no. 6, p. 548, Feb. 2020, doi: 10.1001/jama.2019.22360.
[170] C. J. Hartmann, S. Fliegen, S. J. Groiss, L. Wojtecki, and A. Schnitzler, 'An update on best practice of deep brain stimulation in Parkinson's disease', *Ther Adv Neurol Disord*, vol. 12, p. 1756286419838096, Jan. 2019, doi: 10.1177/1756286419838096.
[171] T. Stoddard-Bennett and R. Reijo Pera, 'Treatment of Parkinson's Disease through Personalized Medicine and Induced Pluripotent Stem Cells', *Cells*, vol. 8, no. 1, Jan. 2019, doi: 10.3390/cells8010026.
[172] E. Arenas, 'Towards stem cell replacement therapies for Parkinson's disease', *Biochemical and Biophysical Research Communications*, vol. 396, no. 1, pp. 152–156, May 2010, doi: 10.1016/j.bbrc.2010.04.037.
[173] T. W. Kim, S. Y. Koo, and L. Studer, 'Pluripotent Stem Cell Therapies for Parkinson Disease: Present Challenges and Future Opportunities', *Front. Cell Dev. Biol.*, vol. 8, 2020, doi: 10.3389/fcell.2020.00729.
[174] A. McTague, G. Rossignoli, A. Ferrini, S. Barral, and M. A. Kurian, 'Genome Editing in iPSC-Based Neural Systems: From Disease Models to Future Therapeutic Strategies', *Front. Genome Ed.*, vol. 3, 2021, doi: 10.3389/fgeed.2021.630600.
[175] S. Jayanti, R. Moretti, C. Tiribelli, and S. Gazzin, 'Bilirubin and inflammation in neurodegenerative and other neurological diseases', *Neuroimmunology and Neuroinflammation*, vol. 7, no. 2, pp. 92–108, May 2020, doi: 10.20517/2347-8659.2019.14.

[176] H. S. Elshony, W. M. El Sheikh, and M. S. Melake, 'Association between serum bilirubin and migraine in children and adolescents', *The Egyptian Journal of Neurology, Psychiatry and Neurosurgery*, vol. 56, no. 1, p. 85, Aug. 2020, doi: 10.1186/s41983-020-00217-9.
[177] J.-N. Jin, X. Liu, M.-J. Li, X.-L. Bai, and A.-M. Xie, 'Association between serum bilirubin concentration and Parkinson's disease: a meta-analysis', *Chin Med J (Engl)*, vol. 134, no. 6, pp. 655–661, Mar. 2021, doi: 10.1097/CM9.0000000000001300.
[178] J. Chen, Y. Tu, C. Moon, E. Nagata, and G. V. Ronnett, 'Heme oxygenase-1 and heme oxygenase-2 have distinct roles in the proliferation and survival of olfactory receptor neurons mediated by cGMP and bilirubin, respectively', *Journal of Neurochemistry*, vol. 85, no. 5, Art. no. 5, 2003, doi: 10.1046/j.1471-4159.2003.01776.x.
[179] J.-S. Park, E. Nam, H.-K. Lee, M. H. Lim, and H.-W. Rhee, 'In Cellulo Mapping of Subcellular Localized Bilirubin', *ACS Chem. Biol.*, vol. 11, no. 8, Art. no. 8, 19 2016, doi: 10.1021/acschembio.6b00017.
[180] T. Takeda, A. Mu, T. T. Tai, S. Kitajima, and S. Taketani, 'Continuous *de novo* biosynthesis of haem and its rapid turnover to bilirubin are necessary for cytoprotection against cell damage', *Scientific Reports*, vol. 5, p. 10488, May 2015, doi: 10.1038/srep10488.
[181] N. G. Abraham and A. Kappas, 'Pharmacological and clinical aspects of heme oxygenase', *Pharmacol. Rev.*, vol. 60, no. 1, Art. no. 1, Mar. 2008, doi: 10.1124/pr.107.07104.
[182] K.-H. Wagner *et al.*, 'Looking to the horizon: the role of bilirubin in the development and prevention of age-related chronic diseases', *Clin. Sci.*, vol. 129, no. 1, pp. 1–25, Jul. 2015, doi: 10.1042/CS20140566.
[183] D. E. Baranano, M. Rao, C. D. Ferris, and S. H. Snyder, 'Biliverdin reductase: a major physiologic cytoprotectant', *Proc. Natl. Acad. Sci. U.S.A.*, vol. 99, no. 25, Art. no. 25, Dec. 2002, doi: 10.1073/pnas.252626999.
[184] M. D. Maines, 'New Insights into Biliverdin Reductase Functions: Linking Heme Metabolism to Cell Signaling', *Physiology*, vol. 20, no. 6, Art. no. 6, Dec. 2005, doi: 10.1152/physiol.00029.2005.
[185] I. D. Diamond and R. S. Schmid, 'Experimental bilirubin encephalopathy. The mode of entry of bilirubin-14C into the central nervous system', *J. Clin. Invest.*, vol. 45, no. 5, Art. no. 5, May 1966, doi: 10.1172/JCI105383.
[186] R. P. Wennberg, J. F. Watchko, and S. M. Shapiro, 'Maternal Empowerment - An Underutilized Strategy to Prevent Kernicterus?',

Curr Pediatr Rev, vol. 13, no. 3, Art. no. 3, 2017, doi: 10.2174/1573396313666170828112038.

[187] R. Stocker, Y. Yamamoto, A. F. McDonagh, A. N. Glazer, and B. N. Ames, 'Bilirubin is an antioxidant of possible physiological importance', *Science*, vol. 235, no. 4792, Art. no. 4792, Feb. 1987, doi: 10.1126/science.3029864.

[188] M. Qaisiya, C. D. Coda Zabetta, C. Bellarosa, and C. Tiribelli, 'Bilirubin mediated oxidative stress involves antioxidant response activation via Nrf2 pathway', *Cell Signal*, vol. 26, no. 3, pp. 512–520, Mar. 2014, doi: 10.1016/j.cellsig.2013.11.029.

[189] C. Mancuso *et al.*, 'Bilirubin as an endogenous modulator of neurotrophin redox signaling', *Journal of Neuroscience Research*, vol. 86, no. 10, pp. 2235–2249, 2008, doi: 10.1002/jnr.21665.

[190] S. R. Datla, G. J. Dusting, T. A. Mori, C. J. Taylor, K. D. Croft, and F. Jiang, 'Induction of heme oxygenase-1 in vivo suppresses NADPH oxidase derived oxidative stress', *Hypertension*, vol. 50, no. 4, pp. 636–642, Oct. 2007, doi: 10.1161/HYPERTENSIONAHA.107.092296.

[191] F. Yang *et al.*, 'The Neuroprotective Effect of Hemin and the Related Mechanism in Sevoflurane Exposed Neonatal Rats', *Front. Neurosci.*, vol. 13, 2019, doi: 10.3389/fnins.2019.00537.

[192] F. Yang, Y. Zhang, Z. Tang, Y. Shan, X. Wu, and H. Liu, 'Hemin treatment protects neonatal rats from sevoflurane-induced neurotoxicity via the phosphoinositide 3-kinase/Akt pathway', *Life Sci.*, vol. 242, p. 117151, Feb. 2020, doi: 10.1016/j.lfs.2019.117151.

[193] T. N. Dang, S. R. Robinson, R. Dringen, and G. M. Bishop, 'Uptake, metabolism and toxicity of hemin in cultured neurons', *Neurochemistry International*, vol. 58, no. 7, pp. 804–811, Jun. 2011, doi: 10.1016/j.neuint.2011.03.006.

[194] H. Kaur, M. N. Hughes, C. J. Green, P. Naughton, R. Foresti, and R. Motterlini, 'Interaction of bilirubin and biliverdin with reactive nitrogen species', *FEBS Letters*, vol. 543, no. 1–3, pp. 113–119, 2003, doi: 10.1016/S0014-5793(03)00420-4.

[195] T. N. Dang, S. R. Robinson, R. Dringen, and G. M. Bishop, 'Uptake, metabolism and toxicity of hemin in cultured neurons', *Neurochemistry International*, vol. 58, no. 7, Art. no. 7, Jun. 2011, doi: 10.1016/j.neuint.2011.03.006.

[196] C. Mancuso *et al.*, 'Inhibition of lipid peroxidation and protein oxidation by endogenous and exogenous antioxidants in rat brain

microsomes in vitro', *Neuroscience Letters*, vol. 518, no. 2, pp. 101–105, Jun. 2012, doi: 10.1016/j.neulet.2012.04.062.
[197] C. Vasavda *et al.*, 'Bilirubin Links Heme Metabolism to Neuroprotection by Scavenging Superoxide', *Cell Chemical Biology*, vol. 26, no. 10, pp. 1450-1460.e7, Oct. 2019, doi: 10.1016/j.chembiol.2019.07.006.
[198] Y. Liu *et al.*, 'Bilirubin Possesses Powerful Immunomodulatory Activity and Suppresses Experimental Autoimmune Encephalomyelitis', *The Journal of Immunology*, vol. 181, no. 3, pp. 1887–1897, Aug. 2008, doi: 10.4049/jimmunol.181.3.1887.
[199] Y. Liu *et al.*, 'Bilirubin Possesses Powerful Immunomodulatory Activity and Suppresses Experimental Autoimmune Encephalomyelitis', *The Journal of Immunology*, vol. 181, no. 3, Art. no. 3, Aug. 2008, doi: 10.4049/jimmunol.181.3.1887.
[200] A. C. Rice and S. M. Shapiro, 'Biliverdin-induced brainstem auditory evoked potential abnormalities in the jaundiced Gunn rat', *Brain Research*, vol. 1107, no. 1, pp. 215–221, Aug. 2006, doi: 10.1016/j.brainres.2006.06.005.
[201] R. Gozzelino, 'The Pathophysiology of Heme in the Brain', *Current Alzheimer Research*, Jan. 31, 2016. https://www.eurekaselect.com/135089/article (accessed Jul. 27, 2020).
[202] C. M. P. Rodrigues, S. Solá, and D. Brites, 'Bilirubin induces apoptosis via the mitochondrial pathway in developing rat brain neurons', *Hepatology*, vol. 35, no. 5, Art. no. 5, May 2002, doi: 10.1053/jhep.2002.32967.
[203] D. Bulters *et al.*, 'Haemoglobin scavenging in intracranial bleeding: biology and clinical implications', *Nature Reviews Neurology*, vol. 14, no. 7, Art. no. 7, Jul. 2018, doi: 10.1038/s41582-018-0020-0.
[204] C. Righy, M. T. Bozza, M. F. Oliveira, and F. A. Bozza, 'Molecular, Cellular and Clinical Aspects of Intracerebral Hemorrhage: Are the Enemies Within?', *Curr Neuropharmacol*, vol. 14, no. 4, Art. no. 4, May 2016, doi: 10.2174/1570159X14666151230110058.
[205] D. Chiabrando, V. Fiorito, S. Petrillo, and E. Tolosano, 'Unraveling the Role of Heme in Neurodegeneration', *Front Neurosci*, vol. 12, Oct. 2018, doi: 10.3389/fnins.2018.00712.
[206] H. M. Schipper, 'Heme oxygenase-1: role in brain aging and neurodegeneration', *Experimental Gerontology*, vol. 35, no. 6, Art. no. 6, Sep. 2000, doi: 10.1016/S0531-5565(00)00148-0.

[207] H. M. Schipper, 'Brain iron deposition and the free radical-mitochondrial theory of ageing', *Ageing Research Reviews*, vol. 3, no. 3, Art. no. 3, Jul. 2004, doi: 10.1016/j.arr.2004.02.001.
[208] V. M. Andrade, M. Aschner, and A. P. Marreilha dos Santos, 'Neurotoxicity of Metal Mixtures', in *Neurotoxicity of Metals*, M. Aschner and L. G. Costa, Eds. Cham: Springer International Publishing, 2017, pp. 227–265. doi: 10.1007/978-3-319-60189-2_12.
[209] M. Qaisiya, C. Brischetto, J. Jašprová, L. Vitek, C. Tiribelli, and C. Bellarosa, 'Bilirubin-induced ER stress contributes to the inflammatory response and apoptosis in neuronal cells', *Arch. Toxicol.*, vol. 91, no. 4, Art. no. 4, Apr. 2017, doi: 10.1007/s00204-016-1835-3.
[210] Y. Liu *et al.*, 'Bilirubin as a potent antioxidant suppresses experimental autoimmune encephalomyelitis: implications for the role of oxidative stress in the development of multiple sclerosis', *Journal of Neuroimmunology*, vol. 139, no. 1, Art. no. 1, Jun. 2003, doi: 10.1016/S0165-5728(03)00132-2.
[211] Z.-Y. Zou *et al.*, 'Biliverdin administration regulates the microRNA-mRNA expressional network associated with neuroprotection in cerebral ischemia reperfusion injury in rats', *International Journal of Molecular Medicine*, vol. 43, no. 3, Art. no. 3, Mar. 2019, doi: 10.3892/ijmm.2019.4064.
[212] N. Atsunori, M. Noriko, H. Chien, T. Hideyoshi, B. T. R., and K. Shinichi, 'Biliverdin Administration Prevents the Formation of Intimal Hyperplasia Induced by Vascular Injury', *Circulation*, vol. 112, no. 4, Art. no. 4, Jul. 2005, doi: 10.1161/CIRCULATIONAHA.104.509778.
[213] K. Bisht *et al.*, 'Biliverdin modulates the expression of C5aR in response to endotoxin in part via mTOR signaling', *Biochem. Biophys. Res. Commun.*, vol. 449, no. 1, Art. no. 1, Jun. 2014, doi: 10.1016/j.bbrc.2014.04.150.
[214] B. Wegiel *et al.*, 'Biliverdin inhibits Toll-like receptor-4 (TLR4) expression through nitric oxide-dependent nuclear translocation of biliverdin reductase', *PNAS*, vol. 108, no. 46, Art. no. 46, Nov. 2011, doi: 10.1073/pnas.1108571108.
[215] J. Chen, 'Heme oxygenase in neuroprotection: from mechanisms to therapeutic implications', *Rev Neurosci*, vol. 25, no. 2, Art. no. 2, 2014, doi: 10.1515/revneuro-2013-0046.

[216] A. Cuadrado and A. I. Rojo, 'Heme oxygenase-1 as a therapeutic target in neurodegenerative diseases and brain infections', *Curr. Pharm. Des.*, vol. 14, no. 5, Art. no. 5, 2008, doi: 10.2174/138161208783597407.
[217] F. Peng *et al.*, 'Serum bilirubin concentrations and multiple sclerosis', *Journal of Clinical Neuroscience*, vol. 18, no. 10, Art. no. 10, Oct. 2011, doi: 10.1016/j.jocn.2011.02.023.
[218] H. Lee and Y. K. Choi, 'Regenerative Effects of Heme Oxygenase Metabolites on Neuroinflammatory Diseases', *International Journal of Molecular Sciences*, vol. 20, no. 1, Art. no. 1, Jan. 2019, doi: 10.3390/ijms20010078.
[219] H. Kaur, M. N. Hughes, C. J. Green, P. Naughton, R. Foresti, and R. Motterlini, 'Interaction of bilirubin and biliverdin with reactive nitrogen species', *FEBS Letters*, vol. 543, no. 1–3, Art. no. 1–3, 2003, doi: 10.1016/S0014-5793(03)00420-4.
[220] T. W. Sedlak, M. Saleh, D. S. Higginson, B. D. Paul, K. R. Juluri, and S. H. Snyder, 'Bilirubin and glutathione have complementary antioxidant and cytoprotective roles', *PNAS*, vol. 106, no. 13, Art. no. 13, Mar. 2009, doi: 10.1073/pnas.0813132106.
[221] T. Sedlak and S. Snyder, 'Bilirubin Benefits: Cellular Protection by a Biliverdin Reductase Antioxidant Cycle', *Pediatrics*, vol. 113, pp. 1776–82, Jul. 2004, doi: 10.1542/peds.113.6.1776.
[222] K.-H. Wagner *et al.*, 'Looking to the horizon: the role of bilirubin in the development and prevention of age-related chronic diseases', *Clin. Sci.*, vol. 129, no. 1, Art. no. 1, Jul. 2015, doi: 10.1042/CS20140566.
[223] F. Yang, Y. Zhang, Z. Tang, Y. Shan, X. Wu, and H. Liu, 'Hemin treatment protects neonatal rats from sevoflurane-induced neurotoxicity via the phosphoinositide 3-kinase/Akt pathway', *Life Sci.*, vol. 242, p. 117151, Feb. 2020, doi: 10.1016/j.lfs.2019.117151.
[224] P. Ayuso *et al.*, 'An association study between Heme oxygenase-1 genetic variants and Parkinson's disease', *Front. Cell. Neurosci.*, vol. 8, 2014, doi: 10.3389/fncel.2014.00298.
[225] E. Barone *et al.*, 'Biliverdin Reductase-A Mediates the Beneficial Effects of Intranasal Insulin in Alzheimer Disease', *Mol Neurobiol*, vol. 56, no. 4, Art. no. 4, Apr. 2019, doi: 10.1007/s12035-018-1231-5.
[226] D. Y. Lee, M. Oh, S.-J. Kim, J. S. Oh, S. J. Chung, and J. S. Kim, 'Bilirubin-Related Differential Striatal [18F]FP-CIT Uptake in

Parkinson Disease', *Clinical Nuclear Medicine*, vol. 44, no. 11, Art. no. 11, Nov. 2019, doi: 10.1097/RLU.0000000000002749.
[227] S.-Y. Hung, H.-C. Liou, K.-H. Kang, R.-M. Wu, C.-C. Wen, and W.-M. Fu, 'Over-expression of Heme oxygenase-1 protects dopaminergic neurons against 1-methyl-4-phenylpyridinium-induced neurotoxicity', *Mol Pharmacol*, Sep. 2008, doi: 10.1124/mol.108.048611.
[228] M. S. Yoo *et al.*, 'Oxidative stress regulated genes in nigral dopaminergic neuronal cells: correlation with the known pathology in Parkinson's disease', *Molecular Brain Research*, vol. 110, no. 1, Art. no. 1, Jan. 2003, doi: 10.1016/S0169-328X(02)00586-7.
[229] D. Y. Lee, M. Oh, S.-J. Kim, J. S. Oh, S. J. Chung, and J. S. Kim, 'Bilirubin-Related Differential Striatal [18F]FP-CIT Uptake in Parkinson Disease', *Clinical Nuclear Medicine*, vol. 44, no. 11, pp. 855–859, Nov. 2019, doi: 10.1097/RLU.0000000000002749.
[230] D. Macías-García *et al.*, 'Increased bilirubin levels in Parkinson's disease', *Parkinsonism & Related Disorders*, vol. 63, pp. 213–216, Jun. 2019, doi: 10.1016/j.parkreldis.2019.01.012.
[231] T. Hatano, S. Saiki, A. Okuzumi, R. P. Mohney, and N. Hattori, 'Identification of novel biomarkers for Parkinson's disease by metabolomic technologies', *J Neurol Neurosurg Psychiatry*, vol. 87, no. 3, pp. 295–301, Mar. 2016, doi: 10.1136/jnnp-2014-309676.
[232] H. Luan, L.-F. Liu, Z. Tang, V. C. T. Mok, M. Li, and Z. Cai, 'Elevated excretion of biopyrrin as a new marker for idiopathic Parkinson's disease', *Parkinsonism & Related Disorders*, vol. 21, no. 11, pp. 1371–1372, Nov. 2015, doi: 10.1016/j.parkreldis.2015.09.009.
[233] M. Moccia *et al.*, 'Increased bilirubin levels in de novo Parkinson's disease', *Eur. J. Neurol.*, vol. 22, no. 6, Art. no. 6, Jun. 2015, doi: 10.1111/ene.12688.
[234] G. Scigliano, F. Girotti, P. Soliveri, M. Musicco, D. Radice, and T. Caraceni, 'Increased plasma bilirubin in Parkinson patients on L-dopa: evidence against the free radical hypothesis?', *Ital J Neuro Sci*, vol. 18, no. 2, Art. no. 2, Apr. 1997, doi: 10.1007/BF01999565.
[235] P. Ayuso *et al.*, 'A polymorphism located at an ATG transcription start site of the heme oxygenase-2 gene is associated with classical Parkinson's disease', *Pharmacogenet Genomics*, vol. 21, no. 9, pp. 565–571, Sep. 2011, doi: 10.1097/FPC.0b013e328348f729.

[236] W. Song *et al.*, 'Evaluation of salivary heme oxygenase-1 as a potential biomarker of early Parkinson's disease', *Mov. Disord.*, vol. 33, no. 4, pp. 583–591, 2018, doi: 10.1002/mds.27328.
[237] H. Luan, L.-F. Liu, Z. Tang, V. C. T. Mok, M. Li, and Z. Cai, 'Elevated excretion of biopyrrin as a new marker for idiopathic Parkinson's disease', *Parkinsonism & Related Disorders*, vol. 21, no. 11, Art. no. 11, Nov. 2015, doi: 10.1016/j.parkreldis.2015.09.009.
[238] C. Li, P. Hossieny, B. J. Wu, A. Qawasmeh, K. Beck, and R. Stocker, 'Pharmacologic induction of heme oxygenase-1', *Antioxid Redox Signal*, vol. 9, no. 12, Art. no. 12, Dec. 2007, doi: 10.1089/ars.2007.1783.
[239] Z. Strasky *et al.*, 'Spirulina platensis and phycocyanobilin activate atheroprotective heme oxygenase-1: a possible implication for atherogenesis', *Food Funct*, vol. 4, no. 11, Art. no. 11, Nov. 2013, doi: 10.1039/c3fo60230c.
[240] E. Barone, F. Di Domenico, C. Mancuso, and D. A. Butterfield, 'The Janus face of the heme oxygenase/biliverdin reductase system in Alzheimer disease: It's time for reconciliation', *Neurobiology of Disease*, vol. 62, pp. 144–159, Feb. 2014, doi: 10.1016/j.nbd.2013.09.018.
[241] H. M. Schipper, A. Liberman, and E. G. Stopa, 'Neural heme oxygenase-1 expression in idiopathic Parkinson's disease', *Exp. Neurol.*, vol. 150, no. 1, Art. no. 1, Mar. 1998, doi: 10.1006/exnr.1997.6752.
[242] D. Macías-García *et al.*, 'Increased bilirubin levels in Parkinson's disease', *Parkinsonism & Related Disorders*, vol. 63, pp. 213–216, Jun. 2019, doi: 10.1016/j.parkreldis.2019.01.012.
[243] J. S. Kim *et al.*, 'Toxicity and tissue distribution of magnetic nanoparticles in mice', *Toxicol Sci*, vol. 89, no. 1, Art. no. 1, Jan. 2006, doi: 10.1093/toxsci/kfj027.
[244] C. Petters, E. Irrsack, M. Koch, and R. Dringen, 'Uptake and metabolism of iron oxide nanoparticles in brain cells', *Neurochem Res*, vol. 39, no. 9, Art. no. 9, Sep. 2014, doi: 10.1007/s11064-014-1380-5.
[245] L. Vitek, C. Bellarosa, and C. Tiribelli, 'Induction of Mild Hyperbilirubinemia: Hype or Real Therapeutic Opportunity?', *Clinical Pharmacology & Therapeutics*, vol. 106, no. 3, Art. no. 3, 2019, doi: 10.1002/cpt.1341.

[246] T. M. Sim, D. Tarini, S. T. Dheen, B. H. Bay, and D. K. Srinivasan, 'Nanoparticle-Based Technology Approaches to the Management of Neurological Disorders', *Int J Mol Sci*, vol. 21, no. 17, Art. no. 17, Aug. 2020, doi: 10.3390/ijms21176070.
[247] D. M. Teleanu, C. Chircov, A. M. Grumezescu, A. Volceanov, and R. I. Teleanu, 'Blood-Brain Delivery Methods Using Nanotechnology', *Pharmaceutics*, vol. 10, no. 4, Art. no. 4, Dec. 2018, doi: 10.3390/pharmaceutics10040269.
[248] L. B. Thomsen, M. S. Thomsen, and T. Moos, 'Targeted drug delivery to the brain using magnetic nanoparticles', *Ther Deliv*, vol. 6, no. 10, Art. no. 10, 2015, doi: 10.4155/tde.15.56.
[249] L. L. Israel, A. Galstyan, E. Holler, and J. Y. Ljubimova, 'Magnetic iron oxide nanoparticles for imaging, targeting and treatment of primary and metastatic tumors of the brain', *Journal of Controlled Release*, vol. 320, pp. 45–62, Apr. 2020, doi: 10.1016/j.jconrel.2020.01.009.
[250] S. Naqvi, A. Panghal, and S. J. S. Flora, 'Nanotechnology: A Promising Approach for Delivery of Neuroprotective Drugs', *Front. Neurosci.*, vol. 14, 2020, doi: 10.3389/fnins.2020.00494.
[251] G. Liu, P. Men, G. Perry, and M. A. Smith, 'Nanoparticle and Iron Chelators as a Potential Novel Alzheimer Therapy', *Methods Mol Biol*, vol. 610, pp. 123–144, 2010, doi: 10.1007/978-1-60327-029-8_8.
[252] Y. Lee, S. Lee, D. Y. Lee, B. Yu, W. Miao, and S. Jon, 'Multistimuli-Responsive Bilirubin Nanoparticles for Anticancer Therapy', *Angewandte Chemie International Edition*, vol. 55, no. 36, Art. no. 36, 2016, doi: 10.1002/anie.201604858.
[253] S. Sundar Dhilip Kumar, N. N. Houreld, and H. Abrahamse, 'Therapeutic Potential and Recent Advances of Curcumin in the Treatment of Aging-Associated Diseases', *Molecules*, vol. 23, no. 4, Art. no. 4, Apr. 2018, doi: 10.3390/molecules23040835.
[254] S. Fuloria *et al.*, 'A Comprehensive Review on the Therapeutic Potential of Curcuma longa Linn. in Relation to its Major Active Constituent Curcumin', *Frontiers in Pharmacology*, vol. 13, 2022, Accessed: Jun. 24, 2022. [Online]. Available: https://www.frontiersin.org/article/10.3389/fphar.2022.820806
[255] European Medicine Agency, 'Assessment report on Curcuma longa L. (C. domestica Valeton), rhizoma'. 2017. [Online]. Available: https://www.ema.europa.eu/documents/herbal-report/draft-

assessment-report-curcuma-longa-l-c-domestica-valeton-rhizome-revision-1_en.pdf
[256] M. Iriti, S. Vitalini, G. Fico, and F. Faoro, 'Neuroprotective herbs and foods from different traditional medicines and diets', *Molecules*, vol. 15, no. 5, pp. 3517–3555, May 2010, doi: 10.3390/molecules15053517.
[257] R. K. Maheshwari, A. K. Singh, J. Gaddipati, and R. C. Srimal, 'Multiple biological activities of curcumin: a short review', *Life Sci*, vol. 78, no. 18, pp. 2081–2087, Mar. 2006, doi: 10.1016/j.lfs.2005.12.007.
[258] P. Anand *et al.*, 'Biological activities of curcumin and its analogues (Congeners) made by man and Mother Nature', *Biochem Pharmacol*, vol. 76, no. 11, pp. 1590–1611, Dec. 2008, doi: 10.1016/j.bcp.2008.08.008.
[259] M. F. Beal, 'Therapeutic approaches to mitochondrial dysfunction in Parkinson's disease', *Parkinsonism Relat Disord*, vol. 15 Suppl 3, pp. S189-194, Dec. 2009, doi: 10.1016/S1353-8020(09)70812-0.
[260] X. Lin *et al.*, 'Curcumin attenuates oxidative stress in RAW264.7 cells by increasing the activity of antioxidant enzymes and activating the Nrf2-Keap1 pathway', *PLoS One*, vol. 14, no. 5, p. e0216711, 2019, doi: 10.1371/journal.pone.0216711.
[261] S. Singh and B. B. Aggarwal, 'Activation of transcription factor NF-kappa B is suppressed by curcumin (diferuloylmethane) [corrected]', *J Biol Chem*, vol. 270, no. 42, pp. 24995–25000, Oct. 1995, doi: 10.1074/jbc.270.42.24995.
[262] A. Jacob, R. Wu, M. Zhou, and P. Wang, 'Mechanism of the Anti-inflammatory Effect of Curcumin: PPAR-gamma Activation', *PPAR Res*, vol. 2007, p. 89369, 2007, doi: 10.1155/2007/89369.
[263] S. C. Gupta, A. K. Tyagi, P. Deshmukh-Taskar, M. Hinojosa, S. Prasad, and B. B. Aggarwal, 'Downregulation of tumor necrosis factor and other proinflammatory biomarkers by polyphenols', *Arch Biochem Biophys*, vol. 559, pp. 91–99, Oct. 2014, doi: 10.1016/j.abb.2014.06.006.
[264] N.-S. Chang, N. Joki, J. Mattison, T. Dinh, and S. John, 'Characterization of serum adhesive proteins that block tumor necrosis factor-mediated cell death', *Cell Death Differ*, vol. 4, no. 8, Art. no. 8, Dec. 1997, doi: 10.1038/sj.cdd.4400301.
[265] H. Yin *et al.*, 'Curcumin Suppresses IL-1β Secretion and Prevents Inflammation through Inhibition of the NLRP3 Inflammasome', *J*

Immunol, vol. 200, no. 8, pp. 2835–2846, Apr. 2018, doi: 10.4049/jimmunol.1701495.

[266] S. A. Jagmag, N. Tripathi, S. D. Shukla, S. Maiti, and S. Khurana, 'Evaluation of Models of Parkinson's Disease', *Frontiers in Neuroscience*, vol. 9, 2016, Accessed: Jun. 25, 2022. [Online]. Available: https://www.frontiersin.org/article/10.3389/fnins.2015.00503

[267] M. F. Beal, 'Parkinson's disease: a model dilemma', *Nature*, vol. 466, no. 7310, Art. no. 7310, Aug. 2010, doi: 10.1038/466S8a.

[268] H. Braak and E. Braak, 'Pathoanatomy of Parkinson's disease', *J Neurol*, vol. 247, no. 2, Art. no. 2, Apr. 2000, doi: 10.1007/PL00007758.

[269] M. Dal Ben *et al.*, 'Earliest Mechanisms of Dopaminergic Neurons Sufferance in a Novel Slow Progressing Ex Vivo Model of Parkinson Disease in Rat Organotypic Cultures of Substantia Nigra', *Int J Mol Sci*, vol. 20, no. 9, Art. no. 9, May 2019, doi: 10.3390/ijms20092224.

[270] C. L. Croft, H. S. Futch, B. D. Moore, and T. E. Golde, 'Organotypic brain slice cultures to model neurodegenerative proteinopathies', *Molecular Neurodegeneration*, vol. 14, no. 1, p. 45, Dec. 2019, doi: 10.1186/s13024-019-0346-0.

[271] C. L. Croft and W. Noble, 'Preparation of organotypic brain slice cultures for the study of Alzheimer's disease', *F1000Res*, vol. 7, p. 592, 2018, doi: 10.12688/f1000research.14500.2.

[272] M. ALAYLIOĞLU, E. DURSUN, S. YILMAZER, and D. G. AK, 'A Bridge Between in vitro and in vivo Studies in Neuroscience: Organotypic Brain Slice Cultures', *Noro Psikiyatr Ars*, vol. 57, no. 4, pp. 333–337, Sep. 2020, doi: 10.29399/npa.26139.

[273] S. Gazzin *et al.*, 'Curcumin Prevents Cerebellar Hypoplasia and Restores the Behavior in Hyperbilirubinemic Gunn Rat by a Pleiotropic Effect on the Molecular Effectors of Brain Damage', *International Journal of Molecular Sciences*, vol. 22, no. 1, Art. no. 1, Jan. 2021, doi: 10.3390/ijms22010299.

[274] E. Vianello *et al.*, 'Histone acetylation as a new mechanism for bilirubin-induced encephalopathy in the Gunn rat', *Sci Rep*, vol. 8, no. 1, Art. no. 1, Sep. 2018, doi: 10.1038/s41598-018-32106-w.

[275] S. E. Wolfensohn and M. Lloyd, 'Practical use of distress scoring systems in the application of humane end points', in *Humane endpoints in animal experiments for biomedical research*, C. Hendriksen and D. Morton, Eds. Royal Society of Medicine Press, 1999.

Accessed: Jan. 13, 2020. [Online]. Available: http://epubs.surrey.ac.uk/827030/

[276] S. Gazzin *et al.*, 'Bilirubin accumulation and Cyp mRNA expression in selected brain regions of jaundiced Gunn rat pups', *Pediatr. Res.*, vol. 71, no. 6, Art. no. 6, Jun. 2012, doi: 10.1038/pr.2012.23.

[277] K. Smith and J. J. Leyden, 'Safety of doxycycline and minocycline: a systematic review', *Clin Ther*, vol. 27, no. 9, Art. no. 9, Sep. 2005, doi: 10.1016/j.clinthera.2005.09.005.

[278] M. Dal Ben, C. Bottin, F. Zanconati, C. Tiribelli, and S. Gazzin, 'Evaluation of region selective bilirubin-induced brain damage as a basis for a pharmacological treatment', *Sci Rep*, vol. 7, no. 1, p. 41032, Jan. 2017, doi: 10.1038/srep41032.

[279] L. Roca *et al.*, 'Factors affecting the binding of bilirubin to serum albumins: validation and application of the peroxidase method', *Pediatr Res*, vol. 60, no. 6, pp. 724–728, Dec. 2006, doi: 10.1203/01.pdr.0000245992.89965.94.

[280] J. Waddell, M. He, N. Tang, C. Rizzuto, and C. F. Bearer, 'A Gunn rat model of preterm hyperbilirubinemia', *Pediatr. Res.*, vol. 87, no. 3, Art. no. 3, 2020, doi: 10.1038/s41390-019-0599-x.

[281] R. K. Ruhela, S. Soni, P. Sarma, A. Prakash, and B. Medhi, 'Negative geotaxis: An early age behavioral hallmark to VPA rat model of autism', *Ann Neurosci*, vol. 26, no. 1, Art. no. 1, Jan. 2019, doi: 10.5214/ans.0972.7531.260106.

[282] D. N. Feather-Schussler and T. S. Ferguson, 'A Battery of Motor Tests in a Neonatal Mouse Model of Cerebral Palsy', *J Vis Exp*, no. 117, Art. no. 117, Nov. 2016, doi: 10.3791/53569.

[283] E. Abranches, A. O'Neill, M. J. Robertson, D. V. Schaffer, and J. M. S. Cabral, 'Development of quantitative PCR methods to analyse neural progenitor cell culture state', *Biotechnol Appl Biochem*, vol. 44, no. Pt 1, pp. 1–8, Apr. 2006, doi: 10.1042/BA20050218.

[284] J. Vandesompele *et al.*, 'Accurate normalization of real-time quantitative RT-PCR data by geometric averaging of multiple internal control genes', *Genome Biol*, vol. 3, no. 7, p. RESEARCH0034, Jun. 2002, doi: 10.1186/gb-2002-3-7-research0034.

[285] S. A. Bustin *et al.*, 'The MIQE Guidelines: Minimum Information for Publication of Quantitative Real-Time PCR Experiments', *Clinical Chemistry*, vol. 55, no. 4, pp. 611–622, Apr. 2009, doi: 10.1373/clinchem.2008.112797.

[286] C. M. Tanner *et al.*, 'Rotenone, Paraquat, and Parkinson's Disease', *Environ Health Perspect*, vol. 119, no. 6, pp. 866–872, Jun. 2011, doi: 10.1289/ehp.1002839.
[287] D. J. Ostrow, L. Pascolo, and C. Tiribelli, 'Reassessment of the Unbound Concentrations of Unconjugated Bilirubin in Relation to Neurotoxicity In Vitro', *Pediatr Res*, vol. 54, no. 1, pp. 98–104, Jul. 2003, doi: 10.1203/01.PDR.0000067486.79854.D5.
[288] D. A. Monti *et al.*, 'N-Acetyl Cysteine May Support Dopamine Neurons in Parkinson's Disease: Preliminary Clinical and Cell Line Data', *PLOS ONE*, vol. 11, no. 6, p. e0157602, Jun. 2016, doi: 10.1371/journal.pone.0157602.
[289] A. M. Gleixner *et al.*, 'N-acetyl-L-cysteine protects astrocytes against proteotoxicity without recourse to glutathione', *Mol Pharmacol*, Jan. 2017, doi: 10.1124/mol.117.109926.
[290] M. K. McCoy *et al.*, 'Blocking Soluble Tumor Necrosis Factor Signaling with Dominant-Negative Tumor Necrosis Factor Inhibitor Attenuates Loss of Dopaminergic Neurons in Models of Parkinson's Disease', *J. Neurosci.*, vol. 26, no. 37, pp. 9365–9375, Sep. 2006, doi: 10.1523/JNEUROSCI.1504-06.2006.
[291] O. J. Adedokun *et al.*, 'Association Between Serum Concentration of Infliximab and Efficacy in Adult Patients With Ulcerative Colitis', *Gastroenterology*, vol. 147, no. 6, pp. 1296-1307.e5, Dec. 2014, doi: 10.1053/j.gastro.2014.08.035.
[292] E. Ficiarà *et al.*, 'Beyond Oncological Hyperthermia: Physically Drivable Magnetic Nanobubbles as Novel Multipurpose Theranostic Carriers in the Central Nervous System', *Molecules*, vol. 25, no. 9, Art. no. 9, Jan. 2020, doi: 10.3390/molecules25092104.
[293] S. F. Larner, J. Wang, J. Goodman, M. B. O'Donoghue Altman, M. Xin, and K. K. W. Wang, 'In Vitro Neurotoxicity Resulting from Exposure of Cultured Neural Cells to Several Types of Nanoparticles', *J Cell Death*, vol. 10, p. 1179670717694523, Mar. 2017, doi: 10.1177/1179670717694523.
[294] J. R. Chowdhury, R. Kondapalli, and N. R. Chowdhury, 'Gunn rat: a model for inherited deficiency of bilirubin glucuronidation', *Adv Vet Sci Comp Med*, vol. 37, pp. 149–173, 1993.
[295] J. W. Conlee and S. M. Shapiro, 'Development of cerebellar hypoplasia in jaundiced Gunn rats: a quantitative light microscopic analysis', *Acta Neuropathol*, vol. 93, no. 5, Art. no. 5, Apr. 1997, doi: 10.1007/s004010050639.

[296] Y. Sawasaki, N. Yamada, and H. Nakajima, 'Developmental features of cerebellar hypoplasia and brain bilirubin levels in a mutant (Gunn) rat with hereditary hyperbilirubinaemia', *J. Neurochem.*, vol. 27, no. 2, Art. no. 2, Aug. 1976.
[297] H. S. Schutta and L. Johnson, 'Bilirubin encephalopathy in the Gunn rat: a fine structure study of the cerebellar cortex', *J. Neuropathol. Exp. Neurol.*, vol. 26, no. 3, Art. no. 3, Jul. 1967.
[298] Y. Takagishi and H. Yamamura, 'Purkinje cell abnormalities and synaptogenesis in genetically jaundiced rats (Gunn rats)', *Brain Res.*, vol. 492, no. 1–2, Art. no. 1–2, Jul. 1989.
[299] A. Barateiro, A. R. Vaz, S. L. Silva, A. Fernandes, and D. Brites, 'ER Stress, Mitochondrial Dysfunction and Calpain/JNK Activation are Involved in Oligodendrocyte Precursor Cell Death by Unconjugated Bilirubin', *Neuromol Med*, vol. 14, no. 4, Art. no. 4, Dec. 2012, doi: 10.1007/s12017-012-8187-9.
[300] A. Barateiro, H. S. Domingues, A. Fernandes, J. B. Relvas, and D. Brites, 'Rat cerebellar slice cultures exposed to bilirubin evidence reactive gliosis, excitotoxicity and impaired myelinogenesis that is prevented by AMPA and TNF-α inhibitors', *Mol. Neurobiol.*, vol. 49, no. 1, Art. no. 1, Feb. 2014, doi: 10.1007/s12035-013-8530-7.
[301] D. Brites and A. Fernandes, 'Bilirubin-induced neural impairment: a special focus on myelination, age-related windows of susceptibility and associated co-morbidities', *Semin Fetal Neonatal Med*, vol. 20, no. 1, Art. no. 1, Feb. 2015, doi: 10.1016/j.siny.2014.12.002.
[302] M. A. Brito, E. Zurolo, P. Pereira, C. Barroso, E. Aronica, and D. Brites, 'Cerebellar axon/myelin loss, angiogenic sprouting, and neuronal increase of vascular endothelial growth factor in a preterm infant with kernicterus', *J. Child Neurol.*, vol. 27, no. 5, Art. no. 5, May 2012, doi: 10.1177/0883073811423975.
[303] A. Fernandes, R. F. M. Silva, A. S. Falcão, M. A. Brito, and D. Brites, 'Cytokine production, glutamate release and cell death in rat cultured astrocytes treated with unconjugated bilirubin and LPS', *J. Neuroimmunol.*, vol. 153, no. 1–2, Art. no. 1–2, Aug. 2004, doi: 10.1016/j.jneuroim.2004.04.007.
[304] A. Fernandes *et al.*, 'Bilirubin as a determinant for altered neurogenesis, neuritogenesis, and synaptogenesis', *Devel Neurobio*, vol. 69, no. 9, Art. no. 9, Aug. 2009, doi: 10.1002/dneu.20727.
[305] S. E. Gambaro, M. C. Robert, C. Tiribelli, and S. Gazzin, 'Role of brain cytochrome P450 mono-oxygenases in bilirubin oxidation-

specific induction and activity', *Arch. Toxicol.*, Nov. 2014, doi: 10.1007/s00204-014-1394-4.
[306] T. W. Hansen, D. Bratlid, and S. I. Walaas, 'Bilirubin decreases phosphorylation of synapsin I, a synaptic vesicle-associated neuronal phosphoprotein, in intact synaptosomes from rat cerebral cortex', *Pediatr. Res.*, vol. 23, no. 2, Art. no. 2, Feb. 1988, doi: 10.1203/00006450-198802000-00018.
[307] J. A. Johnson, J. J. Hayward, S. E. Kornguth, and F. L. Siegel, 'Effects of hyperbilirubinaemia on glutathione S-transferase isoenzymes in cerebellar cortex of the Gunn rat', *Biochem. J.*, vol. 291 (Pt 2), pp. 453–461, Apr. 1993.
[308] M. C. Robert *et al.*, 'Alterations in the Cell Cycle in the Cerebellum of Hyperbilirubinemic Gunn Rat: A Possible Link with Apoptosis?', *PLoS One*, vol. 8, no. 11, Art. no. 11, Nov. 2013, doi: 10.1371/journal.pone.0079073.
[309] S. L. Silva *et al.*, 'Neuritic growth impairment and cell death by unconjugated bilirubin is mediated by NO and glutamate, modulated by microglia, and prevented by glycoursodeoxycholic acid and interleukin-10', *Neuropharmacology*, vol. 62, no. 7, Art. no. 7, Jun. 2012, doi: 10.1016/j.neuropharm.2012.02.002.
[310] G. Harauz and J. M. Boggs, 'Myelin management by the 18.5-kDa and 21.5-kDa classic myelin basic protein isoforms', *Journal of Neurochemistry*, vol. 125, no. 3, Art. no. 3, 2013, doi: 10.1111/jnc.12195.
[311] K. Akiyama, S. Ichinose, A. Omori, Y. Sakurai, and H. Asou, 'Study of expression of myelin basic proteins (MBPs) in developing rat brain using a novel antibody reacting with four major isoforms of MBP', *Journal of Neuroscience Research*, vol. 68, no. 1, Art. no. 1, 2002, doi: https://doi.org/10.1002/jnr.10188.
[312] T. Nguyen *et al.*, 'Axonal protective effects of the myelin-associated glycoprotein', *J Neurosci*, vol. 29, no. 3, Art. no. 3, Jan. 2009, doi: 10.1523/JNEUROSCI.5204-08.2009.
[313] K.-H. Wagner *et al.*, 'Looking to the horizon: the role of bilirubin in the development and prevention of age-related chronic diseases', *Clin Sci (Lond)*, vol. 129, no. 1, pp. 1–25, Jul. 2015, doi: 10.1042/CS20140566.
[314] D. J. Surmeier, J. A. Obeso, and G. M. Halliday, 'Selective neuronal vulnerability in Parkinson disease', *Nat Rev Neurosci*, vol. 18, no. 2, pp. 101–113, Feb. 2017, doi: 10.1038/nrn.2016.178.

[315] N. Giguère, S. Burke Nanni, and L.-E. Trudeau, 'On Cell Loss and Selective Vulnerability of Neuronal Populations in Parkinson's Disease', *Frontiers in Neurology*, vol. 9, p. 455, 2018, doi: 10.3389/fneur.2018.00455.
[316] K.-H. Wagner *et al.*, 'Looking to the horizon: the role of bilirubin in the development and prevention of age-related chronic diseases', *Clin Sci (Lond)*, vol. 129, no. 1, pp. 1–25, Jul. 2015, doi: 10.1042/CS20140566.
[317] L. Vitek, 'The Role of Bilirubin in Diabetes, Metabolic Syndrome, and Cardiovascular Diseases', *Frontiers in Pharmacology*, vol. 3, p. 55, 2012, doi: 10.3389/fphar.2012.00055.
[318] M. Yu *et al.*, 'D-T7 Peptide-Modified PEGylated Bilirubin Nanoparticles Loaded with Cediranib and Paclitaxel for Antiangiogenesis and Chemotherapy of Glioma', *ACS Appl. Mater. Interfaces*, vol. 11, no. 1, pp. 176–186, Jan. 2019, doi: 10.1021/acsami.8b16219.
[319] Y. Liu *et al.*, 'Bilirubin as a potent antioxidant suppresses experimental autoimmune encephalomyelitis: implications for the role of oxidative stress in the development of multiple sclerosis', *Journal of Neuroimmunology*, vol. 139, no. 1, pp. 27–35, Jun. 2003, doi: 10.1016/S0165-5728(03)00132-2.
[320] Y. Zhou *et al.*, 'Sulfiredoxin-1 Attenuates Oxidative Stress via Nrf2/ARE Pathway and 2-Cys Prdxs After Oxygen-Glucose Deprivation in Astrocytes', *J Mol Neurosci*, vol. 55, no. 4, pp. 941–950, Apr. 2015, doi: 10.1007/s12031-014-0449-6.
[321] D. Zagoura, D. Canovas-Jorda, F. Pistollato, S. Bremer-Hoffmann, and A. Bal-Price, 'Evaluation of the rotenone-induced activation of the Nrf2 pathway in a neuronal model derived from human induced pluripotent stem cells', *Neurochemistry International*, vol. 106, pp. 62–73, Jun. 2017, doi: 10.1016/j.neuint.2016.09.004.
[322] P. Scalzo, A. Kümmer, T. L. Bretas, F. Cardoso, and A. L. Teixeira, 'Serum levels of brain-derived neurotrophic factor correlate with motor impairment in Parkinson's disease', *J Neurol*, vol. 257, no. 4, pp. 540–545, Apr. 2010, doi: 10.1007/s00415-009-5357-2.
[323] H. Khalil, M. A. Alomari, O. F. Khabour, A. Al-Hieshan, and J. A. Bajwa, 'Relationship of circulatory BDNF with cognitive deficits in people with Parkinson's disease', *Journal of the Neurological Sciences*, vol. 362, pp. 217–220, Mar. 2016, doi: 10.1016/j.jns.2016.01.032.

[324] S.-Y. Hung, H.-C. Liou, K.-H. Kang, R.-M. Wu, C.-C. Wen, and W.-M. Fu, 'Overexpression of Heme Oxygenase-1 Protects Dopaminergic Neurons against 1-Methyl-4-Phenylpyridinium-Induced Neurotoxicity', *Mol Pharmacol*, vol. 74, no. 6, pp. 1564–1575, Dec. 2008, doi: 10.1124/mol.108.048611.

[325] G. Zhu, J. Li, L. He, X. Wang, and X. Hong, 'MPTP-induced changes in hippocampal synaptic plasticity and memory are prevented by memantine through the BDNF-TrkB pathway', *British Journal of Pharmacology*, vol. 172, no. 9, pp. 2354–2368, 2015, doi: 10.1111/bph.13061.

[326] S. Jayanti, L. Vítek, C. Tiribelli, and S. Gazzin, 'The Role of Bilirubin and the Other "Yellow Players" in Neurodegenerative Diseases', *Antioxidants*, vol. 9, no. 9, Art. no. 9, Sep. 2020, doi: 10.3390/antiox9090900.

[327] D. A. Monti *et al.*, 'N-Acetyl Cysteine Is Associated With Dopaminergic Improvement in Parkinson's Disease', *Clinical Pharmacology & Therapeutics*, vol. 106, no. 4, pp. 884–890, 2019, doi: 10.1002/cpt.1548.

[328] Q. Zhou *et al.*, 'Sulforaphane protects against rotenone-induced neurotoxicity in vivo: Involvement of the mTOR, Nrf2 and autophagy pathways', *Sci Rep*, vol. 6, no. 1, Art. no. 1, Aug. 2016, doi: 10.1038/srep32206.

[329] R. L. Augusto *et al.*, 'Purified anacardic acids exert multiple neuroprotective effects in pesticide model of Parkinson's disease: in vivo and in silico analysis', *IUBMB Life*, vol. 72, no. 8, pp. 1765–1779, 2020, doi: 10.1002/iub.2304.

[330] X. Yuyun *et al.*, 'Effects of Low Concentrations of Rotenone Upon Mitohormesis in SH-SY5Y Cells', *Dose-Response*, vol. 11, no. 2, p. dose-response.12-005.Gao, Apr. 2013, doi: 10.2203/dose-response.12-005.Gao.

[331] G. Tardiolo, P. Bramanti, and E. Mazzon, 'Overview on the Effects of N-Acetylcysteine in Neurodegenerative Diseases', *Molecules*, vol. 23, no. 12, Art. no. 12, Dec. 2018, doi: 10.3390/molecules23123305.

[332] C. H. Williams-Gray *et al.*, 'Serum immune markers and disease progression in an incident Parkinson's disease cohort (ICICLE-PD)', *Movement Disorders*, vol. 31, no. 7, pp. 995–1003, 2016, doi: 10.1002/mds.26563.

[333] E. Kouchaki *et al.*, 'Increased serum levels of TNF-α and decreased serum levels of IL-27 in patients with Parkinson disease and their

correlation with disease severity', *Clinical Neurology and Neurosurgery*, vol. 166, pp. 76–79, Mar. 2018, doi: 10.1016/j.clineuro.2018.01.022.
[334] N. K. Majbour *et al.*, 'CSF total and oligomeric α-Synuclein along with TNF-α as risk biomarkers for Parkinson's disease: a study in LRRK2 mutation carriers', *Translational Neurodegeneration*, vol. 9, no. 1, p. 15, May 2020, doi: 10.1186/s40035-020-00192-4.
[335] Q.-S. Lin *et al.*, 'RIP1/RIP3/MLKL mediates dopaminergic neuron necroptosis in a mouse model of Parkinson disease', *Lab Invest*, vol. 100, no. 3, pp. 503–511, Mar. 2020, doi: 10.1038/s41374-019-0319-5.
[336] M. Dufek, I. Rektorova, V. Thon, J. Lokaj, and I. Rektor, 'Interleukin-6 May Contribute to Mortality in Parkinson's Disease Patients: A 4-Year Prospective Study', *Parkinson’s Disease*, vol. 2015, p. e898192, Aug. 2015, doi: 10.1155/2015/898192.
[337] J. R. Pereira *et al.*, 'IL-6 serum levels are elevated in Parkinson's disease patients with fatigue compared to patients without fatigue', *J Neurol Sci*, vol. 370, pp. 153–156, Nov. 2016, doi: 10.1016/j.jns.2016.09.030.
[338] P. Teismann *et al.*, 'COX-2 and neurodegeneration in Parkinson's disease', *Ann N Y Acad Sci*, vol. 991, pp. 272–277, Jun. 2003, doi: 10.1111/j.1749-6632.2003.tb07482.x.
[339] S.-Y. Song *et al.*, '2-Hydroxy-4-Methylbenzoic Anhydride Inhibits Neuroinflammation in Cellular and Experimental Animal Models of Parkinson's Disease', *International Journal of Molecular Sciences*, vol. 21, no. 21, Art. no. 21, Jan. 2020, doi: 10.3390/ijms21218195.
[340] T. Horiuchi, H. Mitoma, S. Harashima, H. Tsukamoto, and T. Shimoda, 'Transmembrane TNF-alpha: structure, function and interaction with anti-TNF agents', *Rheumatology (Oxford)*, vol. 49, no. 7, pp. 1215–1228, Jul. 2010, doi: 10.1093/rheumatology/keq031.
[341] A. M. Abdelrahman, Y. M. Al Suleimani, P. Manoj, M. Ashique, B. H. Ali, and N. Schupp, 'Effect of infliximab, a tumor necrosis factor-alpha inhibitor, on doxorubicin-induced nephrotoxicity in rats', *Naunyn Schmiedebergs Arch Pharmacol*, vol. 393, no. 1, pp. 121–130, Jan. 2020, doi: 10.1007/s00210-019-01719-x.
[342] M. Moccia *et al.*, 'Increased bilirubin levels in de novo Parkinson's disease', *Eur J Neurol*, vol. 22, no. 6, pp. 954–959, Jun. 2015, doi: 10.1111/ene.12688.
[343] A. Ni and C. Ernst, 'Evidence That Substantia Nigra Pars Compacta Dopaminergic Neurons Are Selectively Vulnerable to Oxidative

Stress Because They Are Highly Metabolically Active', *Frontiers in Cellular Neuroscience*, vol. 16, 2022, Accessed: Jun. 18, 2022. [Online]. Available: https://www.frontiersin.org/article/10.3389/fncel.2022.826193

[344] M. A. Khan, S. Meena, Md. A. Alam, and S. Ghosh, 'A solvent sensitive coumarin derivative coupled with gold nanoparticles as selective fluorescent sensor for Pb2+ ions in real samples', *Spectrochimica Acta Part A: Molecular and Biomolecular Spectroscopy*, vol. 243, p. 118810, Dec. 2020, doi: 10.1016/j.saa.2020.118810.

[345] A. Marchiani, C. Rozzo, A. Fadda, and G. D. and P. Ruzza, 'Curcumin and Curcumin-like Molecules: From Spice to Drugs', *Current Medicinal Chemistry*, Dec. 31, 2013. http://www.eurekaselect.com/118618/article (accessed Jan. 28, 2019).

[346] A. N. Begum *et al.*, 'Curcumin structure-function, bioavailability, and efficacy in models of neuroinflammation and Alzheimer's disease', *J. Pharmacol. Exp. Ther.*, vol. 326, no. 1, Art. no. 1, Jul. 2008, doi: 10.1124/jpet.108.137455.

[347] E. K. Ryu, Y. S. Choe, K.-H. Lee, Y. Choi, and B.-T. Kim, 'Curcumin and dehydrozingerone derivatives: synthesis, radiolabeling, and evaluation for beta-amyloid plaque imaging', *J Med Chem*, vol. 49, no. 20, pp. 6111–6119, Oct. 2006, doi: 10.1021/jm0607193.

[348] S. Perkins *et al.*, 'Chemopreventive efficacy and pharmacokinetics of curcumin in the min/+ mouse, a model of familial adenomatous polyposis', *Cancer Epidemiol Biomarkers Prev*, vol. 11, no. 6, pp. 535–540, Jun. 2002.

[349] K. Chen, Y. An, L. Tie, Y. Pan, and X. Li, 'Curcumin Protects Neurons from Glutamate-Induced Excitotoxicity by Membrane Anchored AKAP79-PKA Interaction Network', *Evid Based Complement Alternat Med*, vol. 2015, p. 706207, 2015, doi: 10.1155/2015/706207.

[350] R. M. Khalil and N. F. Khedr, 'Curcumin Protects against Monosodium Glutamate Neurotoxicity and Decreasing NMDA2B and mGluR5 Expression in Rat Hippocampus', *Neurosignals*, vol. 24, no. 1, Art. no. 1, 2016, doi: 10.1159/000442614.

[351] S. C. Gupta, S. Patchva, and B. B. Aggarwal, 'Therapeutic roles of curcumin: lessons learned from clinical trials', *AAPS J*, vol. 15, no. 1, Art. no. 1, Jan. 2013, doi: 10.1208/s12248-012-9432-8.

[352] M. C. Fadus, C. Lau, J. Bikhchandani, and H. T. Lynch, 'Curcumin: An age-old anti-inflammatory and anti-neoplastic agent', *J Tradit*

Complement Med, vol. 7, no. 3, Art. no. 3, Jul. 2017, doi: 10.1016/j.jtcme.2016.08.002.

[353] M. Heger, R. F. van Golen, M. Broekgaarden, and M. C. Michel, 'The molecular basis for the pharmacokinetics and pharmacodynamics of curcumin and its metabolites in relation to cancer', *Pharmacol. Rev.*, vol. 66, no. 1, Art. no. 1, 2014, doi: 10.1124/pr.110.004044.

[354] S. J. Hewlings and D. S. Kalman, 'Curcumin: A Review of Its' Effects on Human Health', *Foods*, vol. 6, no. 10, Art. no. 10, Oct. 2017, doi: 10.3390/foods6100092.

[355] Y. A. Larasati, N. Yoneda-Kato, I. Nakamae, T. Yokoyama, E. Meiyanto, and J. Kato, 'Curcumin targets multiple enzymes involved in the ROS metabolic pathway to suppress tumor cell growth', *Sci Rep*, vol. 8, Feb. 2018, doi: 10.1038/s41598-018-20179-6.

[356] R. S. Ramsewak, D. L. DeWitt, and M. G. Nair, 'Cytotoxicity, antioxidant and anti-inflammatory activities of curcumins I-III from Curcuma longa', *Phytomedicine*, vol. 7, no. 4, Art. no. 4, Jul. 2000, doi: 10.1016/S0944-7113(00)80048-3.

[357] B. Salehi *et al.*, 'The therapeutic potential of curcumin: A review of clinical trials', *European Journal of Medicinal Chemistry*, vol. 163, pp. 527–545, Feb. 2019, doi: 10.1016/j.ejmech.2018.12.016.

[358] T. Y. Lin, C. W. Lu, C.-C. Wang, Y.-C. Wang, and S.-J. Wang, 'Curcumin inhibits glutamate release in nerve terminals from rat prefrontal cortex: possible relevance to its antidepressant mechanism', *Prog. Neuropsychopharmacol. Biol. Psychiatry*, vol. 35, no. 7, Art. no. 7, Aug. 2011, doi: 10.1016/j.pnpbp.2011.06.012.

[359] C. Kliem, A. Merling, M. Giaisi, R. Köhler, P. H. Krammer, and M. Li-Weber, 'Curcumin Suppresses T Cell Activation by Blocking Ca^{2+} Mobilization and Nuclear Factor of Activated T Cells (NFAT) Activation', *Journal of Biological Chemistry*, vol. 287, no. 13, Art. no. 13, Mar. 2012, doi: 10.1074/jbc.M111.318733.

[360] V. W. Yong, J. Wells, F. Giuliani, S. Casha, C. Power, and L. M. Metz, 'The promise of minocycline in neurology', *The Lancet Neurology*, vol. 3, no. 12, Art. no. 12, Dec. 2004, doi: 10.1016/S1474-4422(04)00937-8.

[361] E. Mhillaj, A. Tarozzi, L. Pruccoli, V. Cuomo, L. Trabace, and C. Mancuso, 'Curcumin and Heme Oxygenase: Neuroprotection and Beyond', *International Journal of Molecular Sciences*, vol. 20, no. 10, Art. no. 10, Jan. 2019, doi: 10.3390/ijms20102419.

[362] H. M. Schipper, W. Song, A. Tavitian, and M. Cressatti, 'The sinister face of heme oxygenase-1 in brain aging and disease', *Progress in*

Neurobiology, vol. 172, pp. 40–70, Jan. 2019, doi: 10.1016/j.pneurobio.2018.06.008.

[363] K. M. Nelson, J. L. Dahlin, J. Bisson, J. Graham, G. F. Pauli, and M. A. Walters, 'The Essential Medicinal Chemistry of Curcumin: Miniperspective', *J. Med. Chem.*, vol. 60, no. 5, Art. no. 5, Mar. 2017, doi: 10.1021/acs.jmedchem.6b00975.

[364] D. L. Suskind, G. Wahbeh, T. Burpee, M. Cohen, D. Christie, and W. Weber, 'Tolerability of curcumin in pediatric inflammatory bowel disease: a forced-dose titration study', *J. Pediatr. Gastroenterol. Nutr.*, vol. 56, no. 3, Art. no. 3, Mar. 2013, doi: 10.1097/MPG.0b013e318276977d.

[365] L. A. Hassell and L. D. Roanh, 'Potential response to curcumin in infantile hemangioendothelioma of the liver', *Pediatr Blood Cancer*, vol. 55, no. 2, Art. no. 2, Aug. 2010, doi: 10.1002/pbc.22538.

[366] J. E. Wolff, R. E. Brown, J. Buryanek, S. Pfister, T. S. Vats, and M. E. Rytting, 'Preliminary experience with personalized and targeted therapy for pediatric brain tumors', *Pediatr Blood Cancer*, vol. 59, no. 1, Art. no. 1, Jul. 2012, doi: 10.1002/pbc.23402.

[367] V. Ferrucci, I. Boffa, G. De Masi, and M. Zollo, 'Natural compounds for pediatric cancer treatment', *Naunyn Schmiedebergs Arch. Pharmacol.*, vol. 389, no. 2, Art. no. 2, Feb. 2016, doi: 10.1007/s00210-015-1191-5.

[368] R. C. Amos, H. Jacob, and W. Leith, 'Jaundice in newborn babies under 28 days: NICE guideline 2016 (CG98)', *Archives of disease in childhood - Education & practice edition*, vol. 102, no. 4, Art. no. 4, Aug. 2017, doi: 10.1136/archdischild-2016-311556.

[369] C. Dani, S. Pratesi, F. Raimondi, C. Romagnoli, and Task Force for Hyperbilirubinemia of the Italian Society of Neonatology, 'Italian guidelines for the management and treatment of neonatal cholestasis', *Ital J Pediatr*, vol. 41, p. 69, Oct. 2015, doi: 10.1186/s13052-015-0178-7.

[370] C. Fan, Q. Song, P. Wang, Y. Li, M. Yang, and S. Y. Yu, 'Neuroprotective Effects of Curcumin on IL-1β-Induced Neuronal Apoptosis and Depression-Like Behaviors Caused by Chronic Stress in Rats', *Front Cell Neurosci*, vol. 12, p. 516, Jan. 2019, doi: 10.3389/fncel.2018.00516.

[371] M. Ikram *et al.*, 'Natural Dietary Supplementation of Curcumin Protects Mice Brains against Ethanol-Induced Oxidative Stress-Mediated Neurodegeneration and Memory Impairment via

Nrf2/TLR4/RAGE Signaling', *Nutrients*, vol. 11, no. 5, p. E1082, May 2019, doi: 10.3390/nu11051082.
[372] M. R. Sarker and S. F. Franks, 'Efficacy of curcumin for age-associated cognitive decline: a narrative review of preclinical and clinical studies', *GeroScience*, vol. 40, no. 2, pp. 73–95, Apr. 2018, doi: 10.1007/s11357-018-0017-z.
[373] J. Jankovic and E. K. Tan, 'Parkinson's disease: etiopathogenesis and treatment', *J Neurol Neurosurg Psychiatry*, vol. 91, no. 8, pp. 795–808, Aug. 2020, doi: 10.1136/jnnp-2019-322338.
[374] E. M. Rocha, B. De Miranda, and L. H. Sanders, 'Alpha-synuclein: Pathology, mitochondrial dysfunction and neuroinflammation in Parkinson's disease', *Neurobiology of Disease*, vol. 109, pp. 249–257, Jan. 2018, doi: 10.1016/j.nbd.2017.04.004.
[375] L. V. Kalia and A. E. Lang, 'Parkinson's disease', *The Lancet*, vol. 386, no. 9996, pp. 896–912, Aug. 2015, doi: 10.1016/S0140-6736(14)61393-3.
[376] R. B. Postuma *et al.*, 'MDS clinical diagnostic criteria for Parkinson's disease', *Mov Disord*, vol. 30, no. 12, pp. 1591–1601, Oct. 2015, doi: 10.1002/mds.26424.
[377] H. Braak, K. Del Tredici, U. Rüb, R. A. I. de Vos, E. N. H. Jansen Steur, and E. Braak, 'Staging of brain pathology related to sporadic Parkinson's disease', *Neurobiol Aging*, vol. 24, no. 2, pp. 197–211, Apr. 2003, doi: 10.1016/s0197-4580(02)00065-9.
[378] I. Rigato, J. D. Ostrow, and C. Tiribelli, 'Bilirubin and the risk of common non-hepatic diseases', *Trends in Molecular Medicine*, vol. 11, no. 6, pp. 277–283, Jun. 2005, doi: 10.1016/j.molmed.2005.04.008.
[379] S. D. Zucker, P. S. Horn, and K. E. Sherman, 'Serum bilirubin levels in the U.S. Population: Gender effect and inverse correlation with colorectal cancer', *Hepatology*, vol. 40, no. 4, pp. 827–835, 2004, doi: 10.1002/hep.1840400412.
[380] C. M. Testa, T. B. Sherer, and J. T. Greenamyre, 'Rotenone induces oxidative stress and dopaminergic neuron damage in organotypic substantia nigra cultures', *Molecular Brain Research*, vol. 134, no. 1, pp. 109–118, Mar. 2005, doi: 10.1016/j.molbrainres.2004.11.007.
[381] W. Song *et al.*, 'Evaluation of salivary heme oxygenase-1 as a potential biomarker of early Parkinson's disease', *Movement Disorders*, vol. 33, no. 4, pp. 583–591, 2018, doi: 10.1002/mds.27328.
[382] I. Mateo *et al.*, 'Serum heme oxygenase-1 levels are increased in Parkinson's disease but not in Alzheimer's disease', *Acta Neurol*

Scand, vol. 121, no. 2, pp. 136–138, Feb. 2010, doi: 10.1111/j.1600-0404.2009.01261.x.

[383] H. M. Schipper, A. Liberman, and E. G. Stopa, 'Neural Heme Oxygenase-1 Expression in Idiopathic Parkinson's Disease', *Experimental Neurology*, vol. 150, no. 1, pp. 60–68, Mar. 1998, doi: 10.1006/exnr.1997.6752.

[384] A. E. Berman *et al.*, 'N-Acetylcysteine Prevents Loss of Dopaminergic Neurons in the EAAC−/− Mouse', *Ann Neurol*, vol. 69, no. 3, pp. 509–520, Mar. 2011, doi: 10.1002/ana.22162.

[385] J. Zhang *et al.*, 'Sulfiredoxin-1 protects against simulated ischaemia/reperfusion injury in cardiomyocyte by inhibiting PI3K/AKT-regulated mitochondrial apoptotic pathways', *Biosci Rep*, vol. 36, no. 2, Art. no. 2, Apr. 2016, doi: 10.1042/BSR20160076.

[386] M. Dal Ben *et al.*, 'Earliest Mechanisms of Dopaminergic Neurons Sufferance in a Novel Slow Progressing Ex Vivo Model of Parkinson Disease in Rat Organotypic Cultures of Substantia Nigra', *International Journal of Molecular Sciences*, vol. 20, no. 9, Art. no. 9, Jan. 2019, doi: 10.3390/ijms20092224.

[387] Z. C. Baquet, P. C. Bickford, and K. R. Jones, 'Brain-Derived Neurotrophic Factor Is Required for the Establishment of the Proper Number of Dopaminergic Neurons in the Substantia Nigra Pars Compacta', *J. Neurosci.*, vol. 25, no. 26, pp. 6251–6259, Jun. 2005, doi: 10.1523/JNEUROSCI.4601-04.2005.

[388] E. Palasz, A. Wysocka, A. Gasiorowska, M. Chalimoniuk, W. Niewiadomski, and G. Niewiadomska, 'BDNF as a Promising Therapeutic Agent in Parkinson's Disease', *International Journal of Molecular Sciences*, vol. 21, no. 3, Art. no. 3, Jan. 2020, doi: 10.3390/ijms21031170.

[389] S. R. Kim, T. Kareva, O. Yarygina, N. Kholodilov, and R. E. Burke, 'AAV Transduction of Dopamine Neurons With Constitutively Active Rheb Protects From Neurodegeneration and Mediates Axon Regrowth', *Molecular Therapy*, vol. 20, no. 2, pp. 275–286, Feb. 2012, doi: 10.1038/mt.2011.213.

[390] N. G. Hernandez-Chan *et al.*, 'Neurotensin-polyplex-mediated brain-derived neurotrophic factor gene delivery into nigral dopamine neurons prevents nigrostriatal degeneration in a rat model of early Parkinson's disease', *Journal of Biomedical Science*, vol. 22, no. 1, p. 59, Jul. 2015, doi: 10.1186/s12929-015-0166-7.

[391] C. A. Lucidi-Phillipi, F. H. Gage, C. W. Shults, K. R. Jones, L. F. Reichardt, and U. J. Kang, 'Brain-derived neurotrophic factor-transduced fibroblasts: Production of BDNF and effects of grafting to the adult rat brain', *Journal of Comparative Neurology*, vol. 354, no. 3, pp. 361–376, 1995, doi: 10.1002/cne.903540306.
[392] J. J. Gagne and M. C. Power, 'Anti-inflammatory drugs and risk of Parkinson disease: A meta-analysis', *Neurology*, vol. 74, no. 12, pp. 995–1002, Mar. 2010, doi: 10.1212/WNL.0b013e3181d5a4a3.
[393] A. Samii, M. Etminan, M. O. Wiens, and S. Jafari, 'NSAID Use and the Risk of Parkinson's Disease', *Drugs Aging*, vol. 26, no. 9, pp. 769–779, Sep. 2009, doi: 10.2165/11316780-000000000-00000.
[394] L. Ren, J. Yi, J. Yang, P. Li, X. Cheng, and P. Mao, 'Nonsteroidal anti-inflammatory drugs use and risk of Parkinson disease', *Medicine (Baltimore)*, vol. 97, no. 37, p. e12172, Sep. 2018, doi: 10.1097/MD.0000000000012172.
[395] A. Håkansson *et al.*, 'Interaction of polymorphisms in the genes encoding interleukin-6 and estrogen receptor beta on the susceptibility to Parkinson's disease', *American Journal of Medical Genetics Part B: Neuropsychiatric Genetics*, vol. 133B, no. 1, pp. 88–92, 2005, doi: 10.1002/ajmg.b.30136.
[396] T.-W. Liu, Y.-R. Wu, Y.-C. Chen, H.-C. Fung, and C.-M. Chen, 'Polymorphisms of Interleukin-6 and Interleukin-8 Are Not Associated with Parkinson's Disease in Taiwan', *Brain Sciences*, vol. 11, no. 6, Art. no. 6, Jun. 2021, doi: 10.3390/brainsci11060768.
[397] H. J. Son *et al.*, 'A novel compound PTIQ protects the nigral dopaminergic neurones in an animal model of Parkinson's disease induced by MPTP', *Br J Pharmacol*, vol. 165, no. 7, pp. 2213–2227, Apr. 2012, doi: 10.1111/j.1476-5381.2011.01692.x.
[398] A. Boireau, F. Bordier, P. Dubédat, C. Pény, and A. Impérato, 'Thalidomide reduces MPTP-induced decrease in striatal dopamine levels in mice', *Neurosci Lett*, vol. 234, no. 2–3, pp. 123–126, Oct. 1997, doi: 10.1016/s0304-3940(97)00685-x.
[399] T. Nagatsu, M. Mogi, H. Ichinose, and A. Togari, 'Cytokines in Parkinson's disease', in *Advances in Research on Neurodegeneration*, Vienna, 2000, pp. 143–151. doi: 10.1007/978-3-7091-6284-2_12.
[400] C. Gómez-Santos, R. Francisco, P. Giménez-Xavier, and S. Ambrosio, 'Dopamine induces TNFalpha and TNF-R1 expression in SH-SY5Y human neuroblastoma cells', *Neuroreport*, vol. 18, no. 16, pp. 1725–1728, Oct. 2007, doi: 10.1097/WNR.0b013e3282f0d3db.

[401] A. L. De Lella Ezcurra, M. Chertoff, C. Ferrari, M. Graciarena, and F. Pitossi, 'Chronic expression of low levels of tumor necrosis factor-alpha in the substantia nigra elicits progressive neurodegeneration, delayed motor symptoms and microglia/macrophage activation', *Neurobiol Dis*, vol. 37, no. 3, pp. 630–640, Mar. 2010, doi: 10.1016/j.nbd.2009.11.018.

[402] S. O. McGuire, Z. D. Ling, J. W. Lipton, C. E. Sortwell, T. J. Collier, and P. M. Carvey, 'Tumor Necrosis Factor α Is Toxic to Embryonic Mesencephalic Dopamine Neurons', *Experimental Neurology*, vol. 169, no. 2, pp. 219–230, Jun. 2001, doi: 10.1006/exnr.2001.7688.

[403] P. Prajapati, L. Sripada, K. Singh, K. Bhatelia, R. Singh, and R. Singh, 'TNF-α regulates miRNA targeting mitochondrial complex-I and induces cell death in dopaminergic cells', *Biochimica et Biophysica Acta (BBA) - Molecular Basis of Disease*, vol. 1852, no. 3, pp. 451–461, Mar. 2015, doi: 10.1016/j.bbadis.2014.11.019.

[404] M. G. Tansey, M. K. McCoy, and T. C. Frank-Cannon, 'Neuroinflammatory mechanisms in Parkinson's disease: potential environmental triggers, pathways, and targets for early therapeutic intervention', *Exp Neurol*, vol. 208, no. 1, pp. 1–25, Nov. 2007, doi: 10.1016/j.expneurol.2007.07.004.

[405] C. A. Adin, 'Bilirubin as a Therapeutic Molecule: Challenges and Opportunities', *Antioxidants*, vol. 10, no. 10, Art. no. 10, Oct. 2021, doi: 10.3390/antiox10101536.

[406] K. M. Park and W. J. Bowers, 'Tumor necrosis factor-alpha mediated signaling in neuronal homeostasis and dysfunction', *Cell Signal*, vol. 22, no. 7, pp. 977–983, Jul. 2010, doi: 10.1016/j.cellsig.2010.01.010.

[407] M. Mogi *et al.*, 'Caspase activities and tumor necrosis factor receptor R1 (p55) level are elevated in the substantia nigra from Parkinsonian brain', *Journal of Neural Transmission*, vol. 107, no. 3, pp. 335–341, Mar. 2000, doi: 10.1007/s007020050028.

[408] I. Peter *et al.*, 'Anti–Tumor Necrosis Factor Therapy and Incidence of Parkinson Disease Among Patients With Inflammatory Bowel Disease', *JAMA Neurology*, vol. 75, no. 8, pp. 939–946, Aug. 2018, doi: 10.1001/jamaneurol.2018.0605.

[409] A. L. Olsen, T. Riise, and C. R. Scherzer, 'Discovering New Benefits From Old Drugs With Big Data—Promise for Parkinson Disease', *JAMA Neurology*, vol. 75, no. 8, pp. 917–920, Aug. 2018, doi: 10.1001/jamaneurol.2018.0345.

[410] M. A. Brito, I. Palmela, F. L. Cardoso, I. Sá-Pereira, and D. Brites, 'Blood–Brain Barrier and Bilirubin: Clinical Aspects and Experimental Data', *Archives of Medical Research*, vol. 45, no. 8, pp. 660–676, Nov. 2014, doi: 10.1016/j.arcmed.2014.11.015.
[411] D. J. Kamothi, V. Kant, B. L. Jangir, V. G. Joshi, M. Ahuja, and V. Kumar, 'Novel preparation of bilirubin-encapsulated pluronic F-127 nanoparticles as a potential biomaterial for wound healing', *European Journal of Pharmacology*, vol. 919, p. 174809, Mar. 2022, doi: 10.1016/j.ejphar.2022.174809.
[412] L. Shan *et al.*, 'Organosilica-Based Hollow Mesoporous Bilirubin Nanoparticles for Antioxidation-Activated Self-Protection and Tumor-Specific Deoxygenation-Driven Synergistic Therapy', *ACS Nano*, vol. 13, no. 8, pp. 8903–8916, Aug. 2019, doi: 10.1021/acsnano.9b02477.
[413] M. J. Kim, Y. Lee, S. Jon, and D. Y. Lee, 'PEGylated bilirubin nanoparticle as an anti-oxidative and anti-inflammatory demulcent in pancreatic islet xenotransplantation', *Biomaterials*, vol. 133, pp. 242–252, Jul. 2017, doi: 10.1016/j.biomaterials.2017.04.029.
[414] C. Moreau *et al.*, 'Iron as a therapeutic target for Parkinson's disease', *Mov. Disord.*, vol. 33, no. 4, Art. no. 4, Apr. 2018, doi: 10.1002/mds.27275.
[415] S. Zullino *et al.*, 'Superparamagnetic Oxygen-Loaded Nanobubbles to Enhance Tumor Oxygenation During Hyperthermia', *Front Pharmacol*, vol. 10, p. 1001, Sep. 2019, doi: 10.3389/fphar.2019.01001.
[416] S. A. M. K. Ansari *et al.*, 'Magnetic Iron Oxide Nanoparticles: Synthesis, Characterization and Functionalization for Biomedical Applications in the Central Nervous System', *Materials (Basel)*, vol. 12, no. 3, p. 465, Feb. 2019, doi: 10.3390/ma12030465.
[417] P. J. Urrutia, D. Bórquez, and M. T. Núñez, 'Iron Neurotoxicity in Parkinson's Disease', in *Handbook of Neurotoxicity*, R. M. Kostrzewa, Ed. Cham: Springer International Publishing, 2021, pp. 1–24. doi: 10.1007/978-3-030-71519-9_11-1.
[418] S. Ayton *et al.*, 'Iron accumulation confers neurotoxicity to a vulnerable population of nigral neurons: implications for Parkinson's disease', *Molecular Neurodegeneration*, vol. 9, no. 1, p. 27, Jul. 2014, doi: 10.1186/1750-1326-9-27.
[419] G. A. Salvador, R. M. Uranga, and N. M. Giusto, 'Iron and Mechanisms of Neurotoxicity', *Int J Alzheimers Dis*, vol. 2011, p. 720658, Dec. 2010, doi: 10.4061/2011/720658.

[420] J.-Y. Wang *et al.*, 'Meta-analysis of brain iron levels of Parkinson's disease patients determined by postmortem and MRI measurements', *Sci Rep*, vol. 6, p. 36669, Nov. 2016, doi: 10.1038/srep36669.
[421] J. Blesa, I. Trigo-Damas, A. Quiroga-Varela, and V. R. Jackson-Lewis, 'Oxidative stress and Parkinson's disease', *Front. Neuroanat.*, vol. 9, 2015, doi: 10.3389/fnana.2015.00091.
[422] B. Wolozin and N. Golts, 'Book Review: Iron and Parkinson's Disease', *Neuroscientist*, vol. 8, no. 1, pp. 22–32, Feb. 2002, doi: 10.1177/107385840200800107.
[423] T. Liang, Z.-M. Qian, M.-D. Mu, W.-H. Yung, and Y. Ke, 'Brain Hepcidin Suppresses Major Pathologies in Experimental Parkinsonism', *iScience*, vol. 23, no. 7, p. 101284, Jul. 2020, doi: 10.1016/j.isci.2020.101284.
[424] C. Mouhape, G. Costa, M. Ferreira, J. A. Abin-Carriquiry, F. Dajas, and G. Prunell, 'Nicotine-Induced Neuroprotection in Rotenone In Vivo and In Vitro Models of Parkinson's Disease: Evidences for the Involvement of the Labile Iron Pool Level as the Underlying Mechanism', *Neurotox Res*, vol. 35, no. 1, pp. 71–82, Jan. 2019, doi: 10.1007/s12640-018-9931-1.
[425] D. Serantes and D. Baldomir, 'Nanoparticle Size Threshold for Magnetic Agglomeration and Associated Hyperthermia Performance', *Nanomaterials (Basel)*, vol. 11, no. 11, p. 2786, Oct. 2021, doi: 10.3390/nano11112786.
[426] U. Engelmann, E. M. Buhl, M. Baumann, T. Schmitz-Rode, and I. Slabu, 'Agglomeration of magnetic nanoparticles and its effects on magnetic hyperthermia', *Current Directions in Biomedical Engineering*, vol. 3, no. 2, pp. 457–460, Sep. 2017, doi: 10.1515/cdbme-2017-0096.
[427] T. L. Moore *et al.*, 'Nanoparticle colloidal stability in cell culture media and impact on cellular interactions', *Chemical Society Reviews*, vol. 44, no. 17, pp. 6287–6305, 2015, doi: 10.1039/C4CS00487F.
[428] H.-C. Cheng, C. M. Ulane, and R. E. Burke, 'Clinical progression in Parkinson disease and the neurobiology of axons', *Ann Neurol*, vol. 67, no. 6, pp. 715–725, Jun. 2010, doi: 10.1002/ana.21995.
[429] R. L. Jayaraj, K. Tamilselvam, T. Manivasagam, and N. Elangovan, 'Neuroprotective effect of CNB-001, a novel pyrazole derivative of curcumin on biochemical and apoptotic markers against rotenone-induced SK-N-SH cellular model of Parkinson's disease', *J Mol*

Neurosci, vol. 51, no. 3, pp. 863–870, Nov. 2013, doi: 10.1007/s12031-013-0075-8.

[430] R. L. Jayaraj, N. Elangovan, K. Manigandan, S. Singh, and S. Shukla, 'CNB-001 a novel curcumin derivative, guards dopamine neurons in MPTP model of Parkinson's disease', *Biomed Res Int*, vol. 2014, p. 236182, 2014, doi: 10.1155/2014/236182.

[431] B. S. Gadad, P. K. Subramanya, S. Pullabhatla, I. S. Shantharam, and K. S. Rao, 'Curcumin-glucoside, a novel synthetic derivative of curcumin, inhibits α-synuclein oligomer formation: relevance to Parkinson's disease', *Curr Pharm Des*, vol. 18, no. 1, pp. 76–84, 2012, doi: 10.2174/138161212798919093.

[432] Y. H. Siddique, F. Naz, and S. Jyoti, 'Effect of Curcumin on Lifespan, Activity Pattern, Oxidative Stress, and Apoptosis in the Brains of Transgenic Drosophila Model of Parkinson's Disease', *Biomed Res Int*, vol. 2014, p. 606928, 2014, doi: 10.1155/2014/606928.

[433] A. A. Farooqui and T. Farooqui, 'Chapter 18 - Therapeutic Potentials of Curcumin in Parkinson's Disease', in *Curcumin for Neurological and Psychiatric Disorders*, T. Farooqui and A. A. Farooqui, Eds. Academic Press, 2019, pp. 333–344. doi: 10.1016/B978-0-12-815461-8.00018-9.

[434] Z. Liu, Y. Yu, X. Li, C. A. Ross, and W. W. Smith, 'Curcumin protects against A53T alpha-synuclein-induced toxicity in a PC12 inducible cell model for Parkinsonism', *Pharmacological Research*, vol. 63, no. 5, pp. 439–444, May 2011, doi: 10.1016/j.phrs.2011.01.004.

[435] M. Ramkumar *et al.*, 'Demethoxycurcumin, a Natural Derivative of Curcumin Abrogates Rotenone-induced Dopamine Depletion and Motor Deficits by Its Antioxidative and Anti-inflammatory Properties in Parkinsonian Rats', *Pharmacogn Mag*, vol. 14, no. 53, pp. 9–16, 2018, doi: 10.4103/pm.pm_113_17.

[436] T. Baj and R. Seth, 'Role of Curcumin in Regulation of TNF-α Mediated Brain Inflammatory Responses', *Recent Pat Inflamm Allergy Drug Discov*, vol. 12, no. 1, pp. 69–77, 2018, doi: 10.2174/1872213X12666180703163824.

[437] E. E. Nebrisi, 'Neuroprotective Activities of Curcumin in Parkinson's Disease: A Review of the Literature', *Int J Mol Sci*, vol. 22, no. 20, p. 11248, Oct. 2021, doi: 10.3390/ijms222011248.

[438] F. Yang *et al.*, 'Curcumin Inhibits Formation of Amyloid β Oligomers and Fibrils, Binds Plaques, and Reduces Amyloid in Vivo*', *Journal of Biological Chemistry*, vol. 280, no. 7, pp. 5892–5901, Feb. 2005, doi: 10.1074/jbc.M404751200.

[439] H. Ghodsi, H. R. Rahimi, S. M. Aghili, A. Saberi, and A. Shoeibi, 'Evaluation of curcumin as add-on therapy in patients with Parkinson's disease: A pilot randomized, triple-blind, placebo-controlled trial', *Clinical Neurology and Neurosurgery*, vol. 218, p. 107300, Jul. 2022, doi: 10.1016/j.clineuro.2022.107300.
[440] V. Donadio *et al.*, 'The Effect of Curcumin on Idiopathic Parkinson Disease: A Clinical and Skin Biopsy Study', *Journal of Neuropathology & Experimental Neurology*, p. nlac034, May 2022, doi: 10.1093/jnen/nlac034.
[441] A. K. Verma, J. Raj, V. Sharma, T. B. Singh, S. Srivastava, and R. Srivastava, 'Epidemiology and associated risk factors of Parkinson's disease among the north Indian population', *Clinical Epidemiology and Global Health*, vol. 5, no. 1, pp. 8–13, Mar. 2017, doi: 10.1016/j.cegh.2016.07.003.
[442] R. B. Mythri and M. M. S. Bharath, 'Curcumin: a potential neuroprotective agent in Parkinson's disease', *Curr Pharm Des*, vol. 18, no. 1, pp. 91–99, 2012, doi: 10.2174/138161212798918995.